CHARACTERISATION OF THE STRUCTURAL MOTIFS INVOLVED IN THE CLEAVAGE AND SECRETION OF HUMAN ANGIOTENSIN-CONVERTING ENZYME

Nailah Conrad

Thesis presented for the degree of

DOCTOR OF PHILOSPHY

in the Division of Medical Biochemistry

UNIVERSITY OF CAPE TOWN

January 2014

Supervisors: Prof. E.D. Sturrock, S.L.U. Schwager

DECLARATION

I, **Nailah Conrad**, declare that this thesis is my own unaided work, both in concept and execution, apart from the normal guidance from my supervisors and where the acknowledgements indicate otherwise.

Neither the substance nor any part of the above thesis has been submitted in the past, or is being, or is to be submitted for a degree at this University or at any other university.

I grant the University of Cape Town free licence to reproduce the above thesis in whole or in part, for the purpose of research.

_____

Candidate's Signature

Signed on this _____day of _____, 2014.

ABSTRACT

Angiotensin converting enzyme is an ectoprotein prone to regulated proteolytic solubilisation by an as yet unknown protease or sheddase. Proteolytic cleavage of membrane proteins is an essential cellular process that controls their expression and function, and modulates cellular and physiological processes. Testis ACE (tACE) is shed at a higher rate than somatic ACE and it has been proposed that regions in its ectodomain direct its shedding. Discrete secondary structures on the surface of the distal ectodomain of tACE were replaced with their N-domain counterparts to determine their role in the ectodomain shedding of ACE. None of the regions investigated proved to be an absolute requirement for shedding, but the mutant ACE proteins were subject to variations in shedding compared to wild-type tACE.

To investigate the role of the proximal ectodomain in shedding the residues H^{610}-L^{614} were mutated to alanines, causing a decrease in shedding. An extension of this mutation on the N-terminal side to seven alanines resulted in a reduction in ACE activity and, more importantly, it affected the processing of the protein to the membrane, resulting in expression of an underglycosylated form of ACE. When E^{608}-H^{614} was mutated to the homologous region of the N-domain, processing was normal and shedding only marginally reduced. These data suggest that this region is more crucial for the processing of ACE than is for regulating shedding. Construction of a P^{628}L mutation in tACE showed an increase in shedding. Furthermore, MALDI analysis of a tryptic digest established that the putative glycosylation site N^{620}WT became glycosylated. Further mutagenesis of the P^{628}L mutant to remove the newly formed glycosylation site, resulted in an even greater increase in shedding.

Soluble fluorogenic peptides mimicking the ACE stalk were used in a cell-based assay to characterise the contribution of the stalk to ACE shedding. Hydrolysis of the wild-type peptide Abz-NSARSEGPQ-EDDnp was not responsive to phorbol ester or the hydroxamate inhibitor (TAPI), however, it was inhibited by EDTA. The aminopeptidase inhibitor bestatin did not inhibit cleavage or alter the cleavage site. Therefore the protease involved in the

cleavage of the ACE stalk peptides is likely different to the sheddase responsible for ACE shedding. Substitution of the P1 and P1’ sites of the peptides did not significantly influence the rate of cleavage. All the peptides were cleaved at the E-G bond, which is C-terminal to the physiological R-S cleavage site. Removal of the fluorogenic capping groups resulted in no cleavage of the peptides and lengthening of the peptide did not result in cleavage. This confirms the need for the ACE sheddase and its substrate to be anchored in the membrane and suggests the use of soluble peptide substrates in a cell assay has limited application for investigating the ectodomain shedding of ACE.

Acknowledgements

I would like to thank the following funders for their financial support throughout my Phd: The National Research Foundation, Medical Research Foundation, The Stella and Paul Loewenstein Foundation, and the Ernst and Ethel Eriksen Trust. Without their generous support, this PhD would not have been possible.

I would like to thank the following people who have contributed to this PhD.

Busiswa Kekana and Marè Vlok at the Centre for Proteomic and Genomic Research (CPGR), Cape Town for the MALDI MS/MS analysis and all the help with analysis.

Diane James (Department of Molecular and Cell Biology, UCT), who conducted nucleotide sequencing.

Adriana Carmona, for the synthesis of the ACE stalk peptides.

I would like to thank Prof. E.D Sturrock for his unwavering support throughout my many years under his supervision. I don't think I could have asked for a more understanding and patient supervisor. Without that understanding I could not have completed this degree.

To Sylva Schwager, thank you for all of your guidance and support throughout my project. Your help with all the proteomic work was invaluable and thank you for the many hours and days (weeks, months…) spent helping me get to grips with the HPLC.

To my fellow lab members with whom I have shared my days with over the years. Thank you for your friendship, company, food, advice, help and everything else. You guys have been great. Ayesha, Wendy, Kerry, Riyad, Tony, Chris, Ross, Colin, Raymond, Trudi, Adele, Kate, Karabelo, Lizelle, Vinasha, Palesa, Albert, Afolake, Sia, Lindile and Moniqah.

For critical reading of thesis, thanks to Sylva, Kerry, Ayesha, Wendy, Amaal, Widaad and Yumna.

To my family and friends for standing by me throughout this journey, cheering me on, keeping me going, for entertaining my child, thanks for everything. Ayesha, Amaal, Suad, Widaad, Yumna, Zulfah.

To my family, I don’t know if I will ever be able to repay this enormous debt of gratitude.

To Maj, Raeesah and Nehal, you have been so wonderful in supporting me and helping with Zaahid. It has truly helped me along in getting me to this point.

To Mummy/Ma, you have been a great help wherever I needed it and shukran for always supporting me and for all your understanding.

To my parents, Mom and Dad, I have to say a big shukran for all your love, support, guidance, all forms of help without which I would have given up a long time ago. I love you both very much. I don’t know what else to say but, thank you and shukran.

To my Zaahid, my darling. You are my greatest teacher at the moment, as I have learnt so much over the last four years about life and how to live it. I hope now we can keep on learning together.

To Saberi, what can I say except thank you from the bottom of heart. Thank you, Shukran, Jazakallah Khayr. You have seen me through every single step of this journey and have experienced my highest high and my lowest low. You have supported me in every possible way and your encouragement has been my lifeblood. I love you so much and I am extremely blessed to have you by my side. Remember, I would be lost in space without you.

To my Creator, shukran for all the opportunities you have presented to me over the years and experiences and you have allowed me to enjoy. All I can ask is that what I have done and what I will do, will be to please you, Insha-Allah.

ABBREVIATIONS

3D	three-dimensional
Å	angstrom
Abz	ortho-aminobenzoic acid
ACE	angiotensin-converting enzyme
ACE2	angiotensin-converting enzyme 2
ACN	acetonitrile
Ac-SDKP	acetyl-SDKP
ADAM	a distintergrin and metalloprotease
ADAMTS-13	a distintergrin and metalloprotease with a thrombospondin type 1 motif
ALCAM	activated leukocyte cell adhesion molecule
AMPS	ammonium persulphate
AngI	angiotensin I
AngII	angiotensin II
APP	amyloid precursor protein
ATR1	angiotensin II receptor type 1
ATR2	angiotensin II receptor type 2
Aβ	amyloid β peptide 1-42
B2	bradykinin 2 receptor
BiP	immunoglobulin binding protein
BK	bradykinin
bp	base pair
BSA	bovine serum albumin
CaM	calmodulin
CC-ACE	ACE with two C-domains
CHO-K1	Chinese hamster ovary
CK2	casein kinase
CN-ACE	ACE with C-domain at N-terminus and N-domain at C-terminus
CO_2	carbon dioxide
COS 7	African green monkey fibroblast-like kidney cells
CRD	carbohydrate recognition domain
Cys	cysteine

DCI	3,4-dichloroisocoumarin
DFP	Diisopropyl fluorophosphate
DMEM	Dulbecco's Modified Eagle Medium
DMSO	Dimethyl sulfoxide
DNA	deoxyribonucleic acid
dNTP	deoxyriboneuclotide
DTT	dithiothreitol
E.coli	Escherischia coli
EDDnp	ethylene diamine-2,4-dinitrophenyl
EDTA	ethylenediaminetetraacetic acid
EGF	epidermal growth factor
EGFR	epidermal growth factor receptor
ELISA	enzyme-linked immunosorbent assay
EM	electron microscopy
ER	endoplasmic reticulum
FAM	6- carboxyfluorescein
FCS	fetal calf serum
Fmoc-Lys(Dnp)-OH	N-α-fluorenylmethyloxycarbonyl-N-ε-2,4-dinitrophenyl-L-lysine
For	forward
FRET	fluorescence resonance energy transfer
GM6001	N-[(2R)-2-(hydroxamidocarbonylmethyl)-4-methylpentanoyl]-L-tryptophan methylamide
GPCR	G-protein coupled receptor
GPI	glycosylphosphatidylinisotol
H_2O_2	hydrogen peroxide
HB-EGF	heparin binding epidermal growth factor
HBSS	hank's buffered salt solution
HEK	human embryonic kidney
HEPES	4-(2-hydroxyethyl)-1-piperazineethanesulfonic acid
HHL	hippuryl-L-His-L-Leu
HL	His-Leu
HMC-1	human mast cell line
HMEC	human microvascular endothelial cell line

HPLC	high performance liquid chromatography
HRP	horseradish peroxidase
HUVEC	human umbilical vein endothelial cells
ICD	intracellular domain
IL	interleukin human mast cell line 1
IL-6R	interleukin-6 receptor
IP	immunoprecipitation
JNK	c-Jun N-terminal kinase
kb	kilobase pairs
kDa	kilo Daltons
KitL	kit ligand
LA	luria agar
LB	luria broth
LC-MS	liquid chromatography mass spectrometry
LPS	lipopolysaccharide
LSF	larger soluble form
mAb	monoclonal antibody
MAP	mitogen-activated protein
MAPK	mitogen-activated protein kinase
MBP	myelin basic protein
MCS	multiple cloning site
MDCK	Madin-Darby canine kidney
MDP	membrane dipeptidase
MHC	major histocompatibility complex
MIC	MHC class I-related chain
MMP	matrix metalloprotease
mRNA	messenger ribonucleic acid
NB-DNJ	N-butyldeoxy-nojirimycin
NCAM	neural cell adhesion molecule
NKG2D	natural killer group 2, D
PAGE	polyacrylamide gel electrophoresis
PAO	Phenylarsine oxide
PBL	peripheral blood lymphocytes

PBS	phosphate buffered saline
PC	proprotein convertase
PCR	polymerase chain reaction
PDBu	phorbol 12,13-dibutyrate
PDI	protein disulphide isomerase
PFA	paraformaldehyde
PKA	protein kinase A
PKC	protein kinase C
PMA	phorbol-12-myristate-13-acetate
PMSF	phenylmethylsulfonyl fluoride
PMT	photomultiplier tube
ProAREG	amphiregulin precursor
RAAS	renin-aldosterone-angiotensin system
RE	restriction enzyme
Rev	reverse
RNA	ribonucleic acid
ROS	reactive oxygen species
RT-PCR	reverse transcriptase polymerase chain reaction
sACE	somatic ACE
SARS-coV	severe-acute respiratory syndrome-coronavirus
SDM	site-directed mutagenesis
SDS	sodium dodecyl sulphate
SEM	standard error of the mean
siRNA	small interference RNA
SSF	smaller soluble form
SVMP	snake venom metalloprotease
tACE	testis ACE
TACE	TNF-α converting enzyme
TAMRA	6-carboxytetramethylrhodamine
TAPI	TNF-α Protease Inhibitor
TBS-T	tris-buffered saline-tween
TCEP	Tris (2-carboxyethyl) phosphine
TEMED	tetramethylethylenediamine

TFA	trifluoroacetic acid
TGF-α	transforming growth factor-α
TIMPs	tissue inhibitor of metalloproteinases
TNF-α	tumour necrosis factor-α
TPCK	tosylphenylalanine chloromethyl ketone
TRANCE	TNF-related activation-induced cytokine
wt	wild-type
ZFHL	benzyloxycarbonyl-Phe-L-His-Leu
Zn	zinc
β−ME	β-mercaptoethanol

LIST OF FIGURES AND TABLES

Chapter 1

Chapter 3

Chapter 4

Chapter 5

Appendix

List of tables

Chapter 1

Chapter 3

Chapter 4

Chapter 5

Appendix

TABLE OF CONTENTS

CHAPTER 1: Literature Review

1.1. Ectodomain shedding

The cell membrane is in constant state of flux due to the action of proteases which cleave ectoprotein domains of membrane-anchored proteins. Cell surface proteins such as Pro-transforming growth factor -α (TGF-α), amyloid precursor protein (APP), L-selectin, interleukin-6 receptor (IL-6R) and tumour necrosis factor-α (TNF-α) are released from the cell membrane by proteolysis, usually at or near a region proximal to the membrane. This event is termed ectodomain shedding. Moreover, ectodomain shedding is exploited ubiquitously to regulate activity and spatial location of chemokines, cytokines, receptors and growth factors involved in inflammation, immunity, cancer, cellular development and a host of other physiologically relevant processes (Hayashida et al., 2010; Overall and Blobel, 2007).

Therefore, the investigation into how ectodomain shedding is controlled has far reaching influences on its role in various cellular processes and disease progression (Overall and Blobel, 2007). Determining the site of cleavage, the enzyme kinetics of the proteolytic action, the susceptibility to antagonists and agonists, may link the function of a protease to its specific substrate in vivo and vice versa. This will expose the cellular pathway involved and may lead to new or alternative avenues that may be evaluated as therapeutic interventions.

The elucidation of common systems and pathways have shown that unrelated proteins are regulated in a similar manner. For example, a common pathway to stimulate shedding may be via protein kinase C-dependant (PKC) and independent mechanisms as evidenced by shared phenotypes displayed by shedding mutants. Serine protease inhibitors, 3,4-dichloroisocoumarin (3,4-DCI), tosylphenylalanine chloromethyl ketone (TPCK) and diisopropyl fluorophosphate (DFP), inhibit shedding of Pro-TGF-α, but not L-selectin and therefore can be used to differentiate between substrates. Testing of the hydroxamate inhibitor TNF-α Protease Inhibitor 2 (TAPI-2), inhibits TNF-α as well as TGF-α shedding. The

general metalloprotease inhibitor 1,10–phenanthroline inhibited phorbol-12-myristate-13-acetate (PMA) -activated shedding, yet EDTA and EGTA were ineffective (Arribas et al., 1996; Hayashida et al., 2010; Merlos-Suárez and Arribas, 1999).

Therefore, it is the purpose of this review to highlight the most appropriate cases that put into context the important physiological role of ectodomain shedding. It will show that there is a multitude of parameters over and above the catalytic activity of the sheddase, i.e. the protease responsible for cleaving the substrate, which influences ectodomain shedding. It will especially concentrate on the structural constraints of the substrate mediating protein-protein interactions to regulate shedding.

1.2 Regulation of ectodomain shedding

There are many contributing factors of both the substrate and sheddase that influence how shedding is regulated. Ectoproteins have been shown to have specific requirements in terms of their stalk length, cytoplasmic domain, transmembrane domain and ectodomain. There exists a complex interplay between these structures that offers a myriad of combinations of regulation conditions or parameters that can result in specific cleavage secretion as it is required.

1.2.1 Stalk length

L-selectin, a glycoprotein expressed in neutrophils, initiates leucocyte migration in inflammation and is downregulated by shedding off the membrane by ADAM 17 (where ADAM is ‘a disintegrin and metalloproteinase’)(Smalley and Ley, 2005; Wang et al., 2009). A study by Zhao et al., (2001) attempted to investigate the structural determinants for the regulation of its shedding. It was found that L-selectin was cleaved 11 residues from the transmembrane domain but this cleavage site had very little sequence specificity. However, proline substitution C-terminal to the cleavage site caused blocking of phorbol-induced shedding (Zhao et al., 2001). The EGF domain, which is distal to the cleavage site, directs phorbol-induced cleavage, but not constitutive shedding. The cleavage site for mouse L-selectin was at the R^{321}-S^{322}bond (Zhao et al., 2001) and in human it is at K^{321}-S^{322} (Migaki et

al., 1995). Additionally, an 8-amino acid deletion in the juxtamembrane region caused a significant reduction in shedding that was likely due to the reduction in the stalk length (Zhao et al., 2001). This suggests that certain residues around the cleavage site influence the cleavage of L-selectin. Other studies have also confirmed the important contribution of the stalk length in controlling the shedding of L-selectin (Hinkle et al., 2003). For example, point mutations around the cleavage site did not affect L-selectin proteolysis neither did alanine mutations of the region K^{327}EGDY in the juxtamembrane stalk. However, short deletions around this region had an effect indicating that the stalk length, not sequence, influenced shedding.

L-selectin shedding was examined in the absence of active ADAM 17 and it was found that constitutive shedding still occurred by another metalloprotease that is dependent on an accessible juxtamembrane stalk of a specific length (Walcheck et al., 2003). Syndecans are transmembrane proteins with a multiplicity of roles in tumour progression. They are cleaved by tumour-related matrix metalloproteinases (MMPs) and regions proximal to the membrane were shown to favour cleavage. In addition syndecans are also cleaved at multiple sites occurring 6 and 15 residues from the transmembrane domain and another was mapped to the region 35-40 residues C-terminal from the “heparin sulphate domain” (Manon-Jensen et al., 2013).

To identify a sequence length that affects shedding, the cleavage site regions of TNF-α and TGF-α were substituted into gp130, which is not usually shed. This resulted in a cleavable gp130. This emphasises once again the need for ample stalk length, allowing access to the substrate. Furthermore, a study by Arribas et al. (1997) used cleavage site regions of TGF-α and amyloid precursor protein (APP) to bring about the shedding of β-glycan, as the 14 amino acid exchange gave sufficient stalk length to allow shedding to occur. While the correct stalk length is important for the shedding of a number of ectoproteins, the conformation and/or flexibility of the juxtamembrane region is also essential (Althoff et al., 2001).

The contribution of the transmembrane, cytoplasmic and juxtamembrane domains of macrophage colony stimulating factor 1 (CSF-1) to its ectodomain shedding was investigated using deletion mutants. Substitution mutations of the 5-residue stretch P^{161}QLQE in the juxtamembrane region was discovered to regulate shedding (Deng et al., 1996). The deletion mutations proved that the stalk length is of utmost importance as it influences the steric availability of the stalk region for the appropriate sheddase. Additional studies whereby residues were inserted into the juxtamembrane stalk, revealed that the amino acid sequence regulated the site of cleavage (Deng et al., 1998). The N-linked glycosylation as a result of the mutations interfered with cleavage, implicating changes in steric conformation and how this influences shedding. Shedding of these cleavable and non-cleavable variants highlighted the importance of stalk length, sequence and glycosylation on the regulation of CSF-1 ectodomain shedding (Deng et al., 2000, 1998).

1.2.2 Regulation of ectodomain shedding by secondary sheddase-substrate interactions

The substrate recognition model for Ephrin A5/EphA3- is an excellent example of a substrate-sheddase complex that requires the ligand to be bound by its receptor in order to be cleaved. Eph is a family of receptor tyrosine kinases which are bound by their ligands called ephrins. They are an important set of proteins that create complexes involved in intercellular communication in development as well as cancer (Nievergall et al., 2012; Surawska et al., 2004). ADAM 10 is the cognate sheddase of ephrins and the shedding process is tightly regulated to ensure that only ephrins bound by an eph receptor is cleaved by ADAM 10. For example, ADAM 10 constitutively associates with the receptor EphA3 (figure 1.1) but does not recognise the individual proteins. The association between Ephrin A5 (ephrin) and Eph A3 (receptor) creates a new molecular recognition motif for the ADAM 10 cys-rich domain, and subsequently Ephrin A5 is cleaved in *trans*.

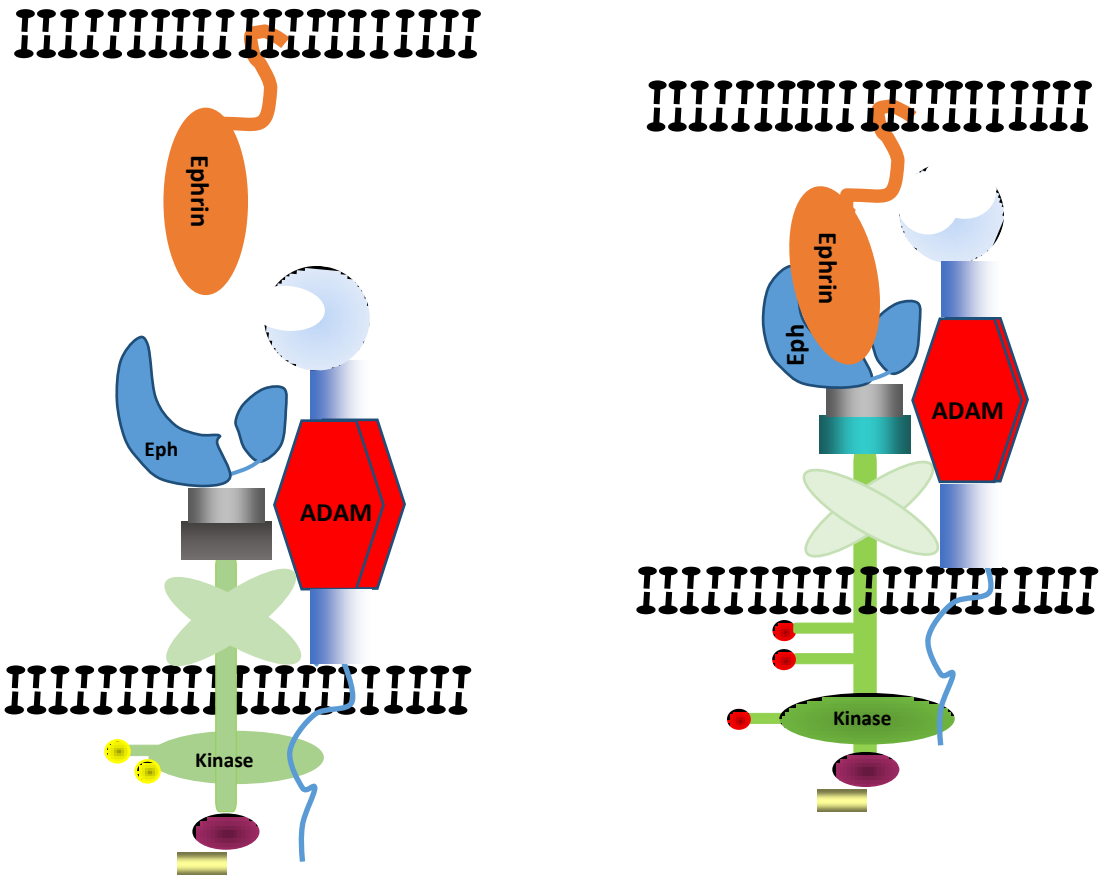

Figure 1.1: Schematic representation of the shedding of Ephrin. ADAM 10 is shown to cleave ephrin on the adjacent cell only when ephrin is bound by Eph. The kinase domains positions Eph in correct orientation to bind to ADAM 10. Mutating ADAM 10 to shorten distance to membrane, resulted in cleavage as ADAM 10 and Eph could interact as wild-type proteins (Adapted from Janes et al., 2009).

An Eph A3 juxtamembrane mutation resulted in the kinase domain being closer to the plasma membrane. This decreases the ADAM 10 interaction and consequently ephrin shedding. Mutations that extend the domain increase ephrin cleavage even if there is no kinase activity. When the Eph kinase domain is closer to the membrane shedding by wild-type ADAM 10 is inhibited. However when ADAM 10 is shortened at the cytoplasmic domain, shedding is restored. This is as a result of the steric hindrance that occurred between a truncated Eph and a full length ADAM 10, which was alleviated by the mutated ADAM 10 (figure 1.1) (Janes et al., 2009). Thus, ephrin shedding by ADAM 10 requires a

sheddase recognition motif to form via the interaction of Eph and ephrin, in conjunction with an accessible stalk region.

Epidermal growth factor receptor (EGFR) is an essential component in the progress of cell growth, development and cancer. Many EGFR ligand precursors are shed, such as amphiregulin precursor (proAREG). By means of immunoprecipitation, deletion mutants and fluorescence or confocal microscopy, its interaction with annexins was established. For example, knock-down of annexin 2 increased shedding of proAREG. In contrast, knockdowns of annexin 8 and 9 caused a decrease in shedding of proAREG. These data suggest that annexins create shedding complexes which mediate substrate selectivity by ADAMs such as ADAM 17 (Nakayama et al., 2012) and offers further evidence for sheddase recognition sites created by the protein-protein interactions between substrate, sheddase and chaperone proteins.

Many well-studied sheddase substrates have structural arrangements which enable them to regulate their processing. Collagen XVII is a type II ectoprotein with a 1008-amino acid ectodomain (Franzke et al., 2004). It has a flexible loop-like triple helical structure and studies have shown that amphipathic residues in its sheddase recognition motif direct shedding and triple helical folding. Coiled-coil heptads are motifs located within the juxtamembrane in the non-collagenous 16Å domain and are responsible for regulation of shedding (Nishie et al., 2012). Deletion studies in this region have shown that the stretch of residues 528-547 is essential for regulating shedding and folding, which in turn influences steric availability (Franzke et al., 2004). The authors propose that due to the positive net charge created in the deletion mutants, the sheddase recognition motif is abolished, as there is a negative net charge in the wild-type.

Kit ligand (KitL) is a membrane-anchored tyrosine receptor and KitL1 and 2 are shed by ADAM 17 and 19. When ADAM 19 is overexpressed it reduces ADAM 17-dependant shedding, which implies that one ADAM competes against the other. Exploration of the ectodomain to determine which domains or motifs are required for shedding indicated that the juxtamembrane of KitL2 was not required, however two non-adjacent stretches of 4 amino acids, SSTL…KAAK, were. When this motif was knocked out, shedding was abrogated

which demonstrates that these residues are secondary binding sites required for shedding (Kawaguchi et al., 2007).

1.2.3 Role of disulphide bonds and redox agents in ectodomain shedding

Many sheddases and their substrates have surface thiol groups in their extractracellular domains. It was proposed that protein disulphide isomerase (PDI) plays a regulatory role in shedding by rearranging disulfide bonds in the stalk region. On the one hand, reducing agents such as dithiothreitol (DTT) blocks shedding, whereas thiol oxidising agents, such as hydrogenperoxide (H_2O_2), increase shedding. Phenylarsine oxide (PAO) is said to be a PDI inhibitor and induces rapid shedding of L-selectin (Bennett et al., 2000). Besides the substrate L-selectin, the sheddase ADAM 17 is influenced by reducing and oxidising conditions in its cleavage of L-selection via its extracellular region, especially the highly conserved disintegrin/cysteine rich region (Wang et al., 2009).

It was suggested that PDI regulates ADAM 17 by keeping ADAM 17 in an inactive form. Down regulation of PDI by the phorbol ester PMA, which alters the redox environment, could render ADAM 17 active. Due to ADAM 17 having 16 cysteine residues, alterations in the redox environment can also result in the isomerisation of disulphide bonds, which causes conformational changes, leading to alterations in shedding. Bacitracin is a general thiol isomerase inhibitor and inclusion of this inhibitor increased only PMA-induced shedding and not constitutive shedding. Furthermore, ELISA binding studies revealed that PDI isomerises disulphide bonds in the non-catalytic domains of ADAM 17 (Willems et al., 2010).

A physiological example of this method of regulation is the activating receptor natural killer group2, D (NKG2D). Their ligands, such as the major histocompatibility complex (MHC) class I-related chain (MIC), are subject to solubilisation by ADAM 17. The soluble ligands are found in cancer sera and lead to the detrimental situation of having reduced levels of natural killer cells and cytotoxic leucocytes. The solubilisation of MICa by ADAM 17 is

dependent on ERp5, a thiol isomerase, which rearranges disulphide bonds and could be involved in the regulation of shedding (Boutet et al., 2009).

1.2.4 Cellular control of shedding via calcium/calmodulin

The shedding of L-selectin is negatively controlled by calmodulin (CaM) which binds to its cytoplasmic tail. A crystal structure of Ca^{2+}-CaM bound by a peptide mimicking the cytoplasmic tail and transmembrane domain of L-selectin illustrated their role in shedding in conjunction with calcium (Gifford et al., 2012). Similarly, CaM in its extended conformation binds a peptide consisting of the transmembrane and cytoplasmic domain of L-selectin (Deng et al., 2013). However, phosphorylation of the L-selectin cytoplasmic tail did not cause CaM to dissociate. During ADAM 17 mediated shedding of L-selectin, different parts of the protein bind and interact to regulate shedding, but CaM does not bind directly to L-selectin. In addition, certain shedding regulation was dependent on PKC signalling and others on p38 mitogen-activated protein kinase (MAPK) signalling (Killock and Ivetić, 2010). Thus, L-selectin utilises binding partners, phosphorylation and signalling to moderate its solubilisation from the membrane.

1.3 ADAMs

The ADAMs are a group of proteases that are responsible for the proteolytic release of membrane bound cytokines, growth factors and cell adhesion molecules. They are involved in a vast array of cellular functions such as immunity, development and tumour progression. ADAMs consist of metalloprotease, disintegrin, cysteine rich and EGF domains and aremembrane anchored (figure 1.2). ADAM 17 and 10 are well-characterised examples of the ADAMs group and have 50% sequence similarity within their catalytic domains. ADAM 17 was identified as responsible for cleaving the cytokine TNF-α and it also releases epidermal growth factor (EGF), transforming growth factors (TGF) and HB-EGF from the cell membrane. ADAM10 has been shown to be critical in development, Notch signaling and the

α–secretase cleavage of APP (Blobel, 2002; Deuss et al., 2008; Kuhn et al., 2010). They play a role in the pathological mechanism of disease and therefore the ADAMs are potential targets for therapeutic intervention (Saftig and Reiss, 2011).

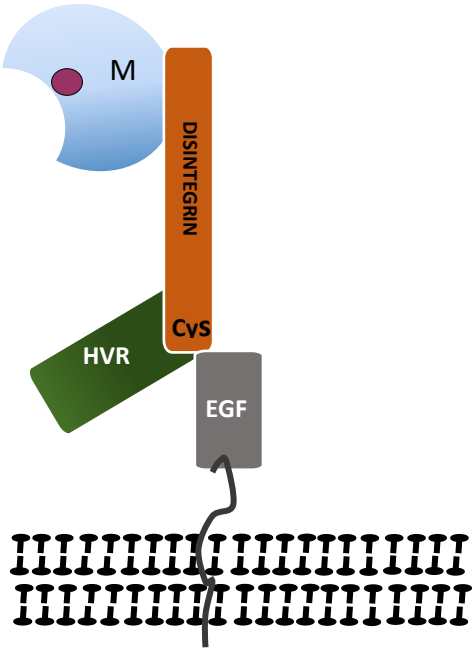

Figure 1.2: Schematic diagram of an ADAM. Blue, M-Metalloprotease, Brown, Disintegrin and Cysteine rich, Grey, EGF-epidermal growth factor, Green, HVR- hypervariable domain.

1.3.1 ADAMs as sheddases

EGFR signalling is involved in development of disease and is regulated by shedding of EGFR ligands such as TGF-α. It was shown that the intact ectodomain is required, but not the cytoplasmic domain or transmembrane domain for phorbol-stimulated cleavage of TGF-α by ADAM 17. The cleavage site of TGF-α was sufficient for PMA-dependant shedding (Le Gall et al., 2010). Similarly, ADAM 17 is responsible for the stimulated shedding of IL-6R. It was shown that when the cleavage site of Pro-TNF-α is substituted in IL-6R, it is still shed. However, when the cleavage site of IL-6R is substituted into Pro-TNF-α, no shedding occurs, suggesting that the cleavage site of Pro-TNF-α is necessary and sufficient to yield a cleavable stalk in IL6R, but not vice versa (Althoff et al., 2000).

EGFR is shed by ADAM 9, 10, 12, 15 and 17. ADAM 17 shedding of EGFR stimulation is rapid, reversible and does not require removal of a pro-domain. (Le Gall et al., 2010). A similar method of regulation is observed in prion disease. Cellular Prion protein (PrPc) is glycosylphosphatidylinisotol (GPI)-anchored and proteolytically shed by ADAM 10. Interestingly, ADAM 9 plays a role in activating ADAM 10 (Parkin and Harris, 2009), thereby involving ADAM 9 indirectly in the shedding of PrPc via ADAM 10 (Altmeppen et al., 2011; Taylor et al., 2009). In contrast, shedding via ADAM 10 of EGFR ligands is stimulated by calcium which is dependent on its cytoplasmic domain (Horiuchi et al., 2007). ADAM 10 functions as both a metalloprotease when bound to the membrane and a potential signalling molecule once cleaved by ADAM 9.

Redundancy within the shedding mechanism is widespread and often more than one sheddase is able to cleave a particular substrate. Calcium stimulation of the purinergenic receptor P2X7(P2X7R) signalling pathway activated ADAM 10 in ADAM 17-/- cells (Le Gall et al., 2009). However, ADAM 17 is the major sheddase of P2X7R as ADAM 10 inhibition had no effect on its shedding when ADAM 17 was expressed endogenously. Prolonged treatment with the ADAM 17 inhibitor SP26 resulted in knockdown of ADAM 17 and thereafter ADAM 10 became the principal sheddase of P2X7R. This interplay between ADAM 10 and 17 demonstrates the importance of ectodomain shedding and the important role it plays in cellular signalling by controlling the spatial availability of a variety of proteins (Le Gall et al., 2009). ADAM 17 and ADAM 10 also act on Desmoglein 2 and activated leucocyte cell adhesion molecules (ALCAM), which are transferrin receptors involved in cell adhesion. These sheddases have been implicated in regulating signalling pathways in tumour development, as loss of cell adhesion is an early indicator in tumour development (Bech-Serra et al., 2006).

ADAM 19 has also been identified as the sheddase of numerous substrates. Recombinant ADAM 19 was shown to cleave myelin basic protein (MBP) and insulin B chain (Chesneau et al., 2003). It is sensitive to the hydroxamate class of inhibitor batimastat (BB94) but not to tissue inhibitor of metalloproteinases (TIMPs) 1 and 3. Overexpression of ADAM 19 in COS7

cells increased shedding of TNF-related activation-induced cytokine (TRANCE) and is a negative regulator of KL-1 in mouse embryonic fibroblasts (Chesneau et al., 2003). ADAM 19 is activated by lipopolysaccharides (LPS) as opposed to PMA and has autocatalytic processing activity in its cysteine domain (Tanabe et al., 2010). An increase in ADAM 19 expression is involved in cancers, inflammation, and fibrosis of the lung and kidney. Therefore, it may be targeted for cell specific inhibition in some tumours (Qi et al., 2009).

1.3.2 The contribution of secondary substrate binding site (exosite) interactions of ADAMs

Vascular apoptosis-inducing protein (VAP) 1 is a snake venom metalloproteinase (SVMP) and a structural analogue of ADAMs. It has a MDC structure similar to ADAMs consisting of a metalloprotease domain (M-domain), a disintegrin domain and a cysteine rich domain (C-domain). A crystal structure of VAP1 showed that the M-domain does not create stable dimers and has calcium binding sites opposite the active cleft (Takeda et al., 2006). The distintegrin domain is structured like a C-shaped arm, where the “shoulder” portion has 3 disulphide bonds and the “arm” portion has 3 disulphide bonds. Together, the calcium binding and disulphide bonds provide a stabilising function. The C-domain consists of the C–hand and C-wrist, but none of these structures are amenable to binding other proteins. The hypervariable region (HVR) points toward the catalytic site and is stabilised by a hydrogen bond network. It is said to be the region that takes part in the secondary engagement or binding with the substrate and is the most divergent part of the structure (figure 1.3) (Takeda et al., 2012, 2006).

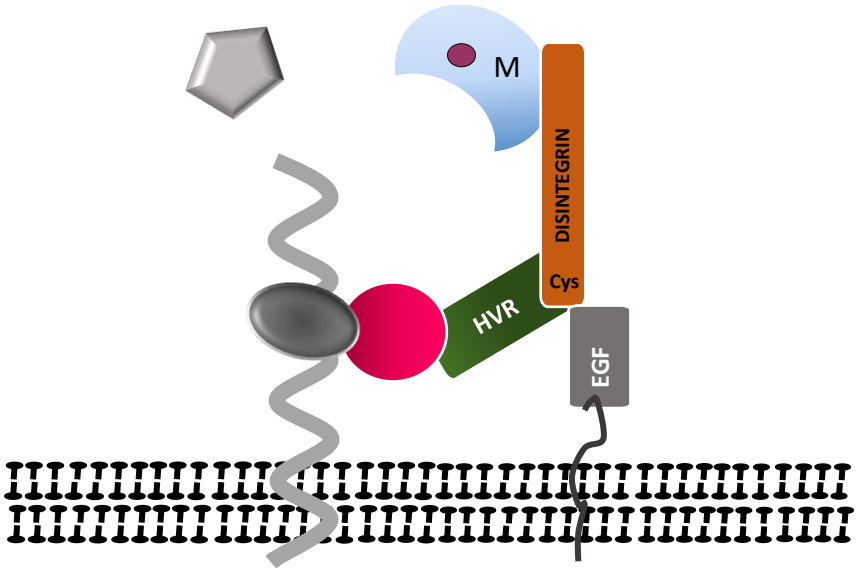

Figure 1.3: Proposed model of HVR binding indirectly to the substrate (grey) via a chaperone protein (red). (Adapted from Takeda et al., 2010).

The crystal structure of ADAMTS-13, which cleaves von Willebrand factors involved in thrombosis, has multiple exosites in non-catalytic domains to recognise its substrates (Akiyama et al., 2009). Mutational analysis proved that particular residues in the HVR loop of ADAMTS-13 was essential for cleavage secretion of von Willebrand factors (Takeda et al., 2006). Similarly, ADAM 12; a sheddase implicated in cancer; was proven to be regulated by non-catalytic domains possibly via its EGF loop (Kveiborg et al., 2010). This demonstrates that ADAMs are regulated by domains outside of their catalytic domains and that the HVR domain is structurally adept at providing such a site.

1.3.3 Cellular trafficking of ADAMs

ADAM 17 needs to be processed to its mature form by furin and the proprotein convertase PC7 (Althoff et al., 2001; Peiretti et al., 2003). However, addition of PMA, which increases ADAM 17 shedding, decreased the maturation of ADAM 17. It does not activate furin activity, indicating that PMA does not increase shedding via activation of ADAM 17 (Endres et al., 2003). CHO-K1 cells defective in ectodomain shedding, had ADAM 17 remain in its inactive form and did not have its prodomain removed. This was not due to lack of furin activity, as zinc metalloproteases were processed normally in these cells. Instead, ADAM 17

inactivity was due to its inability of ADAM 17 to exit the endoplastic reticulum (ER) (Borroto et al., 2003).

Furthermore, it was found that ADAMs are trafficked through the ER and cell signalling via their interaction with catalytically inactive pseudoproteases called rhomboids (Zettl et al., 2011). An important member of this family of intramembrane proteins is iRhom2, which binds ADAM 17 and promotes exit from the ER. If no iRhom2 binds to ADAM 17, it does not exit from the ER and furin activation of ADAM 17 is prevented. Therefore ADAM 17 does not reach the cell surface in a mature and active form (Adrain et al., 2012). A functional example of iRhom2's role in ADAM 17 maturation is its vital role in LPS-stimulated shedding of TNF-α. It was shown that iRhom2 plays a role in ADAM 17 maturation using TNF-α levels in serum as an indication of how the immune system responds to it (McIlwain et al., 2012). Physiologically, ADAM 17 regulates TNF-α dependant diseases such as rheumatoid arthritis and aids in the protection of the skin and the intestinal barrier. Inactivation of the iRhom2 gene, resulted in the disruption of immune cell function (Issuree et al., 2013). This process of arresting the ADAM 17 maturation in the ER, is another regulatory mechanism of shedding.

1.3.4 Use of synthetic peptides in the characterisation of ADAMs in ectodomain shedding

To enable high throughput analysis of proteases and their substrates, soluble synthetic peptides were synthesised and the peptide sequences mimic the region that is cleaved by the protease. Fluorogenic peptides contain groups that fluoresce and have been routinely used as substrates in the development of assays to characterise proteases. Commonly used nomenclature for denoting the residues in the peptide substrate is P1-P2-P3-…Pn on the N-terminal side of the cleavage site scissile bond. Similarly, the C-terminal residues are assigned P1'-P2'-P3'-…Pn (Schechter and Berger, 1967).

Through the analysis of 10 fluorogenic peptides of TNF- α, it was found that ADAM 17 prefers hydrophobic residues at the P1' site such as V, L and I (Table 1.1) . In many of the peptides secondary cleavage products were also identified. Even though ADAM 17 prefers the physiological A-V cleavage site (Black et al., 1997), its substrate specificity is not limited

to this site and may tolerate alternative hydrophobic residues mainly in the P1' position. (Jin et al., 2002).

Table 1.1: Cleavage of fluorogenic peptides by ADAM 17. 10 nM of enzyme was incubated with 50 µM of each peptide in a buffer of 50 mM Tris, pH 7.4, 25 mM NaCl, and 4% glycerol. The reaction was monitored by fluorescence and HPLC. The reaction was terminated after 140 min and percentage cleavage was determined by HPLC using A220 nm (Adapted from Jin et al., 2002).

Peptide	**P1 and P1' residues**	**% Cleavage**
Abz-LAQAVRSSSR-Dpa	AV	90%
Abz-LAQALRSSSR-Dpa	AL	92%
Abz-LAQAIRSSSR-Dpa	AI	66%
Abz-LAQAFRSSSR-Dpa	AF	22%
Abz-LAQFVRSSSR-Dpa	QF	39%
Abz-LAQLVRSSSR-Dpa	QL	34%
Abz-LAQGVRSSSR-Dpa	GV	11%
Abz-LAQVARSSSR-Dpa	AR	19%
Abz-LAQdAVRSSSR-Dpa	dAV	0%

In ADAM 17-expressing cells, only PMA-stimulated cells were able to cleave the TNF-α peptide (Dnp-SPLAQ**AV**RSSSR-NH_2). Moreover, PMA does not increase the expression of ADAM 17, it only increases its activity. Interestingly, the comparison of peptide hydrolysis by the recombinant ADAM 17 and cell lysate, showed that considerably less product was generated using cell lysate (Doedens et al., 2003).

This agrees with the study by Becker et al. (2002) where cleavage of fluorogenic and non-flurogenic TNF-α peptides were analysed with recombinant human ADAM 17 as well as cells endogenously expressing ADAM 17. Cleavage by recombinant ADAM 17 was TAPI-2 inhibitable. In contrast, incubation with HUVEC cells, a human mast cell line-1 (HMC-1) and peripheral blood lymphocytes (PBL) for 1 hour resulted in only 50% peptide reduction and after 24 hours there was no peptide remaining. No specific cleavage products were

identified and stimulation or inhibition by TAPI-2 was not observed (Becker et al., 2002). On the other hand, cleavage was inhibited by an inhibitor cocktail and metalloprotease inhibitor ortho-phenanthroline. HMC-1 in suspension could cleave the fluorogenic peptides but no TAPI-2 inhibition was seen. This clearly indicates that the cleavage of the peptide may differ significantly. This is dependent on whether a purified recombinant protein or a cell lysate with endogenous levels of the enzyme of interest is used.

Peptide mimetics corresponding to the stalk of MBP revealed that ADAM 8 cleaved the peptide TTHYGSLPQKAQGQ at the P-Q site (Schlomann et al., 2002). To find additional substrates for ADAM 8, 10-mer peptides based on extracellular domains of various membrane proteins were synthesised and exposed to soluble ADAM 8 purified from E.coli (figure 1.4). Fourteen out of 34 peptides were cleaved and some were derived from peptides involved in inflammation and neurodegeneration proteins e.g. APP. MBP variants were also synthesised with substitutions in their P1,P1', P2' and P3' sites, although ADAM 8 cleaved these peptides at different efficiencies (Naus et al., 2006). This extensive study demonstrates that basic residues at P1 such as R and K increase cleavage (figure 1.4) (peptide 3 and 4), implying that ADAM 8 has a relaxed sequence specificity at P1 and is less tolerant of changes in P1'.

Position		P5	P4	P3	P2	P1 ↓	P1'	P2'	P3'	P4'	P5'
wild type MBP	1	Y	G	S	L	P	Q	K	A	Q	G
MBP variants	2	Y	G	**L**	L	P	Q	K	A	Q	G
	3	Y	G	S	L	**R**	Q	K	A	Q	G
	4	Y	G	S	L	**K**	Q	K	A	Q	G
	5	Y	G	S	L	P	**E**	K	A	Q	G
	6	Y	G	S	L	P	Q	**E**	A	Q	G
	7	Y	G	S	L	P	Q	**V**	A	Q	G
	8	Y	G	S	L	P	Q	K	**T**	Q	G

Figure 1.4: Cleavage site mutations of MBP peptides. R or K substitution in P1 increases shedding. Mutations in P1' and P2' decreases shedding considerably. Adapted from Naus et al., 2006.

An ADAM 33 substrate profile was determined in a similar manner. It was found that a 10-residue APP peptide (YEVHHQKLVF) was also cleaved by ADAM 33 but at a non-physiological site of H^{14}-Q^{15}. However a KitL peptide was cleaved by ADAM 33 at its physiological site (Zou et al., 2004). The most stringent residues for cleaving the APP substrate (YEVHHQKLVF) were V at P3, Ala at P2 and Q at P1. Changing H at P2 increased cleavage by ADAM 33. It was also found that the minimal length of the peptide for cleavage to occur was 9 residues.

To try and uncover potential substrates for ADAM 8 and ADAM 15, peptide libraries were employed. This method proved unsuccessful for ADAM 15 and only with the overexpression of ADAM 15 could a substrate be identified. ADAM 15 was not stimulated by PMA or Ca^{2+} ionophores but was inhibited by TAPI-2, GM6001 and TIMP3 (Maretzky et al., 2009). This demonstrates that soluble fluorogenic substrates are not always amenable to hydrolysis by recombinant proteases and the characterisation of ADAM 15 could only be achieved via overexpression studies.

To fine map the active site requirements for recognition by ADAM 17 and ADAM 10, peptide libraries were once again utilised. The main differences between these sheddases, lie within their preference for certain residues of the P1' position of the substrate. It was shown that ADAM 17 prefers aliphatic hydrophobic residues whereas ADAM 10 prefers larger residues such as leucine (Krstenansky et al., 2004). Furthermore, ADAM 17 and ADAM 10 select hydrophobic residues at the P1' site, basic and aliphatic residues at P2' site and small residues at the P3'site. ADAM 17 and ADAM 10 are the most selective at the P1' site. ADAM 17 prefers a hydrophobic residues such as V and ADAM 10 prefers L which is much larger. Selectivity of substrates could be determined more by the residues around the cleavage site than by the cleavage motif itself (Caescu et al., 2009).

1.4 ACE

Angiotensin-converting enzyme (ACE) is a vital component of the renin-angiotensin system (RAS) and its most established role is in blood pressure regulation via its dicarboxypeptidase activity. It cleaves the decapeptide angiotensin I (Ang I) to produce the octapeptide

angiotensin II (Ang II), a potent vasoconstrictor, resulting in an increase in blood pressure (figure 1.5) (Skeggs et al., 1956; Yang et al., 1970). It also cleaves and inactivates bradykinin, a vasodilator. It is for these reasons that ACE is a major drug target in hypertensive patients. ACE has numerous other substrates, such as the APP peptide Aβ-42 and Acetyl-SDKP, an antifibrotic agent (Douglas et al., 2013) proving important with respect to ACE inhibition and its peripheral effects.

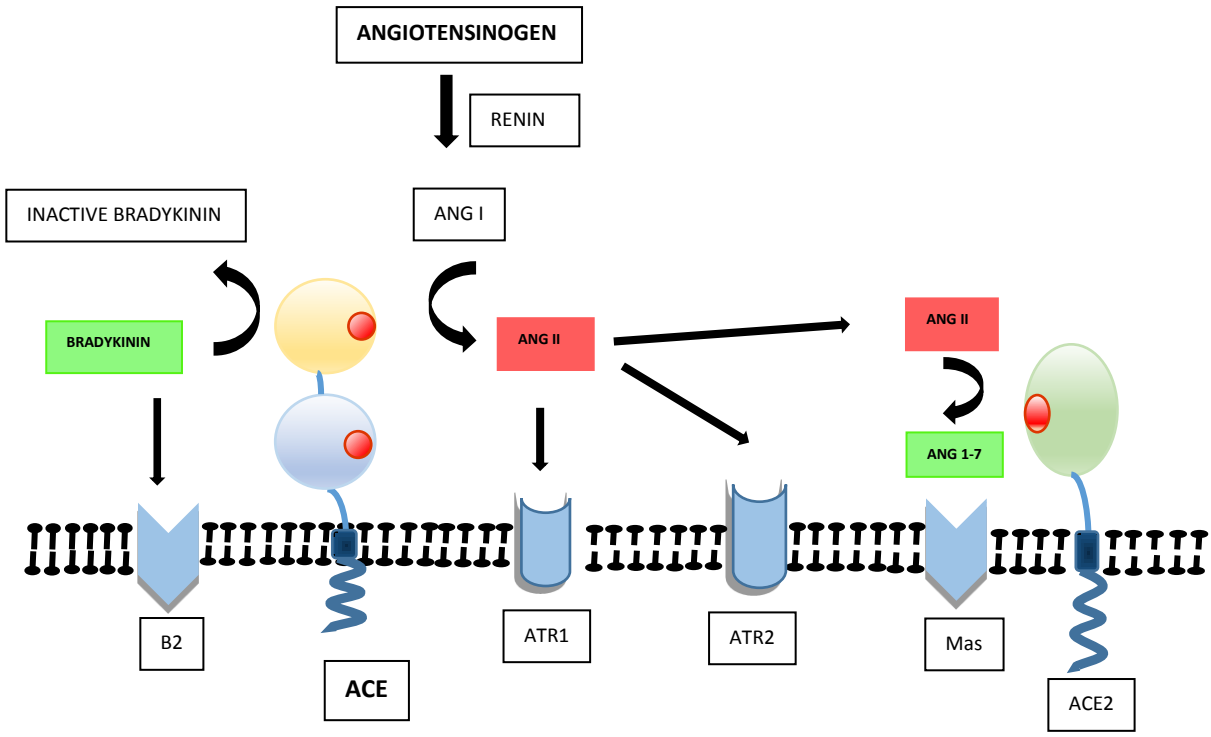

Figure 1.5: Renin angiotensin aldosterone system (RAAS). Simplified schematic to highlight the most important elements of the system. ACE is represented as the double domain membrane anchored protein. The red circles represent the catalytic sites. Ang II binds to the AT1 receptor (AT1R) and results in vasoconstriction (pink). Ang 1-7 and bradykinin both lead to vasodilation (green). The ACE homologue, ACE2, cleaves Ang II to Ang 1-7, promoting vasodilatory parameters.

ACE 2 is single domain homologue of ACE, which produces Ang 1-7. These peptides are vasodilatory and act against the effects of the vasoconstrictor Ang II (Donoghue et al., 2000; Guy et al., 2005). Interestingly, ACE2 was shown to be the functional receptor of the severe acute respiratory syndrome (SARS) coronavirus, which causes a potentially lethal lung infection (Kuba et al., 2005; Wong et al., 2004).

ACE is a highly glycosylated zinc metalloprotease and type I membrane-bound ectoprotein. It consists of two extracellular domains, the N- and C-domain, is attached to the

transmembrane domain by a stalk region and has a short cytoplasmic domain (Alhenc-Gélas et al., 1989). There are two forms of ACE that we will mainly refer to, somatic and testis ACE. Somatic ACE (sACE) consists of the N- and C-domains (Soubrier et al., 1988), whereas testis ACE (tACE) consists only of the C-domain. These are transcribed from the same gene off two different promoters (Hubert et al., 1991; Lattion et al., 1989). Both domains are catalytically active (Soubrier et al., 1988; Wei et al., 1992, 1991a), yet the N- and C- domains have varying inhibitor binding profiles, due to their active sites differing slightly in structure (Nchinda et al., 2006; Watermeyer et al., 2010). To aid in the design of domain-selective inhibitors, the crystal structure of tACE was resolved (Natesh et al., 2003), assessing the key residues participating in ACE activity. Based on this information, inhibitors may be more specifically designed to bring about higher potency with fewer side-effects.

Glycosylation disrupts the crystallisation of protein for x-ray diffraction, therefore minimally glycosylated mutants aid in the crystallisation and structure-function analysis of ACE. It was found that there are seven glycosylation sites in tACE: three are fully glycosylated, three are partially glycosylated and one site (N^{620}) is not glycosylated at all. Testis ACE expressed in the presence of glycosidase inhibitor, NBDNJ, was still fully active, indicating that glycosylation of tACE is not essential for its activity (Yu et al., 1997). More recently, the structure of a minimally glycosylated N-domain mutant was resolved with only sites three, eight and nine available for glycosylation as opposed to the usual eight. It was crystallised with the N-domain selective inhibitor RXP407 (Anthony et al., 2010). The full sACE structure has not been determined, but the C-domain in sACE has been shown to be less dependent on glycosylation than tACE. This is said to be due to the N-domain having stabilising effects on the C-domain within sACE (O'Neill et al., 2008).

Both ACE isoforms undergo cleavage secretion (Ehlers et al., 1997; Wei et al., 1991b) and are shed from the membrane by a sheddase that cleaves within the stalk region. The as yet unknown sheddase has been shown to be a zinc (Zn) metalloprotease, known to be stimulated by phorbol esters and inhibited by hydroxamates. Testis ACE is cleaved more efficiently than somatic ACE. It is therefore imperative to understand the complex structure/function relationships of ACE, and investigate how the posttranslational

mechanisms contribute to other physiological processes in addition to its classical role in Ang I conversion.

1.4.1 Beyond the RAS

ACE has numerous roles besides its dicarboxypeptidase activity. It is perhaps through the suppression of these alternative pathways that the numerous side effects of ACE inhibitors are mediated.

1.4.1.1 Signalling

Casein kinase 2 (CK2) phosphorylates the cytoplasmic tail of ACE at S^{1270} and sets in motion a signalling cascade via mitogen-activated protein kinase (MAPK) and c-Jun N-terminal kinases (JNK). This signalling cascade brings about an increase in ACE expression (Kohlstedt et al., 2002) and incubation with ACE inhibitors has also been linked to the increase in this signalling response (Kohlstedt et al., 2004). Phosphorylation of ACE as well as dimerisation are induced by inhibitors, which could have far reaching physiological impacts and could influence the unknown effects that are related to ACE inhibitors (Fleming, 2006; Fleming et al., 2005).

1.4.1.2 Fertility

Testis ACE or germinal ACE, is essential to male fertility (Fuchs et al., 2005; Kondoh et al., 2005). Kondoh et al., (2005) have previously reported that ACE sheds other GPI-anchored proteins, which are required for fertilization (Kondoh et al., 2009). Furthermore, sperm which expressed a GPI-anchored fluorescent protein and solubilised by ACE, was shown to acquire fertility after the acrosome reaction, an essential step in fertilization. (Watanabe and Kondoh, 2011). This is in agreement with the study that used the monoclonal antibodies 1E10 and 4E3 to identify tACE on sperm and it was shown to be on the post-acrosomal region (Nikolaeva et al., 2006). More recently, the GPI-anchored protein, TEX101, was shown to be regulated by ACE and is currently under further investigation as a mechanism to control male fertility (Fujihara et al., 2013).

1.4.1.3 Amyloid as a substrate

Accumulation of the Aβ 42 peptide, a product of APP cleavage, is believed to contribute to plaque formation in the brain leading to neurodegeneration implicated in Alzheimer's disease (AD). The Aβ 40 peptide has a protective role in AD and reduces plaque deposition. ACE converts Aβ 42 to Aβ40, and ACE inhibition has been shown to increase Aβ 42 deposition and lower the protective effects of Aβ 40 (Zou et al., 2007). The N-domain of ACE has been shown to degrade the Aβ peptide to Aβ 40 more effectively than the C-domain (Oba et al., 2005; Zou et al., 2009). However, another study conducted in CHO-K1 and HEK cells found that both domains of ACE degraded Aβ 40 and Aβ 42 similarly. Morerover, inhibition with the non-selective ACE inhibitor captopril showed an accumulation of Aβ peptides (Hemming and Selkoe, 2005). This supports the need for C-domain selective ACE inhibition and will allow the N-domain catalytic site to be free to degrade the Aβ 42 peptide to the neuro-protective Aβ 40.

1.5 ACE ectodomain shedding

ACE has been shown to undergo regulated proteolytic release of its ectodomain into the extracellular environment, however the physiological relevance for its shedding is unknown. The differences between tACE and sACE are critical as a large proportion of ACE research has been dedicated to the regulation of shedding by delineating the regions of ACE and how they impact the modulation of shedding.

Soluble endothelial ACE was found in serum and it was suggested that ACE could be used as a model to study its associated sheddase. Through the characterisation of tACE expressed in CHO –K1 cells, a soluble form of the enzyme in the medium as well as a membrane-anchored form was discovered (Ehlers et al., 1991a, 1991b). The removal of the first 36 residues of tACE, which is S/T rich and heavily O-glycosylated, did not affect activity or stability (Ehlers et al., 1992). The addition of the phorbol ester phorbol-12,13-dibutyrate (PDBu), increased the level of soluble ACE nearly 50-fold and possibly via the PKC mechanism, as a PKC inhibitor diminished the phorbol-induced shedding (Ehlers et al., 1995). To characterise the regulation and shedding of rabbit tACE, it was transfected into mouse epithelial cells. They found that it accumulates at the cell surface and is then cleaved

off at a slow rate. The phorbol ester PMA stimulated shedding, but not directly through the PKC machinery as PKC inhibitors did not inhibit shedding (Ramchandran et al., 1994). This suggests that other mechanisms are at play to stimulate shedding. Therefore rabbit tACE and human tACE undergo stimulated shedding via different mechanisms.

1.5.1. The effect of the cytoplasmic domain

The characterisation of the ACE tACE mutant with the cytoplasmic domain deleted displayed no phorbol effect, however TAPI decreased shedding (indicating a similar sheddase to wild-type). Addition of cytochalasin D increased basal shedding of wild-type ACE, with little effect on ACEΔCYT. This suggests that the cytoplasmic domain of ACE interacts with actin cytoskeleton. It suggested that there are inhibitory proteins that negatively regulates shedding via the cytoplasmic tail (Chubb et al., 2004).

ACE is serine phosphorylated at S^{730} (tACE numbering) which is situated on the cytoplasmic tail. A CaM inhibitor and CaM kinase inhibitor increased shedding which implicates CaM as associating with the cytoplasmic tail. When S^{730} was mutated to alanine it was not phosphorylated, but was still bound by CaM (Chattopadhyay et al., 2005). Calmodulin therefore regulates shedding of membrane proteins. In an attempt to determine how signalling occurs via ACE, the phosphorylated serine at 1270 (sACE numbering, equivalent to S^{730}) was mutated to an alanine. The resultant loss in phosphorylation of S^{1270}A increased the rate of shedding of ACE, in a similar manner to ACEΔCYT. The addition of cytochalasin D disrupted the association with non-muscle myosin heavy chain 9 (MYH9) (Kohlstedt et al., 2006b). These data demonstrate that the cytoplasmic tail plays an important role in regulating ACE shedding and demonstrates the possible mechanism by which signalling is controlled.

1.5.2 The role of the juxtamembrane stalk

Deletions in the juxtamembrane stalk were made to ascertain its level of involvement in shedding. ACE JM-Δ17 resulted in a 12-fold increase in shedding, ACE JM-Δ24 a 17-fold decrease in shedding and ACE JM-Δ47 was not active and incorrectly processed to the cell membrane (Table 1.2). ACE JMLDL, a mutant where the stalk was replaced with that of the stalk of low density lipoprotein receptor was also cleaved 15 or 17 residues from the

membrane. Wild-type cleavage (as well as ACE JM-Δ24) was shown to occur at the R^{627}-S bond, 24 residues from the membrane. ACE JM-Δ17 was cleaved 10 residues from the membrane (Table 1.2). This suggests that the sheddase requires a minimum of 10 residues in the stalk for cleavage to occur. Significantly, purified full length ACE is not cleaved by CHO-K1 fractions as the sheddase needs the protein to be embedded in membrane (Ehlers et al., 1996). In addition, solubilised ACE 89 cells (which cleave transfected rabbit tACE) and rabbit lung homogenate did not cleave tACE in solution, again suggesting a requirement for ACE to be anchored in the membrane (Sadhukhan et al., 1999). Furthermore, a Triton-X- 100 solubilised pig kidney sheddase preparation did not solubilise ACE, implicating the need for ACE and its sheddase to be anchored in the membrane (Parvathy et al., 1997).

Table 1.2: Effect of deletions in the juxtamembrane stalk region of tACE (Ehlers et al., 1997, 1996).

Mutant	Shedding	Cleavage site/distance from membrane
ACE JM-Δ17	12-fold increase	R^{627}/10 residues from membrane
ACE JM-Δ24	17-fold increase	R^{627}/24 residues from membrane
ACE JM-Δ47	No shedding, no activity	
ACE JMLDL	Yes	A^{628}/15-17 residues from membrane

Many secreted ectoproteins possess a specific sequence that is preferred by its sheddase, as is the case in Pro-TNF-α, which is cleaved preferentially at an A-V site (Althoff et al., 2001; Jin et al., 2002). The determination of the ACE cleavage site was essential in learning more about the shedding requirements of the sheddase.

The cleavage of rabbit ACE occurs between R^{663} and S^{664}, similar to human ACE (Ramchandran et al., 1994). Two cleavage sites were found in mouse and ACE shedding in yeast was inhibited by the hydroxamate inhibitor compound 3 (Sadhukhan et al., 1996). tACE expressed in E.coli was underglycosylated and inactive, and a mutant with five of the N-linked glycosylation sites mutated was inactive and degraded. However, the same mutant expressed in yeast was active (Sadhukhan and Sen, 1996). This suggests that ACE is susceptible to varying expression conditions and cleavage sites may differ.

The cleavage site of human sACE was mapped to R^{1203}-S^{1204} which is 24 residues proximal to the membrane anchoring domain. Trypsin cleaved at the same site and hydroxamate inhibitors showed that ADAM 17 was not involved in constitutive or regulated cleavage of ACE (Hooper and Turner, 2000). This is in agreement with the cleavage site found in human tACE as well as sACE (Woodman et al., 2000). An important finding in this study was that tACE is shed at a much higher rate than sACE, even though they are cleaved at identical sites in the stalk and confirmed the observation that the N-domain of sACE negatively regulates its shedding (Beldent et al., 1995). The initial data accumulated about the ACE sheddase was that it did not require a specific cleavage site sequence, but preferred cleavage after an R or K residue. From these early investigations the ACE sheddase was revealed to be sensitive to protease inhibitors and is inducible.

To investigate whether the ACE sheddase prefers an open, unfolded stalk, an EGF-like domain was introduced into the stalk region of ACE. This mutant was poorly processed and shedding was reduced. However, a phorbol response was still evident. Interestingly, the cleaved protein remained on the cell surface as it was still attached to the stalk via disulphide bonds. The protein was cleaved at the G^{652}-F^{653}, 11 residues proximal to the transmembrane domain (Schwager et al., 1998).

Glycosylation could change the conformation and accessibility of the stalk. To test this theory, serine/threonin(S/T) rich regions (for O-glycosylation) were introduced in the stalk. This mutant, called JGL had increased basal shedding but reduced phorbol shedding. Therefore a modulation of shedding was seen, but not abrogation and the cleavage site shifted to 14 residues from the membrane. Introduction of an N-linked glycan by deleting 6 residues N-terminal from the cleavage site resulted in a cleavage site at the F^{640}-L^{641}, which is C-terminal to the endogenous R^{627}-S^{628}. This shift in cleavage site was probably due to this new glycosylation site as other deletion mutants' cleavage sites were not altered. Removing the S/T region from the N-terminus of tACE did not affect shedding or the cleavage site (Schwager et al., 1999). A further study into the effect of disulphides in the stalk region of ACE revealed that a mutant with the EGF domain of factor IX, (ACE-JMfIX) was only sensitive to DCI and resistant to the effects of PDBu and TAPI. These studies highlight the previous efforts taken to define the involvement of the stalk region to the regulation of tACE

shedding. It is clear that the disulphide bonds and glycosylation modulates shedding and at times shifts the cleavage site. Nevertheless, cleavage still occurs despite the alterations to the stalk region.

In an attempt to determine the boundaries of the tACE ectodomain, sequentially longer deletions of the N and C-termini of tACE were made (Chubb et al., 2002). A mutation between D^{40} and E^{61} (ACE-Δ59) abolished shedding as well as enzymatic activity, suggesting that this region was critical for correct folding of the enzyme and not that it was necessarily involved in the regulation of shedding. D^{40} is the first conserved residue between N and C-domain. ACE-Δ 16 had 16 residues N-terminal of the cleavage site deleted (T^{605}- N^{620}) and this rendered this protein inactive in the cell lysate and no activity or protein was present in the medium. ACE-Δ 11 had residues W^{616}- A^{626} deleted, which caused lowered activity but shedding still occurred. These mutants gave us great insight into the involvement of the juxtamembrane stalk region and proximal ectodomain on the processing and stability of ACE. Thus, Chubb et al. (2002) proposed that the C-terminal boundary of the ectodomain occurred between T^{605}-W^{616}.

1.5.3 The contribution of the ACE ectodomain

In an effort to understand the role of the ectodomain of ACE in shedding, Beldent et al. (1995) investigated the shedding rates of somatic ACE versus a truncated form that consisted only of the C-domain. They noted that the form lacking the N-domain was shed 10-fold more efficiently than the two domain form which is in agreement with the findings of Woodman et al. (2000). They went on to establish that cleavage occurred at the cell membrane and not at the endoplasmic reticulum. This study suggested that the N-domain negatively regulates ACE shedding. Cleavage site of ACE CF (C-domain only) was mapped to R^{1227}-V^{1228} (Beldent et al., 1995).

Rabbit tACE has a major (R^{663}-S^{664}) and minor cleavage site, the former mimicking the endogenous cleavage site found in human ACE. Furthermore, rabbit tACE shedding is sensitive to the hydroxamate-based inhibitor Compound 3 indicating that a metalloprotease is responsible for its shedding (Sadhukhan et al., 1996). Sadhukhan et al. (1998) carried out

an extensive study on rabbit testis ACE to tease out which regions of ACE augments the shedding process. They made swop-over chimeric proteins consisting of different permutations of the ACE stalk or ectodomain with the stalk or ectodomain of CD4, which is usually not cleaved. The chimeric protein which consisted of the ACE ectodomain with the juxtamembrane stalk, transmembrane domain (TM) and cytoplasmic domain of CD4 was cleaved efficiently. ACE deletion mutants were used to determine which region of the ectodomain is responsible. The chimeric protein required residues 1-655 of ACE for shedding to occur and 62 residues of the C-terminal of CD4.

tACE 1-691/CD4-1 which has the full length ACE ectodomain is shed at 95%, tACE1-655/CD4-3 has a reduced ACE ectodomain and a CD4 stalk region of 22 residues. This reduces shedding, but increasing the CD4 stalk to 42 residues, increases shedding. Sixty-two residues of the CD4 stalk in conjunction with residues 1-655 of the ACE ectodomain allows shedding to occur at 99 % (figure 1.6). This once again alludes to a theory that an accessible stalk length is required and that a particular structure created by certain ectodomains and stalk regions results in cleavable proteins.

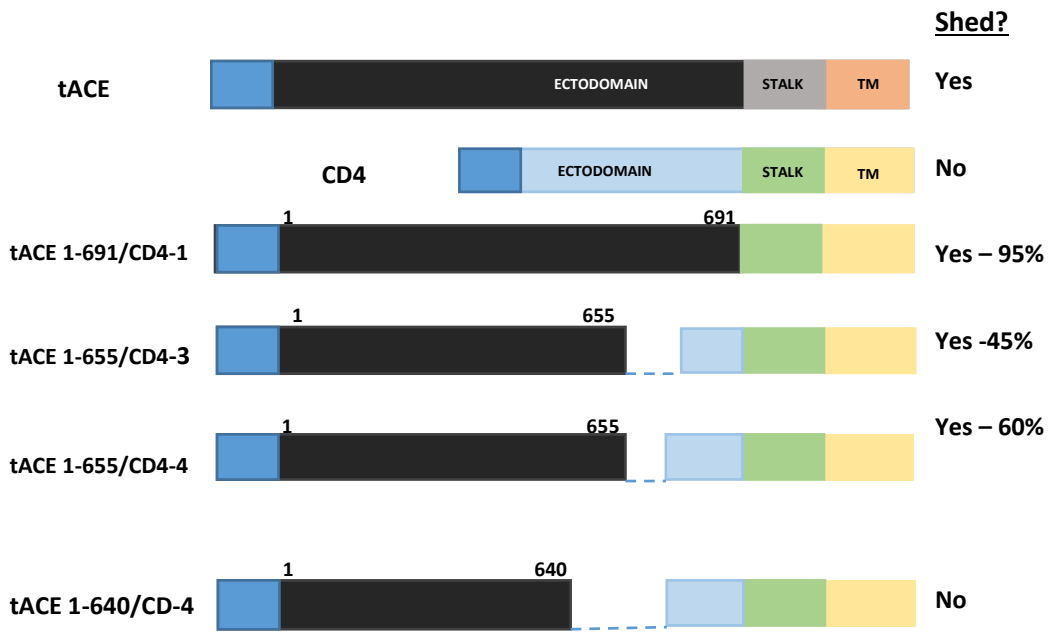

Figure 1.6: ACE/CD4 constructs. Swop-over constructs showing most important constructs. Adapted from Sadhukhan et al., (1998) and Chattopadhay et al., (2008).

The region in the ectodomain of ACE proximal to the stalk region said to direct cleavage secretion was fine-mapped via alanine mutagenesis (Sadhukhan et al., 1998). A five residue motif was shown to be vital for the cleavage of rabbit tACE (Chattopadhyay et al., 2008). This provides definitive evidence that shedding of ACE not only requires the availability of a suitable cleavage site, sufficient stalk length and membrane anchorage, but also a specific secondary binding site for the candidate sheddase.

To further investigate the roles of the stalk and extracellular domain of ACE in shedding, Pang et al. (2001) replaced the GPI anchor of membrane dipeptidase (MDP), which is not usually shed, with the ACE stalk and transmembrane region (Pang et al., 2001). MDP-STM was shed, but the MDP-TM chimera with no stalk was not, suggesting that the juxtamembrane stalk is critically important for shedding. Importantly, another construct comprising of N-domain fused to the stalk and TM (i.e. Δ C) was not shed, but was active at the cell surface (Pang et al., 2001)indicating that a sheddase recognition motif (RM) within the C-domain is an essential requirement for shedding. This supports the hypothesis that the overall structure of the ectodomain, stalk and transmembrane domain combination results in a conformation that allows access for the sheddase to cleave the stalk (Deng et al., 1998).

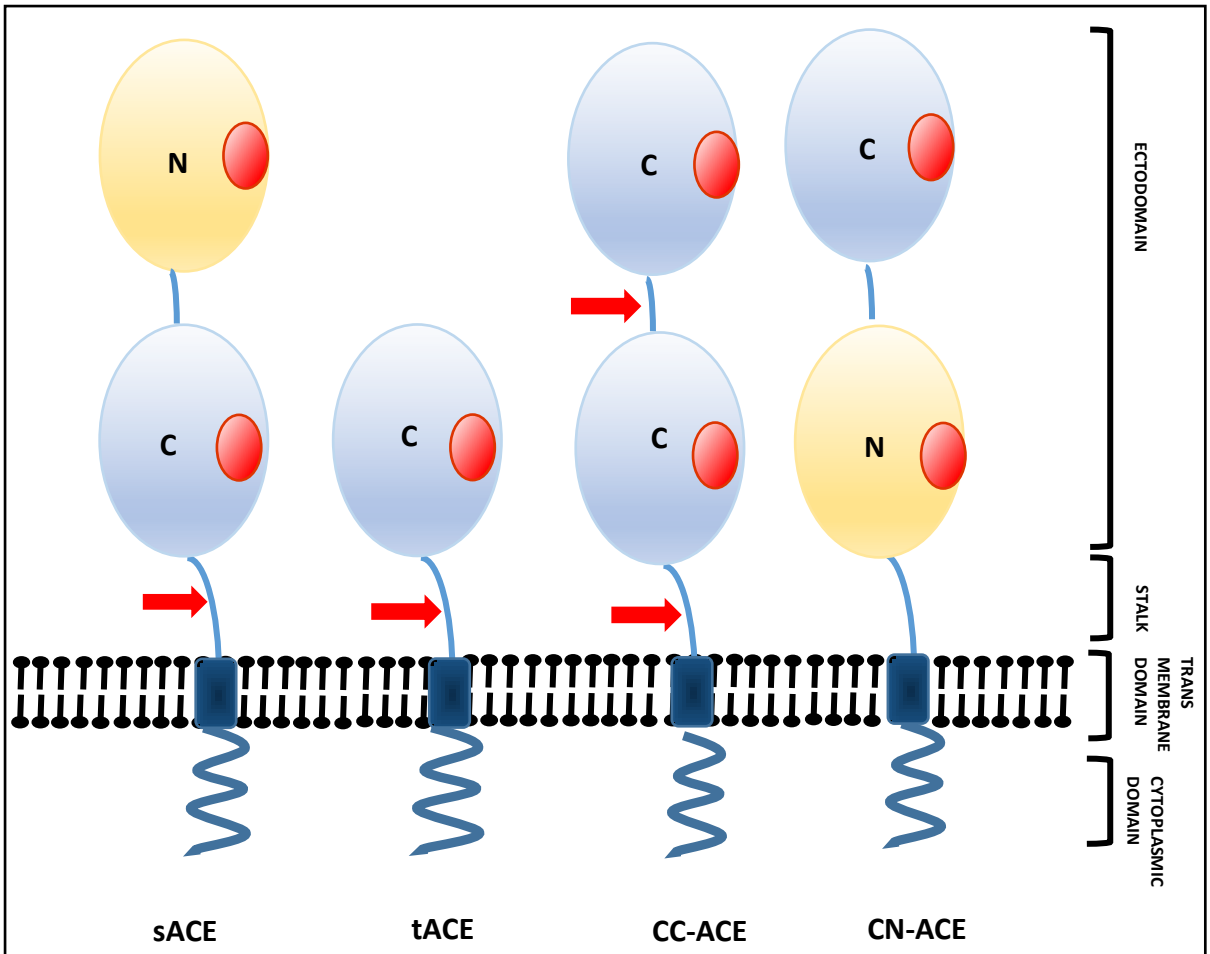

Figure 1.7: ACE isoforms and mutant constructs. Representative figure of ACE isoforms, viz, sACE and tACE highlighting the N- (yellow) and C-domain (blue) in sACE and the single C-domain in tACE. The catalytic site is represented in red. The swop-over constructs are shown alongside it. Red arrows indicate the site of cleavage (Woodman et al., 2005).

Based on the knowledge that tACE is shed more efficiently than sACE (Woodman et al., 2000), the N-domain negatively regulates shedding (Beldent et al., 1995) and that the ACE ectodomain elicits shedding of non-shed proteins (Pang et al., 2001; Sadhukhan et al., 1998), N- and C-domain swop-over mutants were constructed to determine if shedding was regulated by merely the presence of two domains, or whether the N-domain occludes a sheddase recognition domain in the C-domain (figure 1.7). The construct with the C-domain fused to the N-terminus of the N-domain (CN-ACE) was not shed (Woodman et al., 2005). The CC-ACE, which had two C-domains attached by the linker region, was cleaved off the membrane at the stalk as well in the linker region. This suggests that the C-domain contains a motif that could direct the sheddase to cleave within the linker as well as the stalk. It was also proposed that the conformation of two C-domains is more favourable than having an

N-domain in the construct. These findings clearly show that the shedding of ACE is highly regulated and its structural conformation plays a pivotal role in directing cleavage. As the C-domain was identified to potentially harbour a sheddase recognition domain, the single domain tACE was further investigated to identify this domain. Homologous regions between the N- and C-domains were sequentially swopped in order to determine which region restricts shedding (Woodman et al., 2006). It was found that a region corresponding to residues 164-416 in tACE was crucial for the shedding as well as activity of ACE. A smaller mutation within this region also rendered the protein inactive and not shed, suggesting that this region requires further investigation.

1.5.4 The ACE sheddase

The characterisation of the ACE sheddase activity from kidney microvilli, lung, testis (pig) and human lung and placenta tissue showed that the sheddase activity was membrane associated and occurred at a pH of 8.4. Serine, thiol or aspartic protease inhibitors did not affect ACE sheddase activity, though 2.5mM of EDTA and phenatroline inhibited ACE sheddase activity by 50%, signifying a clear role for metalloproteases in the sheddase activity (Oppong and Hooper, 1993). From ADAM 17 deficient mice, mouse fibroblasts were made and tACE cDNA was transfected into this cell line, but shedding of ACE remained normal (Sadhukhan et al., 1999) demonstrating that ADAM 17 was not involved in shedding of ACE. To investigate its role in the shedding of ACE and APP, antisense (ASO) technology was used to silence the activity of ADAM 10 and 17. APP shedding by ADAM 10 and ADAM 17 was reduced by 60% and 30%, respectively, but ADAM 10 and ADAM 17 ASO had no effect on ACE shedding (Allinson et al., 2004). APP and ACE have similar shedding profiles and are activated by DCI. This is evidence that ADAM 10 and ADAM 17 are not involved in ACE shedding (Parkin et al., 2002; Parvathy et al., 1998).

After many attempts to identify the ACE sheddase, one team of investigators yielded positive results. The study focussed on the shedding of endogenous sACE in HUVEC cells. They found that shedding was stimulated by LPS and not PMA, as was the case with most ACE shedding. Shedding of ACE was analysed in the medium after 16 hours. It was inhibited by the metalloprotease inhibitor BB-94 and ADAM 9 was identified as the LPS-stimulated sheddase of via siRNA. HEK cells transfected with ACE and ADAM9 showed that ADAM9 needs to be anchored in the membrane with a catalytic domain in order for it to be shed as ACE. Interestingly, TNF-α and TNFRI were involved in the stimulation of ACE shedding via

ADAM9. It was concluded that ADAM 9 is most likely not involved in unstimulated shedding of ACE in HUVEC (English et al., 2012). Therefore ADAM 9 is unlikely the primary sheddase of ACE. BB94 inhibits ACE shedding at an IC_{50} of 0.47μM and TAPI-2 has an IC_{50} of 18μM. This indicated that the inhibitors of ACE shedding are separate from the matrix metalloproteases (Parvathy et al., 1997).

1.5.5 ACE 2 shedding

The ACE homologue ACE 2, is membrane-anchored and undergoes regulated ectodomain shedding. Extensive studies has been conducted on this newly identified homologue and ADAM 17 was identified as the sheddase responsible for constitutive shedding in various cell lines (Iwata et al., 2009). ACE 2 is shed into two forms a larger soluble form (LSF) and a smaller soluble form (SSF). The shedding of LSF is decreased in ADAM 17 mutant CHO-M2 cells as well as EC-2 cells from ADAM 17-null mice. Rescued ADAM 17 activity in EC-2 cells reinstated the shedding of LSF but not SSF. ACE 2 juxtamembrane stalk deletion mutants were made and also affected the appearance of the LSF in the medium. This indicates that ADAM 17 is the main protease involved in the cleavage of the LSF and in conjunction with the juxtamembrane stalk regulates the shedding of the soluble forms of ACE2 (Iwata et al., 2009). Calmodulin was also shown to regulate shedding as CaM inhibitors increased ACE2 shedding (Lambert et al., 2008). The juxtamembrane and cytoplasmic domains were non-essential in the regulation of shedding and the cleavage site was mapped to the region 716-741 (Jia et al., 2009). As with ACE, a region distal to the transmembrane domain was identified to be essential for shedding. As a result, a point mutation at L^{584} was discovered via sequential mutagenesis to be a requisite for ACE 2 shedding.

To investigate the P1 and P1' requirements of ADAM 17 in the shedding of ACE2, 20-amino acid peptides corresponding to the stalk region of ACE2 were incubated with ADAM 17 (Lai et al., 2011). Substitutions were used to determine the effect on peptide cleavage of alanine and glutamate in the P1 and P1' positions, respectively. Cleavage was established to occur at R^{708}, and a glutamate substitution at position 708 and/or 710 resulted in an attenuation of cleavage. When these mutations were made in full length ACE2, only PMA induced

shedding was decreased and basal shedding was unaffected (Lai et al., 2011). This further demonstrates that multiple levels of regulation are involved in the shedding of ectoproteins such as ACE2. It is apparent that some shedding mechanisms are shared between ACE and ACE 2, while some remain different. These similarities and differences can be investigated for further characterisation of ACE shedding.

1.5.6 Polymorphisms that affect the ectodomain shedding of ACE

A polymorphism was found in unrelated individuals which increased the level of serum ACE but with no clinical abnormalities (Kramers et al., 2001). This was said to be due to an increase in shedding possibly as a result of a point mutation at Pro1199Leu, which is found in the stalk region. The Pro1199Leu mutants expressed in CHO-K1 and COS cells were shed 1.5-fold more efficiently than wild-type after 24 hours. An increase in the PMA response was also evident (Eyries et al., 2001). The cleavage site was mapped to R^{1137}-L^{1138}, however the cleavage site from the serum ACE was cleaved at the endogenous ACE site of R-S. The role of proline in the structure of ACE was predicted via a hydrophobic cluster analysis (HCA) plots due to the lack of three-dimensional structural information. Proline is predicted to form twists in the structure and the replacement with a leucine relieves this constraint and the loop becomes more flexible, allowing for a more favourable conformation of the ACE stalk for the sheddase. It is also interesting to note that the P^{1199} is the last conserved residue between the N- and C– domains before the C-domain specific loop with the cleavage site.

The Y^{465}D polymorphism in N-domain of somatic ACE causes an increase in plasma ACE. Analysis of this mutation suggested conformational changes in sACE causes the N- and C-domains to open up and allow access for the sheddase, leading to an increase in the rate of shedding (figure 1.8) (Danilov et al., 2011). A stop codon at W^{1197} lead to a dramatic increase in serum ACE (Nesterovitch et al., 2009). It is important to be aware of these polymorphisms that cause increased serum ACE due to aberrant shedding as these could lead to misdiagnosis of sarcoidosis which is identified via elevated serum ACE, but is caused by disparities in immune responses.

1.5.7 ACE shedding and dimerisation

ACE is involved in protein-protein interactions that could have implications in its activity, signalling and ectodomain shedding. To study these interactions, a large set of monoclonal antibodies directed to the various epitopes on the surface of ACE was used (Balyasnikova et al., 2005; Balyasnikova et al., 2003; Gordon et al., 2010; Kost et al., 2003). The monoclonal antibodies 9B9 and 3G8 blocked ACE dimerisation in reverse micelles via a proposed carbohydrate recognition domain. 3G8 blocked shedding and 9B9 increased shedding (Kost et al., 2003). 3G8 is likely shielded by the C-domain and is carbohydrate dependent, but 9B9 is not affected. This implies that this region of the N-domain negatively regulates shedding. These studies have shown that dimers occur via two interactions, one that is non-covalent occurring through the N-domain and the other disulphide-linked dimerisation occurring via the C-domain (Gordon et al., 2010). The dimerisation of ACE was found to be a key initiator of the signalling cascade, particularly ACE inhibitor-induced dimerisation. Interestingly, an enzymatically active C-domain was essential for inhibitor-induced dimerisation (Kohlstedt et al., 2006a).

Stauroporine, an inhibitor of PKC, stimulated antibody induced shedding, but inhibits PMA shedding suggesting that there are different signaling pathways for PMA-induced and antibody-induced shedding (Balyasnikova et al., 2002). This study also showed the sequential epitope for 5C8 is P^{1193}-R^{1203} and residues within this region create the three dimensional epitope for 1B3, along with the distal motif of A^{837}-H^{839} (tACE numbering). IB3 binds the C-terminus of sACE in its catalytically active form, whereas 5C8 binds its denatured form indicating that this epitope is prone to protein-protein interactions. Also, based on a molecular representation of ACE, it was found that these residues possibly interact with the stalk region (figure 1.8)(Irina V Balyasnikova et al., 2005) as the stalk deletion mutant Δ 11JM abolishes the epitope for 1B3. Furthermore, epitopes for 1B3, 1B8 and 3F10 are occluded in sACE expressed on the cell surface (Naperova et al., 2008).

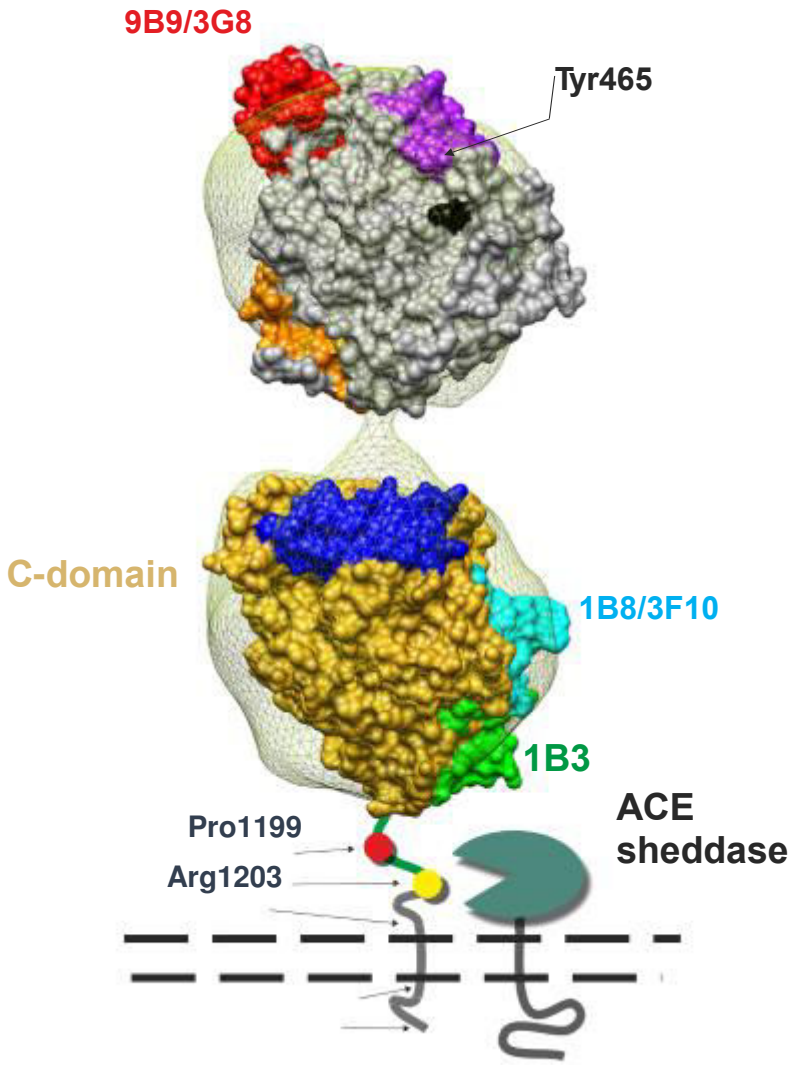

Figure 1.8: Model of human sACE with relevant epitopes and residues highlighted. 1B3 epitope coloured in green showing orientation towards stalk and putative sheddase. Epitopes for 1B8/3F10 in turquoise and 9B9/3G8 in red. Y^{465} is indicated by a black dot, P^{1199} in red, R^{1203} (cleavage site). Adapted from Danilov et al., 2011.

1.6 Aims of research

It is evident that ectodomain shedding is an important and vital cellular mechanism that is used by the cell to modulate the cell surface expression of ACE in response to various stimuli. Moreover, ACE shedding is influenced by amino acids in the juxtamembrane region as well as the conformation of the stalk in respect of promoting access and binding to ACE by its cognate sheddase. Fine-mapping of the structural contribution of the C-domain residues and motifs in the ectodomain and stalk is likely to identify the putative ACE

sheddase recognition motif. Therefore, it is the aim of this investigation to characterise the structural motifs necessary in the ectodomain cleavage of ACE.

This will be addressed by these main research objectives:

1. To analyse the distal ectodomain of ACE for a sheddase recognition motif
2. To investigate residues in the proximal ectodomain of ACE and their effect on shedding
3. To investigate the role of stalk glycosylation in the ACE shedding
4. To use soluble peptides mimicking the juxtamembrane region of ACE to understand the specificity of the ACE sheddase

CHAPTER 2: Materials and Methods

2.1. Recombinant DNA analysis

2.1.1. Plasmids and primers

Plasmid pcDNA 3.1 (-/+) and pGEM 117f (-/+) were purchased from Invitrogen (USA). Primers were purchased from Inqaba Biotech (South Africa). Primer sequences are listed in the appendix (table A3.1, A3.2, A3.3, A3.4). The restriction enzymes were purchased from Fermentas Life Sciences (Canada) or Roche (Switzerland).

2.1.2 Agarose gels

1% (w/v) agarose in 1X TBE (89mM Tris base, 89mM boric acid, 2mM EDTA) containing 0.2mg/ml ethidium bromide. Electrophoresis took place over approximately 1 hour at 70 volts in 1X TBE buffer. The gels were exposed to UV light at 260nm to visualise DNA bands. Images were captured on a gel documentation system (Syngene, UK) and analysed with GeneSnap and GeneTools software.

2.1.3 Restriction enzyme digestion

1µg of DNA was incubated with 10 units of enzyme/s (being less than 10% of the total volume), 1X compatible buffer and sterile water to bring up to the final volume. Reactions were incubated at 37°C for 2-4 hours and stopped with 6X loading dye.

2.1.4 DNA purification from agarose gels

The desired DNA bands were excised from agarose gels using a sterile blade. The DNA was purified from the gel slice using the Wizard SV® gel and PCR Clean-up System (Promega, USA).

2.1.4 DNA ligations

A 10:1 ratio of insert to vector was used, 2 units of T4 DNA ligase (Promega, USA) and 1X ligation buffer, thawed and well-mixed, and water made up to a final volume of 20µl. The ligation was incubated at room temperature overnight and transformed in competent E.coli cells. The Kapa Biosystems DNA ligase was also used, but incubation was allowed up to 6 hours.

2.1.5 DNA quantitation

DNA was diluted 1:100 and the absorbance was measured at 260nm and 280nm using a spectrophotometer. This was used to calculate its concentration and purity. Low concentrations of DNA were measured via the Nanodrop (Thermo Scientific) and 1.5µl was used.

2.1.6 DNA sequencing

Sequencing reactions were performed by the Molecular and Cell Biology DNA Sequencing Service, UCT (South Africa) utilising the Big Dye® Terminator v3.1 Cycle Sequencing kit (Applied Bio systems, USA) and Half-dye Mix (Bioline, UK). Further analysis was performed by Macrogen Inc. (Korea) using a 3730XL DNA sequencer (Applied Biosystems, USA).

2.1.7 Preparation of competent E.coli cells

A 5ml overnight culture of E.coli was inoculated into 100ml flask of LB (1% (w/v) tryptone, 0.5% (w/v) yeast extract, 0.5% (w/v) NaCl). The flask was incubated at 37°C until the culture reached an OD_{530nm} of 0.35. The culture was chilled on ice for 15 minutes before the cells were collected by centrifugation at 4000 × g for 5 minutes. The supernatant was removed and the cell pellet was resuspended in 10ml of chilled TFBI (30mM KOAc; 100mM RbCl; 10mM $CaCl_2$; 50mM $MnCl_2$; 15% (v/v)glycerol; adjusted to pH 5.8). These cells were again incubated on ice for 90 minutes and centrifuged at 4000 × g for 5 minutes. The collected

cells were resuspended in 3.5ml of chilled TFBII (10mM MOPS; 10mM $RbCl_2$; 75mM $CaCl_2$; 15% (v/v) glycerol; adjusted to pH 6.5). The final suspension was divided into 100µl fractions and flash frozen in liquid nitrogen. The competent cells were stored at -80°C until used.

2.1.8 DNA transformation

Competent cells were thawed on ice where after a maximum of 20µl of plasmid DNA was added. These were left on ice for 20 minutes and heat shocked in a 42°C waterbath for 45 seconds. The tubes were then incubated on ice for a further 2 minutes. Luria broth (LB) medium was added to bring the volume to 1ml and then were incubated at 37°C with shaking for at least an hour. After this growth period, the cells were centrifuged at high speed for 2 minutes. The supernatant was removed and the pellet was resuspended in 100µl of medium. This was plated out under sterile conditions onto Luria Agar (LA) plates supplemented with 100µg/ml of the antibiotic Ampicillin, which allows for selection of plasmid-containing cells.

2.1.9 Plasmid DNA isolation from E.coli transformed cells

Crude plasmid preparation for use in screening of mutant constructs:
One ml of an overnight E.coli culture was pelleted by centrifugation for 2 minutes at maximum speed in a microcentrifuge. The supernatant was discarded and the pellet was resuspended in 70µl of cell lysis buffer (10mM Tris, pH 8.0; 1mM EDTA; 15% (w/v) sucrose; 100µg/ml BSA; 20µg/ml ribonuclease A; 2mg/ml lysozyme). This was incubated at 37°C for 30 minutes and then boiled for 1 minute. An incubation period of 10 minutes followed on ice. The suspension was centrifuged at maximum speed for 10 min. The resultant supernatant was used in subsequent restriction digests.

Large quantities of DNA plasmids were prepared according to the manufacturer's protocol supplied with the Qiagen Plasmid Midi Kits (GmbH, Germany).

2.1.10 Site-directed mutagenesis

Site-directed mutagenesis reactions were performed according to an amended protocol from the PCR-based Quickchange® Site-Directed Mutagenesis protocol (Stratagene La Jolla,

CA, USA). Sets of complementary primers (Table 4.1) were designed using the WATCUT programme (http://watcut.uwaterloo.ca/watcut, University of Waterloo, Canada) and synthesised by Inqaba Biotechnical Industries (South Africa). The desired mutations were introduced as well as silent mutations to create restriction enzyme sites which were necessary for the screening of the mutation of interest (Table 4.1). High Fidelity Taq polymerase from Kapa Biosystems, (South Africa) were used in all reactions and they were carried out using either a HybaidExpress thermocycler (Hybaid Ltd, UK) or a Bio-Rad MyCycler^{TM} thermal cycler (Bio-Rad Laboratories, Inc, USA). To confirm that the correct sized PCR was produced, a small aliquot of the PCR was separated on a 1% agarose gel. The remaining portion of the reaction was incubated with the restriction enzyme DpnI overnight at 37°C to remove the un-mutated, unmethylated template DNA (Zheng et al., 2004). The reaction was then transformed (2.1.8) into either E.coli JM109 competent cells (2.1.7) or the methylation deficient JM110 if the restriction enzyme is sensitive to methylation patterns (such as BclI) and plated on LA plates supplemented with 100 µg/ml ampicillin. Colonies were picked from the plates and grown overnight in 5ml LB. The plasmid DNA was then isolated and screened with the appropriate restriction enzyme (listed with respective primers). Positive colonies were prepared for DNA sequencing (2.1.6) by DNA isolation using the Zyppy Plasmid Miniprep Kit (Zymo Research, USA).

2.2 Tissue culture

2.2.1 Maintenance of cells

The cell culture of choice was Chinese Hamster Ovary K1 (CHO-K1) cells and these were grown in an incubator at 37°C with 85% humidity and 5% carbon dioxide (CO_2). The growth medium used comprised of 10% foetal calf serum [(FCS)(Gibco)] heat inactivated at 56°C for 30 minutes, 50% Dulbeccos modified eagles medium(DMEM), 50% Hams F12 (Sigma, USA), 20mM N-2-hydroxyethylpiperazine-N'-2-ethanesulphonic acid (HEPES) pH 7.5. Cells were seeded into a 75mm^2 flask (Nunc) containing 30% FCS growth medium. After the cells attached, the medium was replaced with 10% FCS growth medium. Cells were grown until confluent and cells were split into culture dishes as needed.

2.2.2. Lifting of cells

Cells were split by adding trypsin-EDTA (0.5% trypsin in phosphate-buffered saline (PBS)) and incubating for 2 minutes. The lifted cells and trypsin suspension were centrifuged for 30 seconds at 2000 x g and the pellet was resuspended in the appropriate medium. This was used to seed flasks or dishes for further use.

To store cells under liquid nitrogen, the pellet was resuspended in a solution of 10% dimethyl sulphoxide (DMSO) in FCS.

2.2.3 Transfections

Stable transfections with pcDNA 3.1 constructs were conducted using the calcium phosphate method according to the Pro® Fection Mammalian Transfection System (Promega, USA) technical manual. Cells grown to approximately 40% confluency in 100mm dishes were used with 10-15µg of DNA. A glycerol shock was done 4 hours after DNA was added to cells. The antibiotic G418 (Sigma, USA) was used to select for resistant clones (Graham and van der Eb, 1973). These individual clones were isolated with cotton swabs dipped in trypsin-EDTA to lift them off the dish and then grown and tested for appropriate enzyme activity using hippuryl-L-His-L-Leu (HHL) or benzyloxycarbonyl-Phe-His Leu (Z-FHL) as a substrate.

2.2.4 Shedding assay

CHO-K1 cells expressing tACE proteins were grown to confluence in a 6-well plate. The complete growth medium was removed, cells were washed with PBS and replaced with 500µl Optimem (Gibco), supplemented either with 1µM of phorbol 12, 13-dibutyrate (PDBu) or 50µM TAPI (Peptides International). Cell lysates were harvested by adding 500µl of triton lysis buffer [1% Triton X-100, 50mM Hepes pH 7.5, 0.5M NaCl, 1mM phenylmethylsulphonyl fluoride (PMSF)] to each well and after cells started lifting, the lysates were pipetted to a sterile microfuge tube. The assay was conducted over 4 hours. The percentage ACE shed was calculated as the ratio of total ACE activity in the medium to total ACE activity in the medium and cell lysate [% ACE shed=ACE activity in the medium/ (ACE activity in the medium + ACE activity in the cell lysate)].

2.3 Western blot analysis

2.3.1 Protein concentration

The Bradford method was used to quantify proteins. Samples were diluted to a final volume of 800µl of water and then mixed with 200µl of Bradford reagent (BioRad) (Bradford, 1976). After a 5 minute incubation the sample was read at 595nm on a spectrophotometer blanked against a zero protein sample. These absorbance readings were converted to concentrations in µg/ml against standard curve of IgG or albumin (Appendix A2.2).

2.3.2 SDS-Polyacrylamide gel electrophoresis (SDS-PAGE)

The BioRad PROTEAN ®II gel system was used to cast and run the polyacrylamide gels (Laemmli, 1970). For shedding experiments, 20µl of medium samples and 15µl of cell lysate samples were used with 5µl of SDS sample buffer (62.5 mM Tris-HCl pH 6.8, 2% SDS, 10% glycerol, 0.001% bromophenol blue, 5% β-mercaptoethanol). This was boiled for 5 minutes and kept on ice until loaded onto gel. The 10% stacking gel consisted of running gel buffer (0.375M Tris pH8.8, 0.1% SDS), 0.1% ammonium persulphate (AMPS) and 7µl TEMED made to a final volume of 10ml with water. The 3% stacking gel was made up of stacking gel buffer (0.125M Tris pH6.8, 0.1% SDS), 0.3% AMPS and 20µl TEMED. The gels were run in 1X running buffer (0.025M Tris pH 8.3, 0.192M glycine, 0.1% SDS) at 50 mAMPs.

2.3.3 Coomassie staining of gels

Gels were incubated in a staining solution of 50% (v/v) methanol, 10% (v/v) acetic acid, 0.25% (w/v) Coomassie brilliant blue and then destained in 25% (v/v) ethanol, and 10% (v/v) acetic acid until background was clear.

2.3.4 Western blotting

The separated proteins from the SDS-PAGE were transferred to nitrocellulose membranes (Hybond-C, Amersham Biosciences) using the BioRad blotting apparatus. Transfer occurred at 100 volts for 1 hour. The system was cooled by an ice pack and stirring and the blotting buffer composed of 25mM Tris pH 8.2, 200mM Glycine, 20% v/v methanol.

The membrane was blocked in 5% (w/v) skimmed milk in Tris-buffered saline [(TBS) 0.05M Tris pH 7.4, 0.2M NaCl)]. The primary antibody (rabbit polyclonal anti- ACE) (Ehlers et al., 1991a) was added at a dilution of 1:1000 in 5% skimmed milk in TBS and incubated

overnight at 4°C with shaking. Thereafter the antibody was removed and washed for 15 minutes thrice with 5% skimmed milk in TBS. The secondary antibody [anti-rabbit conjugated to horse-radish peroxidase (Amersham Biosciences, Sweden)] was added at a dilution of 1:2000 in 5% skimmed milk in TBS and incubated for 1 hour at room temperature with shaking. The membrane was then washed as before but with TBS containing 0.1% Tween-20. The detection reagent (Immun-Star™ HRP Chemiluminescence kit) was then applied for 5 minutes. The membranes were drained of excess reagent and placed between clear plastic sheets. The chemiluminescent bands were captured on a G-BOX (Syngene) and analysed via GeneTools.

2.4 ACE activity assay of transfected membrane-bound tACE

The peptide Z-FHL (Sigma, USA) was used as a synthetic substrate to detect ACE activity (Depierre and Roth, 1975). O-phthaldialdehyde (Sigma, USA) was used to derivatise the His-Leu (HL) released (Friedland and Silverstein, 1976). 6µl of each sample to be analysed for ACE activity was placed in a 96-well microtitre plate (Schwager et al., 2006) and 30µl of the Z-FHL (1mM) substrate was added to each well. For the blank zero time (BZT), no sample was added. The plate was incubated at 37°C in a plate incubator with shaking 30-60 minutes. 120µl of 0.4M NaOH was added to stop the reaction. An ACE sample was added to the BZT and mixed. 10µl of 24mg/ml (in methanol) of *o*-phthaldialehyde was added and incubated for 10 minutes. 30µl of 3N HCl was added to stop the reaction. Fluorescence was detected in a fluorescence spectrophotometer (Varian Inc., USA) with an excitation wavelength of 360nm and an emission wavelength of 485nm. 1 milliunit (mU) of ACE activity was calculated as nmol His-Leu (HL) formed/minute from a standard curve of fluorescent units (FU) versus HL concentration (refer to Appendix A1.1 for composition of reagents and A1.2 for the standard curve).

CHAPTER 3: Analysis of the distal ectodomain of tACE to identify distinct regions that serve as a sheddase recognition motif

3.1 Introduction

A large body of work has been carried out to determine the structural requirements of the ACE sheddase(s) (Ehlers et al., 1995, 1992, 1991b; Sadhukhan et al., 1998). Recombinant ACE expressed in CHO-K1 cells was found in a soluble form, leading to the initial suggestion that ACE is shed off the membrane in a regulated manner (Ehlers et al., 1991b). Removal of the O-glycosylation region at the N-terminus of tACE had no effect on its shedding (Ehlers et al., 1992) and the addition of the phorbol ester dramatically increased shedding (Ehlers et al., 1995; Ramchandran and Sen, 1995) . Deletions of the juxtamembrane stalk showed that a minimum stalk length was required for ectodomain shedding. It was proposed that the stalk needed to be accessible to the sheddase as well as have a minimum length of 11 amino acids (Ehlers et al., 1996). Inclusion of the O-glycosylation region and disulphide bridge in the stalk did not abolish shedding but altered the regulation and rate of shedding. This argues that even though they modulate the shedding profile, the regions mutated did not abrogate shedding and therefore are not the primary sites of regulation for the shedding process (Schwager et al., 2001, 1999). These mutations in the stalk suggested that the modulation of shedding was directed by other regions of the ACE protein. Moreover, Chubb et al., (2002) determined that the cytoplasmic tail was not an absolute requirement for shedding.

An investigation into the role of the two domains of ACE demonstrated that a single C-domain variant was cleaved at a much faster rate than sACE (Beldent et al., 1995). Further studies have shown that tACE is cleaved 2-3 fold more rapidly than sACE even though they are cleaved at the same site in the stalk (Woodman et al., 2000). This points towards the N-domain of sACE negatively regulating shedding and that the single domain tACE/C-domain is shed more efficiently. However, a mutant where the N-domain was fused to the stalk and anchored in the membrane was not shed at all and suggested that the mere presence of a single domain was

not sufficient for cleavage off the membrane (Pang et al., 2001). This led to the theory that the C-domain may have a recognition motif that interacts with the sheddase and regulates ectodomain cleavage. Domain swop-over mutants reinforced the notion of a sheddase recognition motif within the ectodomain of the C-domain as the double C-domain mutant was cleaved within the linker region as well as at the stalk, which does not occur in sACE. The inverse orientation of the N- and C-domains of sACE was shed poorly and had very low activity, implying that the conformation was not conducive to proper processing and shedding (Woodman et al., 2005). This, taken together with the fact that sACE is shed less efficiently than tACE, suggests that the recognition motif may be occluded in the C-domain of sACE. It was also shown using monoclonal antibodies that certain epitopes within the N-domain may be involved in the control of shedding. The monoclonal antibody 3G8, whose epitope was mapped to the lid region of the N-domain, was shown to decrease shedding upon binding to sACE (I V Balyasnikova et al., 2005; Balyasnikova et al., 2002). This indicates that perhaps these antibodies shielded the protein interaction site needed for shedding to occur.

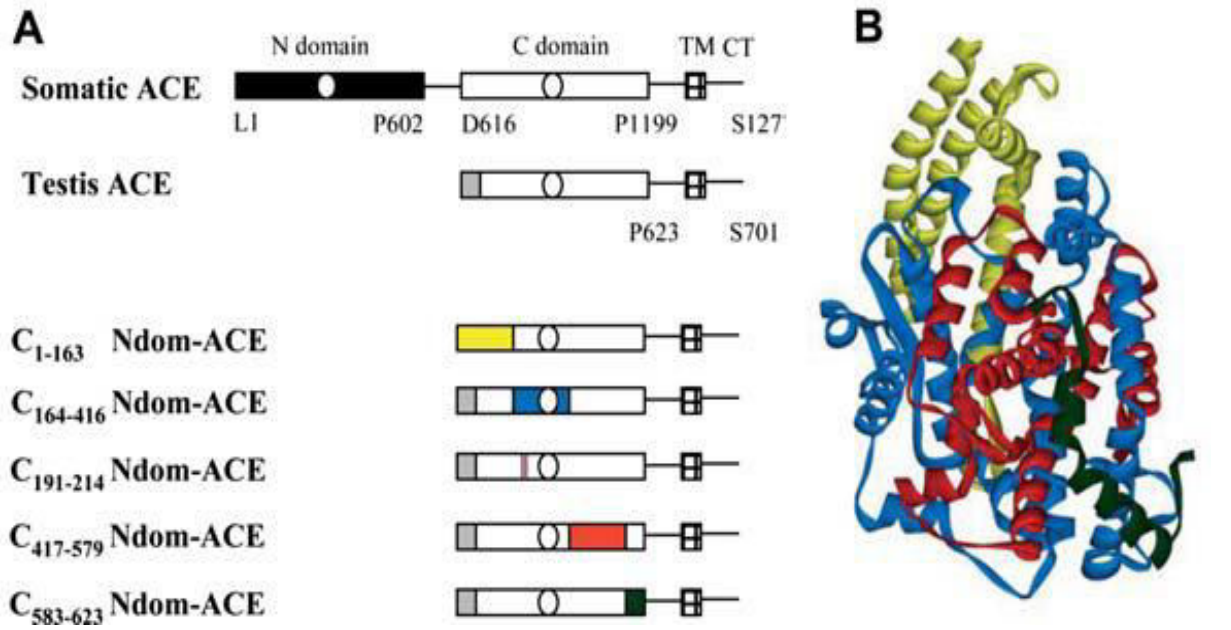

Figure 3.1: Schematic representation of constructs utilised in the study from Woodman et al., (2006). A) Grey boxes represent the 36 residue O-glycosylated region of tACE. The various colours represent the regions substituted with N-domain residues. A) is a linear representation and in B) are the corresponding regions in relation to its three-dimensional structure (Picture reproduced from (Woodman et al., 2006).

The shedding profiles of swop-over chimeras between rabbit tACE and the unshed ectoprotein CD4, suggested that the ACE ectodomain directed cleavage of the CD4 stalk (Sadhukhan et al., 1998). To fully examine the tACE/C-domain ectodomain, five chimeric tACE proteins were constructed by substituting regions of tACE with the corresponding regions from the N-domain in an attempt to identify the sheddase recognition domain, namely, $C_{1\text{-}163}$Ndom-ACE, $C_{164\text{-}416}$Ndom-ACE, $C_{197\text{-}214}$ Ndom-ACE, $C_{417\text{-}579}$ Ndom-ACE and $C_{583\text{-}623}$Ndom-ACE (figure 3.1) (Woodman et al., 2006). The $C_{164\text{-}416}$Ndom-ACE chimera was neither processed nor shed, proposing that a putative sheddase recognition motif within the distal ectodomain of testis ACE might be localised within the region between residues D^{164}-V^{416}. This region of ACE spatially influences the entire protein when viewing the three dimensional structure of ACE (Natesh et al., 2003) and would explain why such a substitution mutation with the N-domain residues might result in an inactive protein. The region disrupts the active site, removes 2 glycosylation sites and affects the junction of the 2 subdomains of tACE. It also introduces another potential glycosylation site within α-helix 11. The various mutants made in the Woodman study (2006) were designed by sequentially substituting regions of the entire C-domain with the corresponding region of the N-domain (figure 3.1). Because these mutants were designed without the benefit of a three dimensional structure of the enzyme, the secondary structural elements were not taken into consideration. The smaller $C_{197\text{-}214}$ Ndom-ACE chimera was made based on the fact that it had the lowest homology between the C and N-domains, and it was postulated that it would be the most likely candidate region for a putative recognition motif as it was further away from the active site. This mutant was also catalytically inactive demonstrating that this region was also necessary for folding and processing of the protein.

In this study, we then re-analysed the region D^{164}-V^{416} with the aim of identifying a recognition motif within this region. The following regions could be excluded due to reasons listed here: 1) it was shown previously that mutating residues R^{191}-Y^{214} causes a loss of enzymatic activity and poor cellular processing, indicating that this region is essential for correct processing (figure 3.2)(Woodman et al., 2005), and 2) a mutation reported by Williams et. al*.,* (1996) of the

residues H^{353}-I^{413} (figure 3.2) resulted in an active, correctly processed protein. Thus, it was decided to focus efforts on finding suitable regions that could coordinate shedding without negatively affecting the processing or activity of the protein. Residues 164-196 make up helix 5-6 of tACE and helix 5 of tACE is highly homologous with helix 5 of the N-domain. Furthermore, helix 6 forms part of the 197-214 chimera, which was inactive. This suggests that this region is important for processing and activity and unlikely to be part of the sheddase recognition motif. I^{261}-M^{340} incorporates helix 9-12 which also displays high sequence homology between the N- and C-domains, as well as the glycosylation sites that could affect processing if mutated. The only other potential candidate region, which had low homology to N-domain, was α helix 10 as it only had 50 % homology between the N and the C domains. However, it was not studied further due to the fact that it borders the subdomain junction which could affect folding (Woodman et al., 2006). The regions chosen to be mutated were located on the N-terminal subdomain and more proximal to the cleavage site according the three-dimensional crystal structure (Natesh et al., 2003) (figure 3.3).

Incorporating the knowledge learnt from previous attempts to locate the recognition motif, several factors were taken into account to rationally design further chimeras. An alignment was done between the C-domain and the N-domain of the 164-416 regions (figure 3.2). To further investigate this region, smaller N-domain substitutions were made by focussing on regions of least homology between the N- and the C-domain of which α helix 7 (D^{215}-Y^{225}) and 8 (S^{228}-H^{258}) met these criteria. The proximity of these regions to the cleavage site of tACE on the crystal structure was also taken into account. The basis for this was to identify regions most likely to interact with the sheddase secondary to the cleavage site interaction (Woodman et. al. 2000). The secondary structure of ACE was also taken into account where helices and loops were depicted (Natesh et al., 2003). This was done to prevent disrupting structures and thereby possibly preventing inactivation. Regions that included important features such as active sites and glycosylation sites were also avoided as mutations to these areas could lead to inactive proteins or incorrectly folded and processed proteins. Besides α helix 7 and 8, another three residue motif, A^{261}QH, immediately after helix 8 was also analysed. A^{261}QH creates a motif that

is closely associated with the most C-terminal residues of the ACE structure making it an excellent candidate for a recognition motif. Furthermore, it was also shown previously to be a part of a functional epitope for the monoclonal antibody 1B3 (Irina V Balyasnikova et al., 2005a; Naperova et al., 2008), indicating it may be involved in protein-protein interactions.

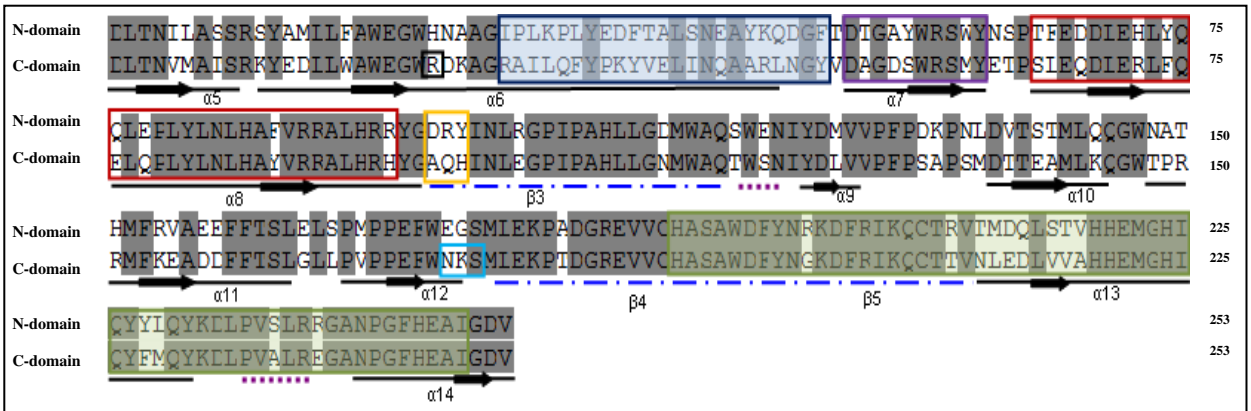

Figure 3.2: Alignment of the C-domain residues 164-416 and the complementary N-domain residues highlighting key structural features. Regions underlined in black with arrows represent α helices, regions underlined with purple dashed lines are 3_{10} helices, the residue boxed in black represents the chloride 1 site; the residues boxed in turquoise represents the glycosylation site that would be removed with the substitution of N-domain residues. Blue dashed lines represent β sheets, the region boxed in blue is the 191-214 mutation, and the region boxed in green represents the 353-413 mutation. The mutations made pertaining to this chapter are boxed in purple (α helix 7), red (α helix 8) and $A^{261}QH$ (yellow). This will highlight how these mutations maintain the structural boundaries of the protein.

A more recent publication confirmed our predictions that the secondary contact region with the sheddase would occur in closer proximity to the cleavage site (Chattopadhyay et al., 2008). They hypothesised that a 5-residue motif in the ectodomain directly proximal to the cleavage site alters shedding of rabbit tACE. The implications of their findings will be detailed and discussed further with respect to the human tACE cleavage in chapter 4.

3.1.1 Project objectives

The main aim of this study was to identify residues or regions within the distal ectodomain of testis ACE that interact with the ACE sheddase and directs its proteolytic activity. This was achieved via the following objectives:

1. Examining the role of the region encompassing residues D^{164}-V^{416} in tACE by constructing chimeric tACE mutants within this region using overlap PCR and SDM

2. Determining the effects of the above mutations on the enzymatic activity of ACE
3. Analyse the shedding profiles of the mutants with respect to their response to stimulation by PDBu and inhibition by TAPI

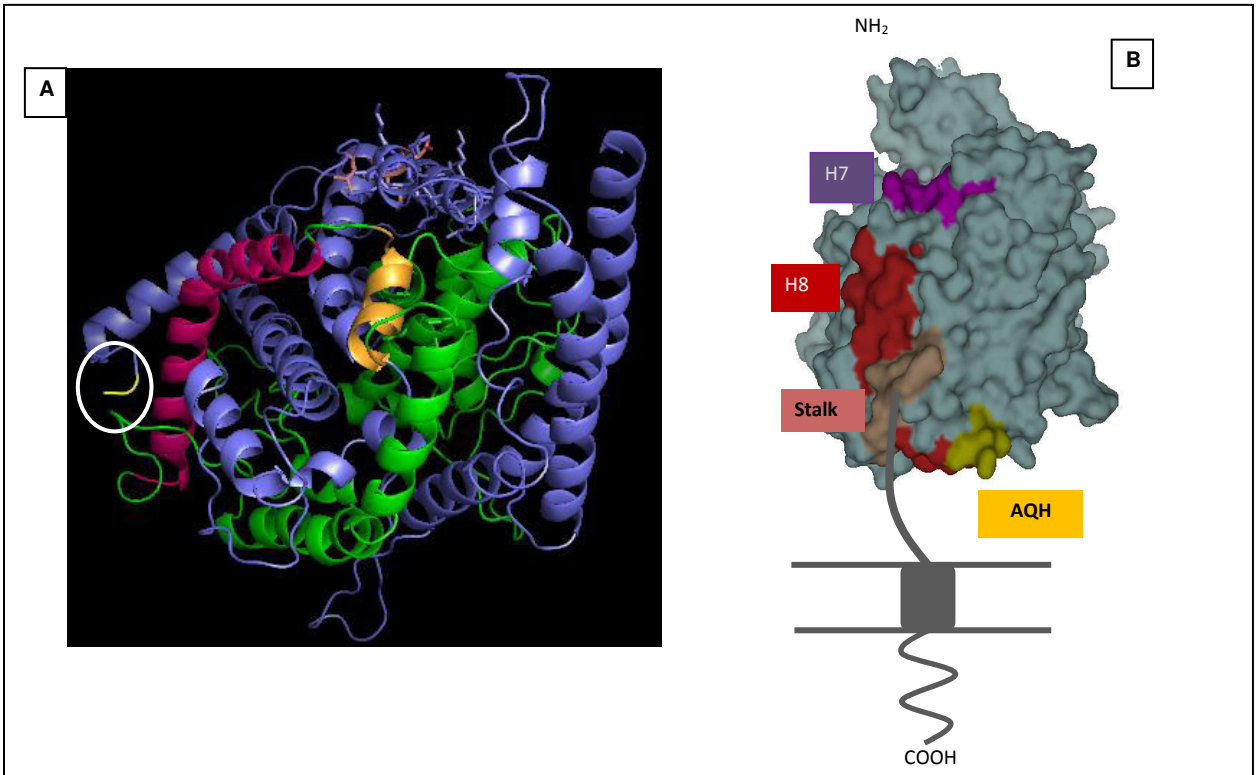

Figure 3.3: Selected mutants represented on the structure of tACE. A) Ribbon representation of tACE structure (Natesh et. al. 2003). Green represents the residues 164-416, α helix 7 is coloured in orange, α helix 8 is coloured in pink, the 3-residue motif AQH is coloured in yellow. The C-terminal end of the structure ends at (Pro 623) and is circled in white. B) Surface representation of the tACE structure with the mutations made coloured in purple (H7), red (H8) and yellow (AQH). The stalk residues are coloured in pink and a schematic representation has been added to orientate the structure in the relation to the transmembrane and cytoplasmic domains.

3.2 Materials and Methods

Based on the analysis of the ACE ectodomain, the region between residues D^{164}-V^{416} was further evaluated for potential sheddase recognition motifs. Three mutants were made to determine their contribution to the regulation of shedding using the methods summarised in table 3.1 and detailed in section 3.2.1.

Table 3.1: List of mutants made and method used.

Mutant Construct	Method used to introduce N-domain residues
pcDNA tACE H7	Overlap PCR
pcDNA tACE H8	Overlap PCR
pcDNA tACE AQH	Site directed mutagenesis

3.2.1 Cloning of swop-over ACE mutants

3.2.1.1 Subcloning of tACE into pGEM -Z11f (-) and pcDNA 3.1 (-)

Human wild-type tACE was cloned into pGEM -Z11f (-) via compatible BamHI and HindIII restriction sites from pLENtACE (Ehlers et al., 1991a). From pGEM -Z11f (-) tACE, the insert was cloned into pcDNA 3.1(-) with BamHI and HindIII.

3.2.1.2. Cloning of pcDNA-tACE H7

The D164-V416 region of tACE was flanked by the restriction sites BglII at the 5' site and NheI at the 3' site. Two sets of primers were designed and utilised overlap PCR (Urban et al., 1997) to mutate the 33bp α-helix 7 of tACE to the N-domain residues (figure 3.4). Mid For and Mid Rev primers (table A.3.1) contain regions complementary to tACE as well as the N-domain residues of α-helix 7. The restriction enzyme EheI was introduced to facilitate screening of colonies with the correct mutation. The tACE specific primer BglII For and the Mid Rev primers used in conjunction with the BglII-NheI tACE fragment as the DNA template produced a 600bp fragment. The Mid For primer and tACE specific NheI Rev primer produced a smaller 186bp fragment (figure 3.4, step 1). These PCR products were purified from agarose gels using the Wizard® SV Gel and PCR Clean-Up System (Promega, USA). The "zipper reaction" consisted of 5µl of each purified band, dNTPs, PCR buffer, $MgCl_2$ and nuclease free H_2O. It was boiled for 10 minutes, placed on ice for 2 minutes, Pfu polymerase (Promega) was then added and incubated at 75°C for 10 minutes (step 2). This reaction was then used as the template with BglII For and NheI Rev primers for the reaction to amplify the entire fragment. General PCR conditions were used i.e. 95°C for 5 minutes (initial denaturation), 95°C for 30 seconds, 62.7°C for 45 seconds, 72°C for 1 minute (x25 cycles), 72°C 1 minute. This resultant PCR fragment was gel purified,

digested with BglII and NheI, and then subcloned into the tACE fragment with the BglII and NheI restriction sites (step 3).

The ligated fragments were transformed into E.coli JM109 competent cells, as previously described (chapter 2.1.8). Colonies were screened using small scale DNA preparations and digestions of the DNA with the screening enzyme EheI. Positive colonies were sent for sequencing and after the mutation was confirmed, the tACE DNA insert was subcloned from pGEM tACE H8 into the expression vector pcDNA3.1 (-) using the compatible restriction enzymes BamHI and HindIII. The ligated plasmids were transformed into competent JM109 E.coli cells, positive colonies were identified from them and DNA was isolated using the Qiagen Maxi Kit in quantities sufficient for transfections into CHO-K1 cells. 10-15µg of this DNA was used to transfect CHO-K1 cells using the calcium phosphate method (refer to chapter 2.2.3). Stable cell lines were assayed for changes in shedding under control, PDBu and TAPI conditions (chapter 2.2.4). Western blot analysis (chapter 2.5) and ZFHL enzyme assays (chapter 2.6) were conducted.

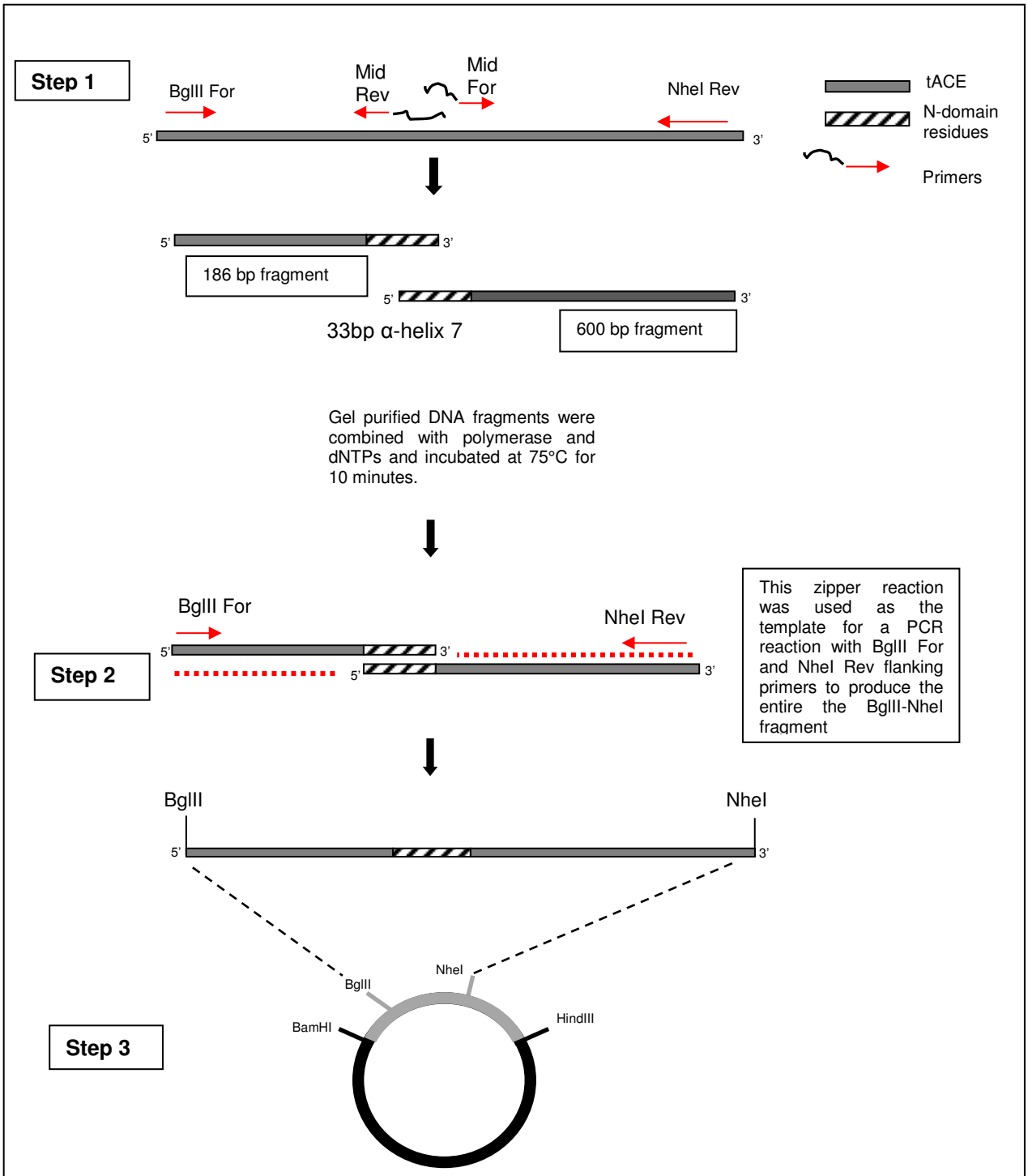

Figure 3.4: Schematic diagram representing the PCR and cloning steps involved in creating the construct pcDNA-tACE H7.

3.2.1.3. Cloning of pcDNA-tACE H8

Helix 8 is 96 base pairs long and overlap PCR was used to mutate this region to N-domain residues. Primers were designed with a portion targeted to the corresponding 96bp N-domain region and a portion that will target the surrounding testis ACE flanking regions of helix 8 (figure 3.5, step 1). The template that was used was Ndomain D629 (P. Redelinghuys, PhD thesis, 2006). These primers were used to produce an N-domain fragment with tACE flanking regions. The resultant DNA fragment was purified using PCR clean-up kits (Wizard kit, Promega) and the 128bp fragment now becomes a "megaprimer" when used in conjunction with tACE specific primers to produce two larger tACE fragments (fragments A and B) each with the complementary N-domain region at the 3'and 5'prime regions, respectively (figure 3.5, step 2).

Optimisation of the megaprimer reaction required that the megaprimer concentration needed to be in excess compared to the flanking primer and PCR conditions needed to favour the megaprimer initially. Therefore, an initial 5 cycles of the PCR was conducted at an annealing temperature specific to the megaprimer. Thereafter the annealing temperature is reduced to 50°C for a further 25 cycles (Wu et al., 2005). This DNA fragment was cut out and purified. The overlap zipper reaction was set up using both fragments and adding Pfu and dNTPs. This was incubated for 10 minutes at 75°C, which is the optimal temperature at which Pfu acts as a polymerase (step 3). This reaction was used as the template for a PCR reaction with BglII and NheI primers to create DNA fragments incorporating N-domain residues with BglII and NheI restrictions sites. This fragment was cut out and gel purified. It then underwent restriction endonuclease digestion with BglII and NheI to create the correct 5' and 3' ends required for ligation into similarly digested and purified pGEM-w.t. tACE (step 4).

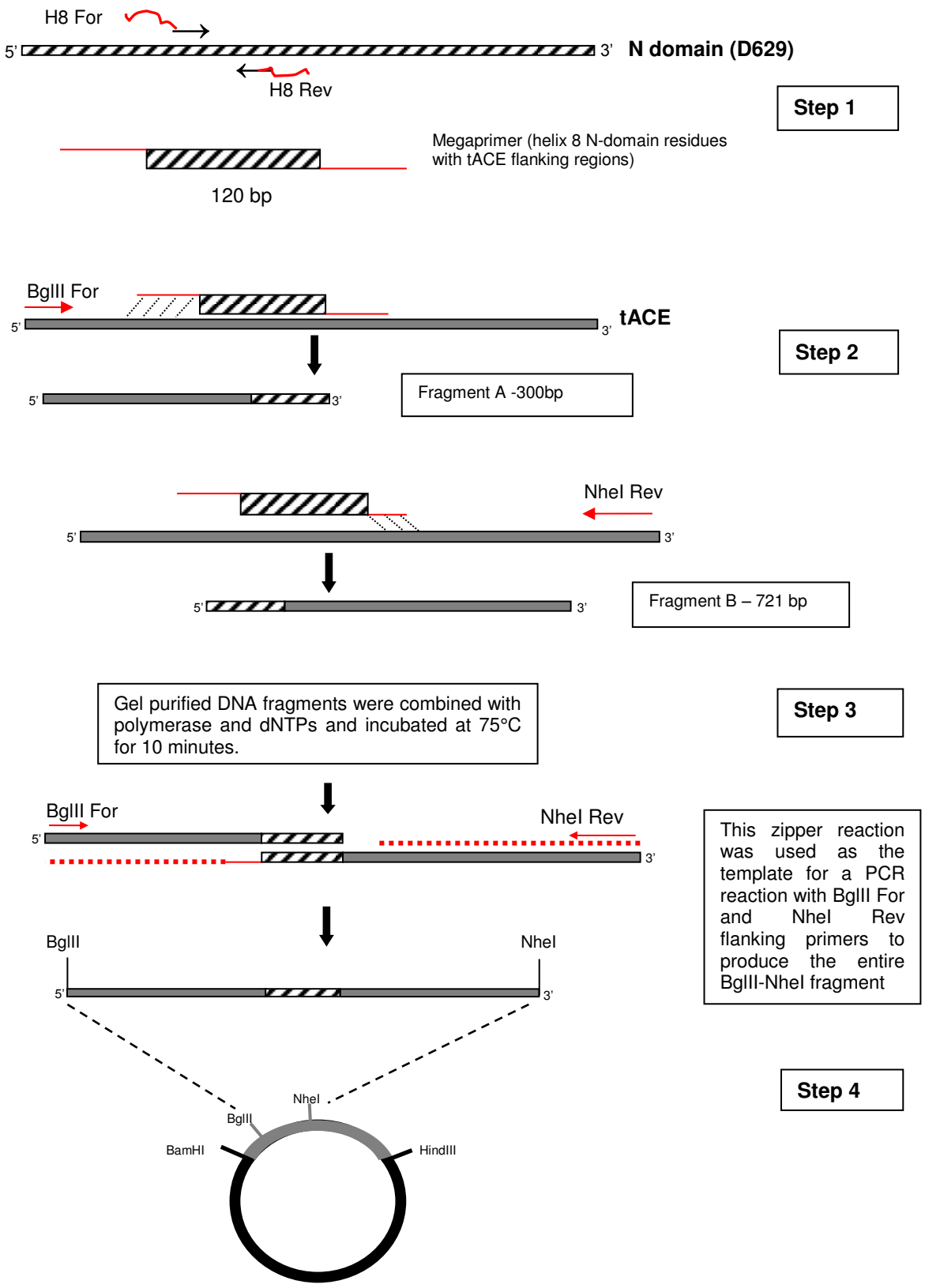

Figure 3.5: Schematic diagram representing the PCR and cloning steps involved in creating the construct pcDNA- tACE H8.

The ligated fragments were transformed into E.coli JM109 competent cells as previously described. Colonies were screened using small scale DNA preparations and digestions of the DNA with the screening enzyme SphI. Positive colonies were sent for sequencing and after the mutation was confirmed, the tACE DNA insert was subcloned from the pGEM- tACE H8 into the expression vector pcDNA3.1 (-) using the compatible restriction enzymes BamHI and HindIII.

3.2.1.4 Site-directed mutagenesis of pcDNA-tACE AQH

The 3 residue motif was mutated via site-directed mutagenesis using the primers presented in Appendix, table A3.3 according to the method outlined in chapter 2.

3.2.1.5 Expression of mutants in CHO-K1 cells

The ligated plasmids were transformed into competent JM109 E.coli cells, positive colonies were identified and from them DNA was isolated using the Qiagen Maxi Kit in quantities sufficient for transfections into CHO-K1 cells. 10-15µg of this DNA was used to transfect CHO-K1 cells using the calcium phosphate method (refer Method and materials). Stable cell lines were assayed for changes in shedding under control, PDBu and TAPI conditions. Western blot analysis and ZFHL enzyme assays were conducted.

3.3 Results

3.3.1 Cloning of tACE mutants

3.3.1.1 Subcloning of tACE into pGEM -Z11f (-) and pcDNA 3.1 (-)

In preparation for the subcloning of the mutated fragments into wild-type tACE, the wild-type tACE DNA insert was subcloned from pLEN-tACE into pGEM -Z11f(-) and then into the expression vector pcDNA 3.1 (-). pLEN-tACE has 3 HindIII restriction sites (figure 3.6 A) and BamHI and ClaI sites flanking the tACE insert. However, ClaI could not be used in the subcloning as it is not compatible with pGEM -11Zf (-). Therefore HindIII was used in conjunction with BamHI. The fragment released with the digestion of BamHI and ClaI (figure 3.6 B, lane 1) was gel purified and ligated with a similarly digested pGEM 11Zf (-). Digestion of pGEM 11Zf (-)-tACE with BamHI and HindIII produced a fragment of approximately 2500bp (figure 3.6 D, lane 2), indicating the successful ligation of tACE and pGEM 11Zf (-).

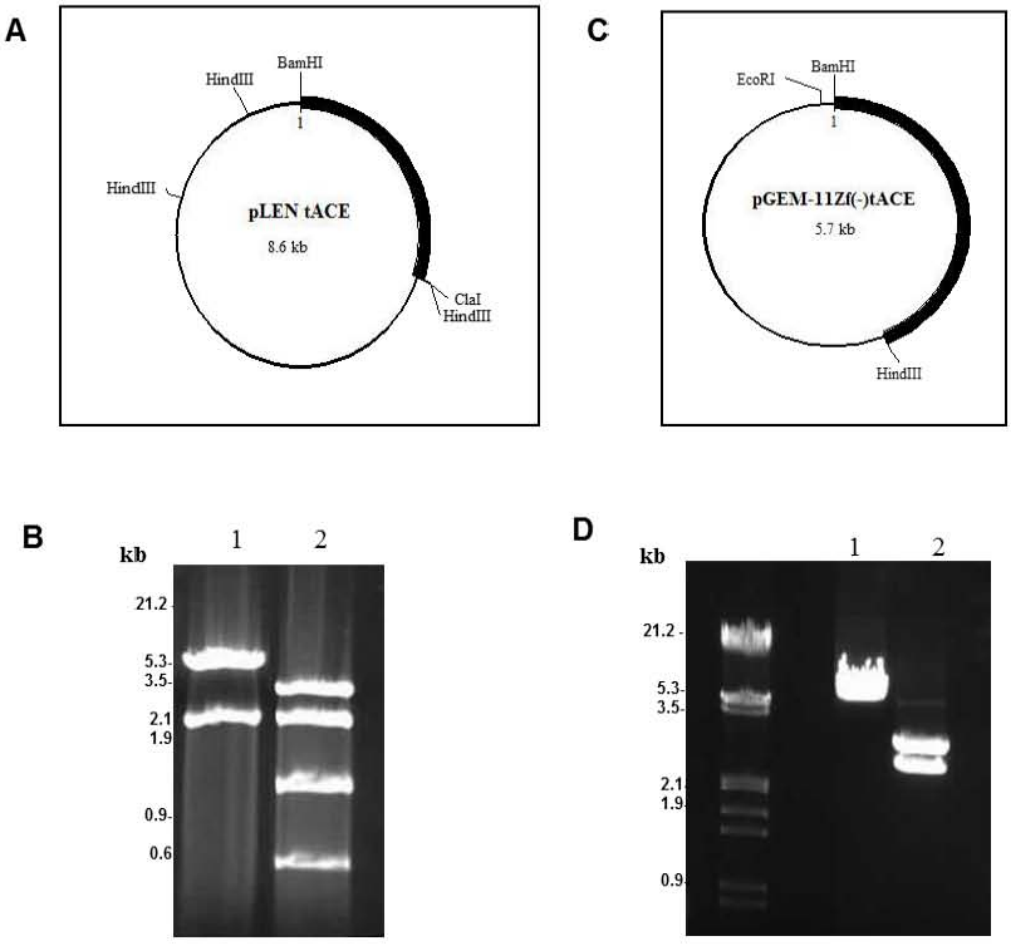

Figure 3.6: **Cloning of tACE into pGEM -11Zf(-).** A) pLEN-tACE plasmid map highlighting the position of ClaI and HindIII restriction sites. B) 1% agarose gel showing digested pLEN-tACE; lane 1- BamHI and ClaI, lane 2- BamHI and HindIII. λ DNA digested with HindIII and EcoRI are used as the DNA sizing marker as indicated on the left in kilobases (kb). C) pGEM -11Zf(-) tACE plasmid map highlighting BamHI and HindIII restriciton sites. D) 1% agarose gel of restriction digested pGEM 11Zf(-) tACE; lane 1- HindIII, lane 2- BamHI and HindIII. λ DNA digested with HindIII and EcoRI are used as the DNA sizing marker as indicated on the left in kilobases (kb).

3.3.1.2 Subcloning of pcDNA-tACE H7

pGEM -Z11f(-) tACE was used as template for construction of all the chimeras. The tACE H7 chimera was constructed using overlap PCR (Woodman et. al. 2006) to mutate the region spanning D^{215}-Y^{225} to corresponding N-domain residues according to the strategy outlined in figure 3.4 and using the primers in table A3.1 (Appendix). The resultant fragment with BglII and NheI restriction sites at the 5' and 3' termini was subcloned into pGEM Z11f(-)-tACE and the correct insertion verified by DNA sequencing. The tACE H7 insert was then subcloned into the pcDNA 3.1 (-) using compatible restriction sites BamHI and HindIII. An EheI restriction site was engineered into the primer to assist in screening for the mutation. Thus, digestion of pcDNA-tACE H7 with EheI yielded two fragments of 4.8kb and 3.1kb, indicating the correct incorporation of the mutation (figure 3.7).

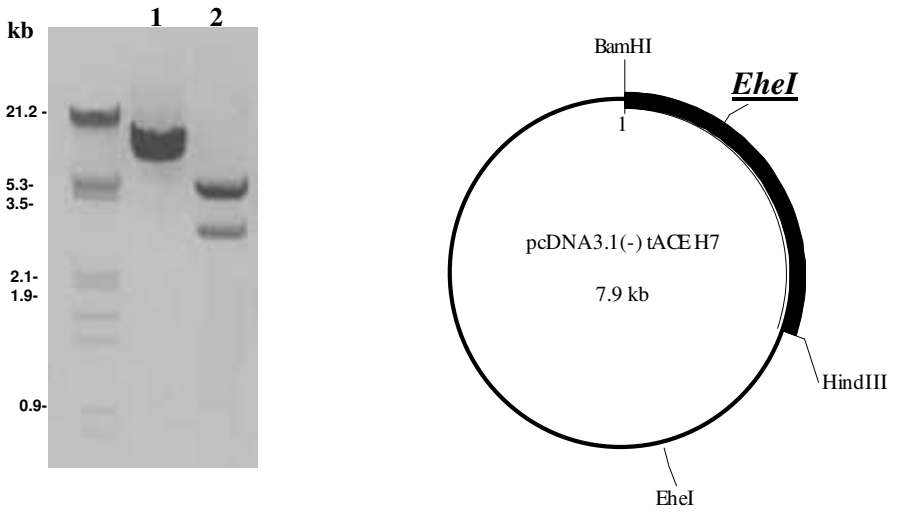

Figure 3.7: Restriction digest and plasmid map of pcDNA 3.1 (-) tACE H7. On the left is a 1% DNA agarose gel of EheI digests of wild-type tACE (lane 1) and tACE H7 (lane 2). λ DNA digested with HindIII and EcoRI are used as the DNA sizing marker as indicated on the left in kilobases (kb). The plasmid map highlights the restriction enzyme sites pertinent to the construct. The underline italicised EheI site was introduced to aid in the screening of the mutation that was introduced.

3.3.1.3 Cloning of pcDNA-tACE H8

To substitute the N-domain residues of α-helix 8 for the corresponding region in tACE, the strategy outlined in figure 3.5 was followed using the PCR primers presented in table A3.2. (Appendix). S^{228}-H^{258}Ndom/tACE H8 was constructed using Megaprime (Wu et al., 2005) and overlap PCR to mutate the tACE residues S^{228}-H^{258} to N-domain residues L^{230}-H^{258}. The PCR products depicted in figure 3.5 as fragment A and B, together with primers which flank the mutated regions and incorporate BglII and NheI restriction sites, respectively, were used to produce a final PCR product that was subcloned into pGEM -Z11f(-) tACE digested similarly with BglII and NheI. After confirming the sequence of tACE H8, it was subcloned from the pGEM Z11f (-) into the pcDNA 3.1 (-) vector. Digestion with SphI confirmed that the correct residues were incorporated as the there was a loss of the C-domain SphI site. The pcDNA vector also contributes five SphI sites to the plasmid construct and thus five bands are expected. Lane 1 represents the wild-type banding pattern, showing all the resultant bands except for a 0.072kb that is not visible on the gel represented here. The sizes of the resultant bands were 5.0kb, 1.2kb, 0.8 and 0.6kb (figure 3.8). When the SphI site is absent, as in tACE H8 (lane 2), the 1.2kb band is lost and included with the 5.3kb DNA fragment to produce a larger 6.4kb fragment.

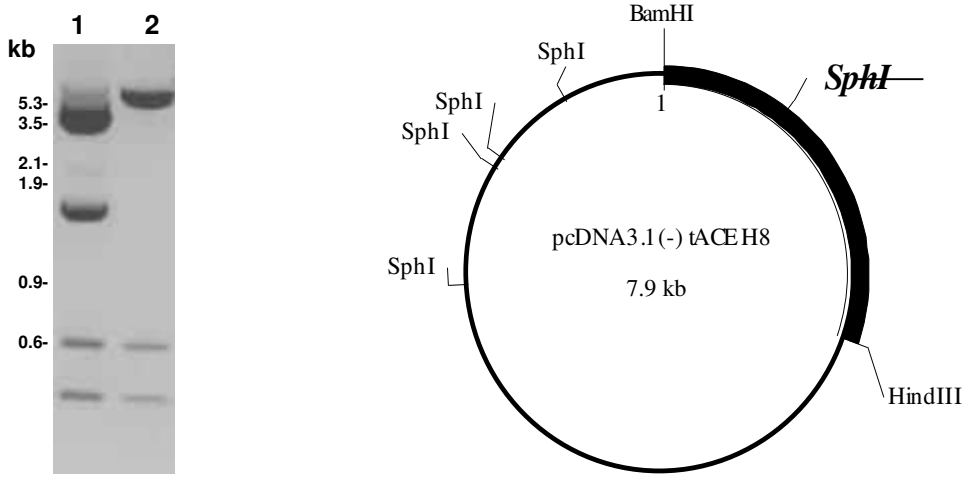

Figure 3.8: Restriction digest and plasmid map of pcDNA 3.1 (-) tACE H8. On the left is a DNA agarose gel of SphI digests of wild-type tACE (lane 1) and tACE H8 (lane 2). λ DNA digested with HindIII and EcoRI are used as the DNA sizing marker as indicated on the left in kilobases (kb). The plasmid map highlights the restriction enzyme sites pertinent to the construct. The italicised SphI site was removed with the introduction of the N-domain residues and was used to screen the introduction of the correct mutation.

3.3.1.4 Cloning of pcDNA tACE AQH

The residues A^{261}-H^{263} were replaced with their N-domain counterparts by SDM (chapter 2, section 2.1.10) using the primers detailed in table A3.3 (Appendix). DNA sequencing confirmed the incorporation of the correct mutation and the DNA insert was subcloned into pcDNA 3.1(-) using BamHI and HindIII restriction sites. A unique AgeI restriction enzyme site was included in the SDM primers for screening purposes. Thus, digestion of pcDNA 3.1(-) tACE with AgeI did not produce any distinct bands (figure 3.9, lane 1), while digestion of pcDNA 3.1 (-) tACE A^{261}QH yielded a single band, representing a construct that was linearized by a single restriction site digestion.

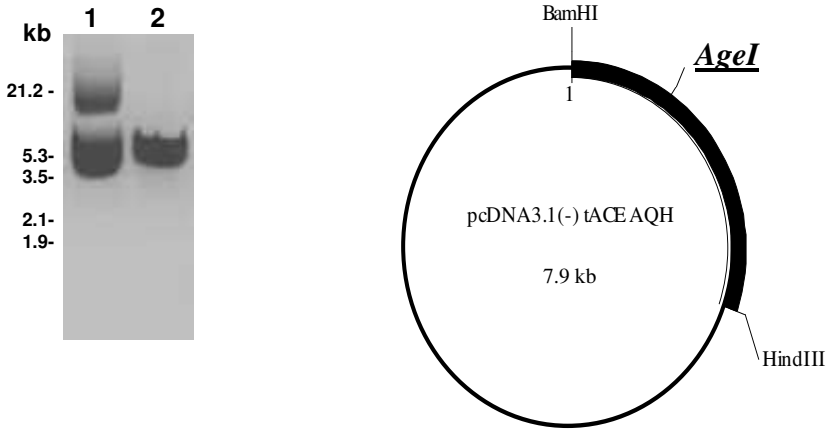

Figure 3.9: Restriction digest and plasmid map of pcDNA 3.1 (-) tACE AQH. On the left is a DNA agarose gel of AgeI digests of wild-type tACE (lane 1) and tACE A^{261}QH (lane 2). λ DNA digested with HindIII and EcoRI are used as the DNA sizing marker as indicated on the left in kilobases (kb). The plasmid map highlights the restriction enzyme sites pertinent to the construct. The underlined italicised AgeI site was introduced to aid in the screening of the mutation that was introduced.

3.3.2 Expression and shedding of swop-over mutants

Mutant and wild-type tACE DNA was stably transfected into CHO-K1 cells. The ectodomain shedding of the swop-over tACE H7 and tACE H8 chimeras and the tACE A^{261}QH mutant was analysed as described before (refer to chapter 2, section 2.2.3 and 2.2.4). Western blot analysis was performed in order to confirm the molecular weight of the proteins and their presence in the cell medium and lysate. Wild-type tACE in pcDNA 3.1(-) was released into the medium at a rate of 25% of the total ACE (Figure 3.10) which was higher than the pLEN construct previously described (Ehlers et al., 1991a). The addition of 1µM of the phorbol ester PDBu results in a two-fold increase in shedding consistent with previous reports (Ehlers et al., 1995). The addition of the hydroxamate inhibitor TAPI reduced shedding to below 5% and this confirmed that the protease cleaving the juxtamembrane region of ACE is a metalloprotease.

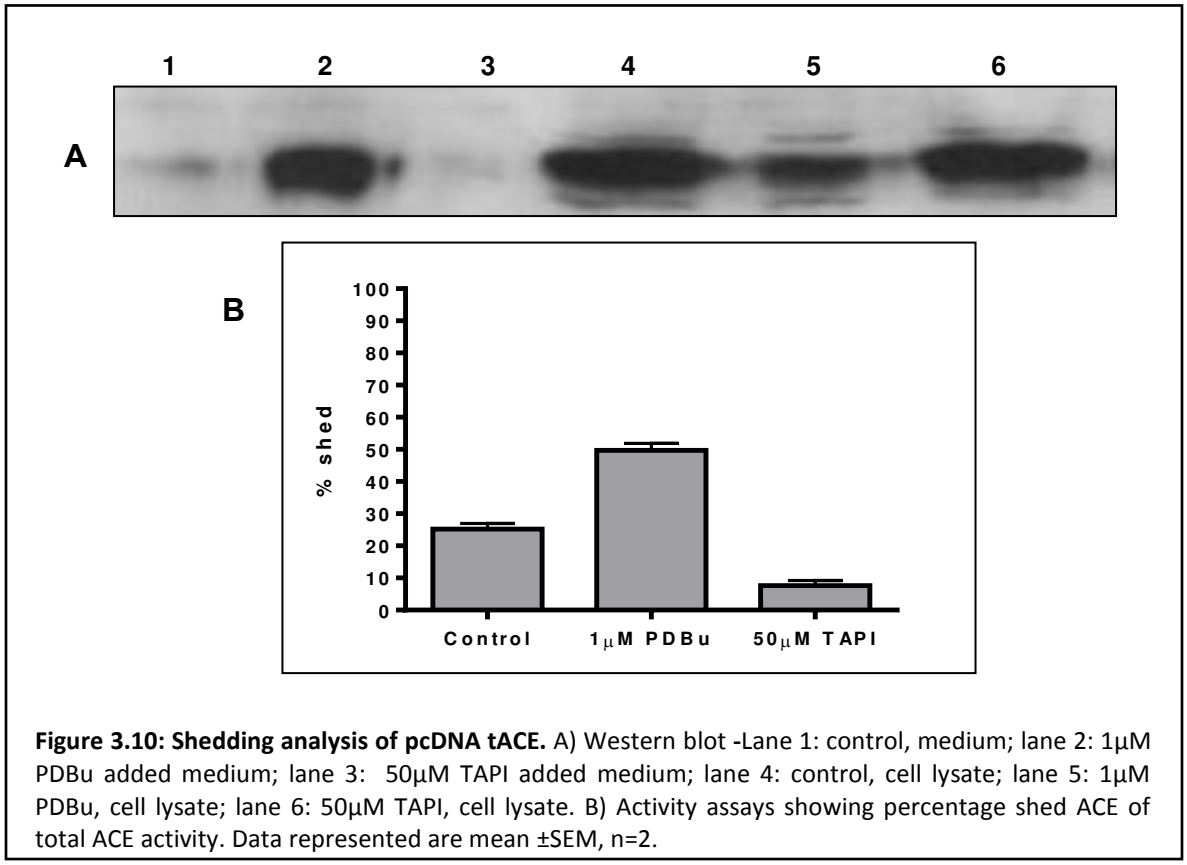

Figure 3.10: Shedding analysis of pcDNA tACE. A) Western blot -Lane 1: control, medium; lane 2: 1µM PDBu added medium; lane 3: 50µM TAPI added medium; lane 4: control, cell lysate; lane 5: 1µM PDBu, cell lysate; lane 6: 50µM TAPI, cell lysate. B) Activity assays showing percentage shed ACE of total ACE activity. Data represented are mean ±SEM, n=2.

3.3.2.1 tACE H7

The ectodomain shedding of tACE H7 was analysed via western blot analysis and ACE activity assays using the substrate ZFHL. Shedding was marginally, but not significantly, lower (19%) than wild-type (24%) (figure 3.11, B). tACE shedding was stimulated by phorbol ester and shedding was inhibited by TAPI. Thus, the replacement of α helix 7 of the C-domain with the corresponding N-domain residues does not significantly alter its modulation of ectodomain shedding.

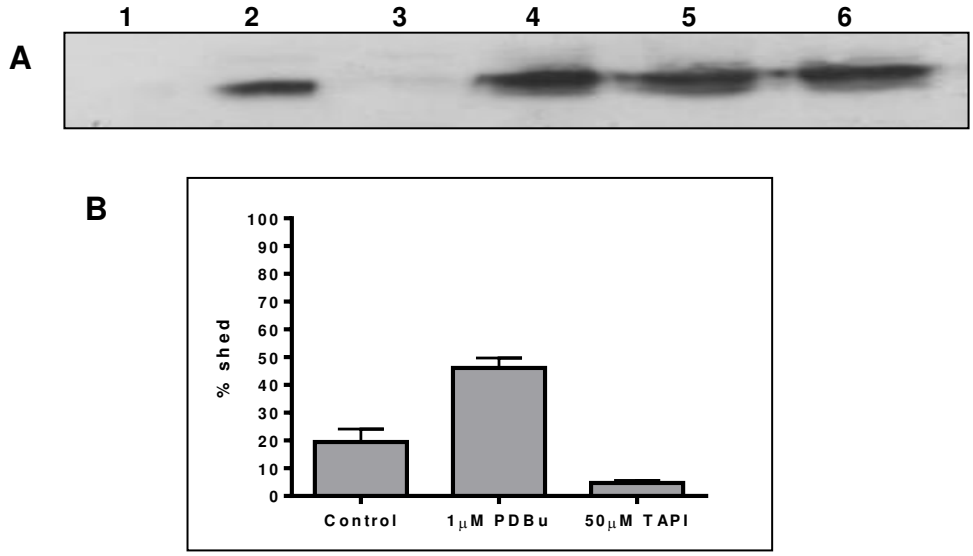

Figure 3.11: Shedding analysis of pcDNA tACE H7. A) Western blot- Lane 1: control, medium; lane 2: 1μM PDBu added medium; lane 3: 50μM TAPI added medium; lane 4: control, cell lysate; lane 5: 1μM PDBu, cell lysate; lane 6: 50μM TAPI, cell lysate. B) Activity assays showing percentage shed ACE of total ACE activity. Data represented are mean ±SEM, n=2.

3.3.2.2 tACE H8

The replacement of C-domain residues within α helix 8 with their N-domain counterparts increased basal shedding by 8% and the presence of the phorbol ester resulted in stimulated shedding of 62% (figure 3.12). This mutation had the unexpected result of increased shedding instead of reduced shedding. This puts forward that this region is not vital for the regulation of shedding. Nevertheless, the introduction of N-domain residues at this site has modulated shedding by causing an increase in shedding to 30%.

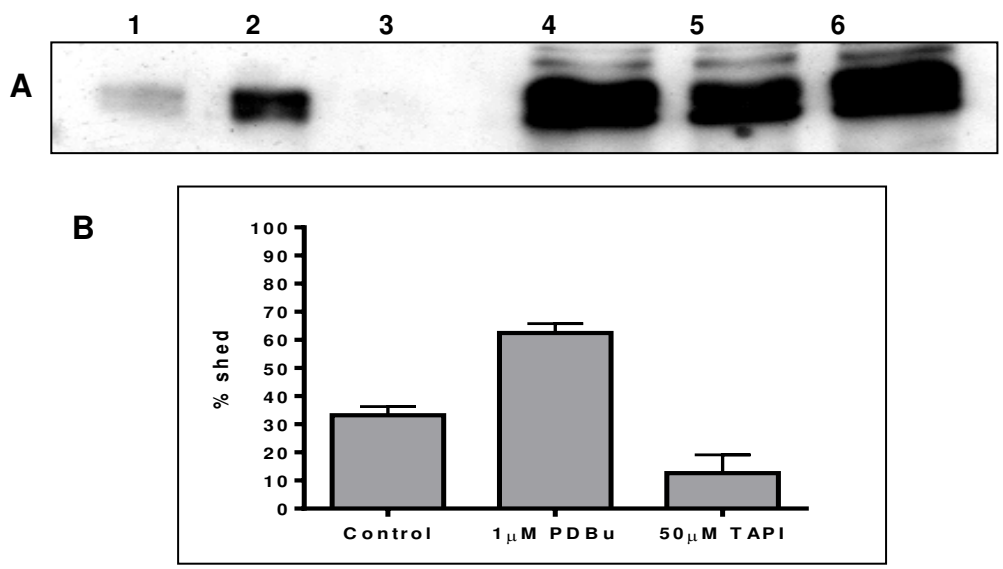

Figure 3.12: Shedding analysis of pcDNA tACE H8. A) Western blot - Lane 1: control, medium; lane 2: 1μM PDBu added medium; lane 3: 50μM TAPI added medium; lane 4: control, cell lysate; lane 5: 1μM PDBu, cell lysate; lane 6: 50μM TAPI, cell lysate. B) Activity assays showing percentage shed ACE of total ACE activity. Data represented are mean ±SEM, n=2.

3.3.2.3 tACE AQH

Compared to wild-type shedding (figure 3.10, B), basal shedding of tACE AQH was reduced by 10% according to the activity assay (figure 3.12, B). However, this mutant was still sensitive to PDBu as well as TAPI as there is an increase in shedding with the addition of PDBu and decrease with TAPI demonstrating a similar shedding profile to the H7 and H8 mutants. The rationale behind making this mutant was based on the fact that these residues contribute to a specific epitope in the stalk region of ACE for the monoclonal antibody 1B3 (Irina V Balyasnikova et al., 2005a). They suggested that these residues encompass the 1B3 epitope along with an 11-residue sequential epitope in the stalk. Therefore, it is likely that these residues create a structural motif that is in close enough proximity with the stalk region to possibly interact with it, and direct cleavage of ACE in the stalk. Alteration of this motif, however, was not sufficient to knock out the shedding of ACE.

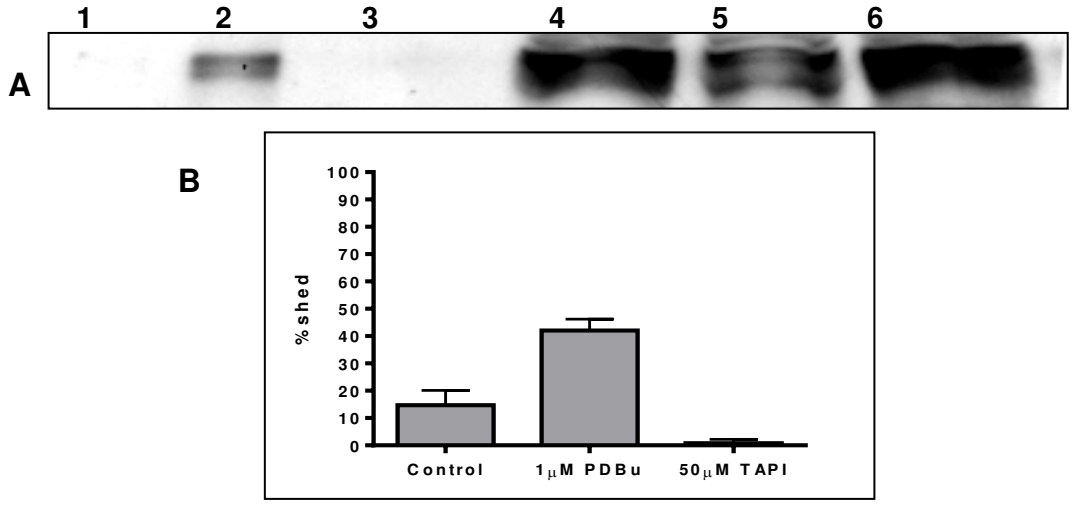

Figure 3.13: Shedding analysis of pcDNA tACE AQH. A) Western blot - Lane 1: control, medium; lane 2: 1μM PDBu added medium; lane 3: 50μM TAPI added medium; lane 4: control, cell lysate; lane 5: 1μM PDBu, cell lysate; lane 6: 50μM TAPI, cell lysate. B) Activity assays showing percentage shed ACE of total ACE activity. Data represented are mean ±SEM, n=2.

In figure 3.14 the percentage of shed ectodomain of all the mutants is compared. tACE H7 and wild-type tACE are most similar in their responses to phorbol stimulation and TAPI inhibition. tACE H8 has increased shedding compared to wild-type tACE for all conditions indicating that the mutation in helix 8 might have caused a conformational change which promotes shedding. The addition of 50μM TAPI did not reduce shedding to the same extent as with tACE AQH and wild-type. tACE AQH is also the only mutant whose basal shedding was less than that of wild-type, although not statistically significant. This may support that these three residues may possibly contribute to a sheddase recognition motif or it may induce the action of another sheddase.

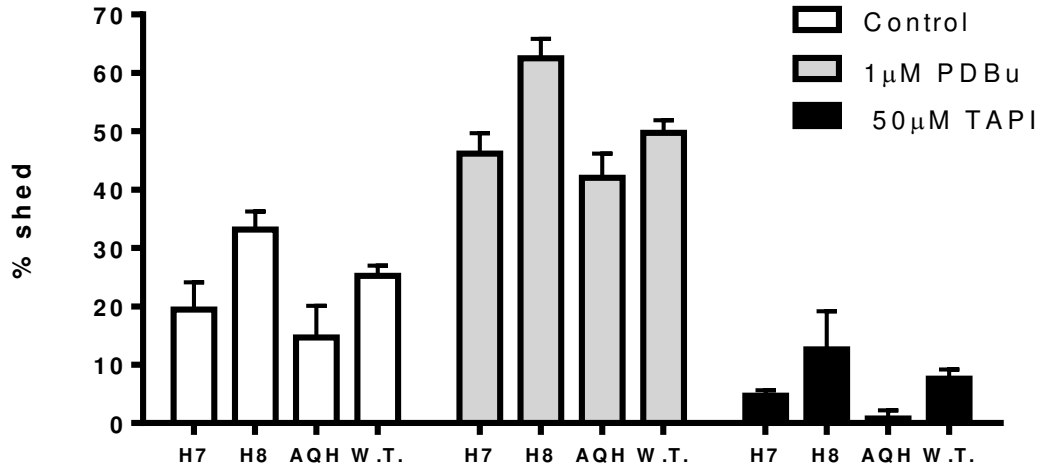

Figure 3.14: Comparison of shedding between mutants showing untreated control, stimulated (1μM PDBu) and inhibited (50μM TAPI) conditions. The abbreviations H7, H8, AQH and W.T. represent the constructs tACE H7, tACE H8, tACE AQH and tACE wild-type, respectively. Data represented are mean ±SEM, n=2.

3.4 Discussion

Previous work has alluded that a putative recognition motif within the distal ectodomain of testis ACE may be localised within the region D^{164}-V^{416}. However, this swop-over mutation encompassed 252 residues and resulted in a protein that was incorrectly processed, inactive and not shed. This region of ACE spatially influences the entire protein when viewing the three dimensional structure of ACE and would explain why such a substitution mutation with the N-domain residues would likely result in an inactive protein. The region includes the active site and two glycosylation sites. The various mutants made in the Woodman study (2006) were designed by following the compatible restriction sites between the C and N-domain, so as to essentially cover the entire ectodomain. They did not take the secondary structure of the protein into account in the design.

Therefore, in this study discreet mutations were made by focussing on regions of least homology between N- and C-domains, at the surface of the protein, regions with close proximity to the cleavage site (to increase the likelihood of interaction with the sheddase), and

to make sure that structural elements remained intact by referring to the secondary structure of ACE. Overlap PCR was successfully used to introduce a desired mutation by replacing C-domain residues with N-domain residues at helix 7 (figure 3.7). The mutation of helix 7 and helix 8 (figure 3.8) did not alter shedding significantly and the protein was processed to the cell surface as was seen in the western blot (figure 3.11 and figure 3.12), suggesting that these residues do not play a vital role in directing ACE shedding. The replacement of the three residue motif A^{261}QH immediately following α helix 8 with N-domain residues had the most notable influence on shedding. The alteration of the A^{261}QH reduced basal shedding, but the mutant was active and shed, and responded to the addition of PDBu (figure 3.13), which increased shedding. Within α helix 7, there was a mutation of M223W, which is within the chloride 2 pocket (Tzakos et al., 2003). This agrees with a more extensive investigation of a point mutation of this residue within tACE (C. Yates, PhD thesis 2012). There was no alteration in either shedding or ACE activity, indicating that this residue did not play essential role in the chloride activation of ACE. With these mutations we have made specific N-domain substitution mutants of residues within the region D^{164}-V^{416}, which has been previously identified as a potential sheddase recognition motif (Woodman et al., 2006). We have managed to produce chimeric mutants that are catalytically active and correctly processed by maintaining the structural integrity of the protein.

Other examples of proteins that show that ectodomains may contribute to their shedding are tumour necrosis factor (TNF-α) and L-selectin (Zhao et al., 2001; Zheng et al., 2004). These studies demonstrate the presence of a sheddase recognition motif within their ectodomains. TNF-α is cleaved by TNF-α convertase (TACE/ADAM 17) as well as ADAMs 9 and 10. The TNF-α ectodomain was shown to be responsible for selective stimulated cleavage by ADAM 17 (Zheng et al., 2004). L-selectin, a leukocyte transmembrane glycoprotein which undergoes slow, constitutive shedding and fast, stimulated shedding was also cleaved by ADAM 17 and it was shown that its EGF domain was essential for stimulated shedding (Zhao et al., 2001).

Having established a premise for the role of a sheddase recognition motif, it is necessary to discuss it in the context of alternative/additional regulatory mechanisms that influence shedding such as the dimerisation of ACE. Studies conducted in reverse micelles showed that homodimerisation occurs between the two molecules of sACE via their respective N-domains (Kost et al., 2003). Furthermore, dimerisation was blocked by monoclonal antibodies 9B9 and 3G8 (I V Balyasnikova et al., 2005; 2005b) whose epitopes were mapped to the N-terminal lid region of the N-domain, and were also found to influence shedding (Irina V Balyasnikova et al., 2005b). Deglycosylated ACE did not form dimers (Kost et al., 2003) and 9B9 increased shedding in the presence of 5mM galactose. Balyasnikova et al. (2005a) confirmed that 3G8 decreased the rate of shedding by 30% and 9B9 stimulated shedding by 2-4 fold. Further studies conducted by Gordon et.al. (2010) found that 3G8 is shielded by the C-domain and is carbohydrate dependant, establishing that the epitopes for 9B9 and 3G8 form the carbohydrate recognition motif that mediate dimerization. They also put forward a model where dimers occur via two interactions: namely, non-covalently linked dimers which occur through the N-domain and disulphide-linked dimerization which occurs via the C-domain (K. Gordon, PhD thesis 2011). Collectively, we can see that the epitopes involved in dimerization have a role in shedding as well.

In sACE, a cooperative effect may exist between the N- and the C-domains that could result in the inhibition of the accessible recognition motif for the sheddase, which does not occur in tACE. There are many scenarios where it would be possible to relate these events to the recognition motif. It could be possible that the dimerization of sACE does not allow accessibility to the sheddase, or even still causes a conformational change that prevents the recognition motif from being accessed. Another possibility would be that because the C-domain forms disulphide-mediated dimers and the N-domain non-covalent linked dimers, possibly via glycans, the C-domain or tACE is more susceptible to changes in the redox environment. It was shown that ADAM17 is modulated by protein disulphide isomerise (PDI), which keeps it in an inactive form (Bennett et al., 2000; Willems et al., 2010). Perhaps it is this chaperone (PDI) that is

required to mediate the disulphide bond rearrangement to facilitate an increase in shedding in tACE.

It is also encouraging that it has been hypothesised that many ADAMs or ADAM-like structures possess a non-catalytic region called the hypervariable region (HVR), said to be the sight of target recognition for ADAMs. Based on homologous structures found in the snake-venom homologue VAP1, it was shown that the HVR forms a disulphide bridge-stabilised fold that is highly conserved (Takeda et al., 2012, 2006). The authors put forward exciting models of the HVR region being the exosite contact with the substrate and thereby coordinating proteolysis at the cleavage site distal to the initial contact at the HVR. Once again, there is an indication that disulphide bonding may have a critical role in the interaction of the HVR and its substrate, thus giving further support to the theory that a change in the redox environment acts as the regulation switch in the shedding of ACE.

Another factor that may affect domain interactions and shedding is the complex glycosylation that ACE undergoes. There has been consistent effort into the construction of minimally glycosylated sACE, which aimed to reduce heterogeneity caused by glycans and promote the formation of protein crystals for the crystal structure determination of sACE. However, it was shown that when the number of *N*-linked glycans was reduced in sACE, there is an increase in cleavage in the interdomain linker region of sACE (Anthony C., PhD thesis, 2011). It was proposed that this was attributable to the lack of glycans protecting the linker region. These results shed new light on the analysis of the previously mentioned CC-domain construct. This protein consisted of two C-domains joined by the linker region and were shown to be cleaved within the linker as well as the stalk (Woodman et al., 2005). This led to the assertion that the presence of a sheddase recognition domain in the C-domain directed cleavage in both the linker region and stalk. Alternatively, one can argue that considering that the C-domain had less glycosylation (6 sites) than the N-domain (9 sites), that it was cleaved in the bridge region. Yu et. al. (1997) showed that endoproteinase Asp-N cleaved sACE in the linker region between T^{615} and D^{616}, suggesting that this region was more susceptible to proteolysis. It was also found that

a non-glycosylated cellulose degrading enzyme from the bacterium *C.fimi* undergo autolysis, which is not seen in the fully glycosylated form, indicating that glycosylation offers protection against degradation. If the explanation for the cleavage within the bridge region is that either the lack of glycans no longer protects the bridge region or that the conformational change that results from having two C-domains creates greater accessibility for the sheddase, we would then need to further discuss the contribution of glycans to sACE stability as well as the steric relationship between the N-and the C-domain and how it relates to shedding.

Based on previous work, we have further dissected the tACE ectodomain in an attempt to identify the sheddase recognition motif. We did not conclusively identify a region within the tACE/C-domain that, when substituted with the N-domain, significantly altered its rate of shedding. We have thus furthered our body of knowledge about the structural contribution that the distal ectodomain of tACE has made. We have succeeded in making swop over mutations that resulted in active and fully processed ACE proteins whereby shedding can still be analysed and we have managed to maintain the structural integrity of ACE by following the structural boundaries based on the published crystal structure. Considering that mutating exact secondary structure elements of tACE did not have a dramatic effect on its shedding, we refocused our attention (chapter 4) on the proximal ectodomain of ACE and its stalk region.

CHAPTER 4: Role of the proximal ectodomain and stalk region of tACE in the shedding of ACE

4.1 Introduction

We have previously discussed the stalk and ectodomain contributions to the regulation of the shedding of ACE. In this chapter we revisit the important findings of Sadhukhan et al. (1998) that showed when the ectodomain and stalk regions of CD4 were swopped with the ectodomain or stalk region of testis ACE, the CD4-ACE chimera consisting of the ACE ectodomain and CD4 stalk was cleaved within the CD4 stalk region. CD4 is a membrane protein that is not usually cleaved from the membrane, hence these experiments proposed there were elements in the ACE ectodomain directing a protease to cleave the stalk region and shed the protein from the membrane. It must also be reiterated that sACE shedding is inefficient compared to tACE as it was suggested to be due to the N-domain shielding the C-domain or stalk (Beldent et al., 1995). The binding of ACE monoclonal antibodies that modulate its rate of shedding demonstrated that certain regions may be involved in shedding (Balyasnikova et al., 2005a; Balyasnikova et al., 2005b; Gordon et al., 2010; Kost et al., 2003). It was however the ACE-CD4 study conducted by Sadhukhan et al. (Sadhukhan et al., 1998) that prompted further exploration of the distal ectodomain of ACE for a sheddase recognition motif (Pang et al., 2001; Woodman et al., 2006, 2005)(Chapter 3 of this thesis).

Further experiments by the same group (Sadhukhan et al., 1998) sought to delineate which region/s of the ectodomain were involved in the sheddase recognition by making chimeric mutants of the ACE and CD4 ectodomains (Chattopadhyay et al., 2008). They initially tried to make sequential deletions of the rabbit tACE ectodomain, but this affected processing to the cell surface and they therefore chose to use chimeric proteins instead. The region of ACE that was required for processing and shedding was residues 343-655 (rabbit tACE numbering). A mutant that contained ACE residues 1-655 was secreted into the medium but when the ectodomain was further restricted to residue 640, the protein was expressed in cells but was not secreted, indicating that residues 640-655 were important for shedding.

They then performed alanine scanning mutagenesis on this 15 residue region and established that the 5 residue motif HGEKL attenuated cleavage secretion when these residues were changed to alanines (Chattopadhyay et al., 2008). The 5 residue mutation in sACE had a similar effect, suggesting that it directs cleavage secretion in the single and double domain forms of rabbit ACE. The constructs were expressed in *Pichia pastoria* as well as HeLa cells, showing that they are processed in yeast cells as well as mammalian. It was these key experiments that encouraged our investigation of the role of this 5 amino acid motif HGEKL in human tACE.

The potential rabbit tACE recognition motif within the proximal ectodomain is underlined in figure 4.1. The stalk region starts at residue W^{616} (Chubb et al., 2002). It can be seen that it is 17 residues N-terminal of the cleavage site, 13 residues N-terminal to P^{623} and 10 residues N-terminal to the seventh potential glycosylation site of the C-domain. Therefore, the region directly proximal to the cleavage has many important hallmarks. Considering Pro623/1199-Leu polymorphism was associated with a 5-fold increase in shedding (Kramer et al., 2001), we extended our investigations of the stalk region to determine whether glycosylation of the N^{620} occurs when the L is present at 623 instead of P.

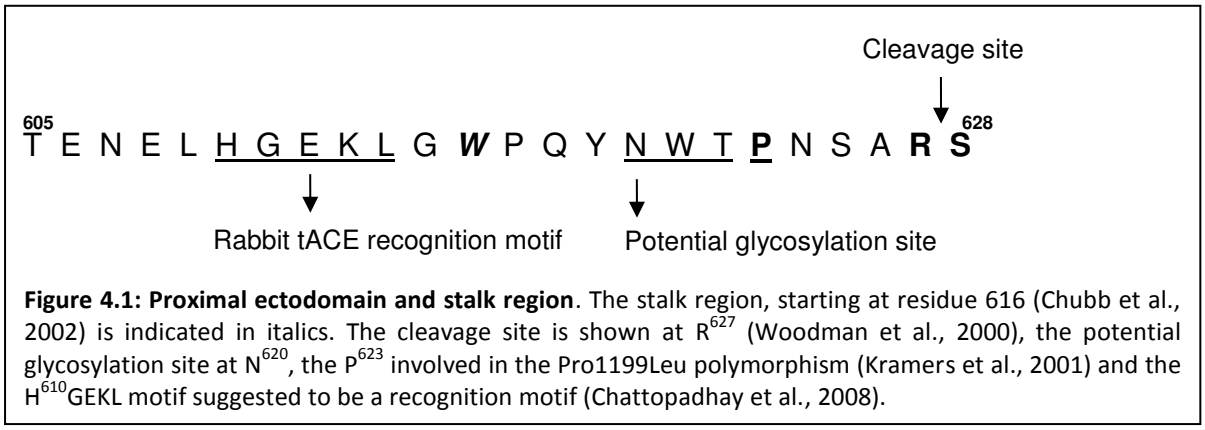

Figure 4.1: Proximal ectodomain and stalk region. The stalk region, starting at residue 616 (Chubb et al., 2002) is indicated in italics. The cleavage site is shown at R^{627} (Woodman et al., 2000), the potential glycosylation site at N^{620}, the P^{623} involved in the Pro1199Leu polymorphism (Kramers et al., 2001) and the H^{610}GEKL motif suggested to be a recognition motif (Chattopadhay et al., 2008).

Eyries et al. (2001) conducted further investigations into this polymorphism by generating a sACE P^{1199}L variant as well as a C-domain variant. In both CHO-K1 and COS cell lines the P^{1199}L mutant was shed 1.5-fold higher than wild-type. It would seem, from the in vitro data that the introduction of the proline has a significant effect on shedding. Based on their 2D structural analysis, it was suggested that proline induces conformational constraints by forming twists in the structure. Leucine, on the other hand, is more flexible and possibly

released the stalk from the restricted formation, allowing for better access by the sheddase. This plasma ACE polymorphism substantiated the theory of the stalk being more important for cleavage secretion than the cleavage site sequence; however the CD4/ACE (Sadhukhan et al., 1998) mutants still alluded to the contribution of the ectodomain to the regulation of shedding.

These tie in with the suggestions made by Ehlers et al., (1996), which suggested the cleavage secretion process to be dependant on topographical parameters. The removal of the proline could also allow for the normally unglycosylated N^{620} (Yu et al., 1997) (figure 4.1), to be glycosylated. This pattern of residues has been extensively researched and using peptides containing proline at various positions, it was shown that proline positioned C-terminal to the N-glycosylation recognition sequence of Asn-Xaa-Thr (Ser) (Bause and Legler, 1981; Marshall, 1974) resulted in highly diminished glycosylation (Bause, 1983) as it changes the conformation of the peptide and affects the potential of glycans attaching. An introduction of a glycan in this region could perhaps re-direct the sheddase to a more favourable position and thus increase shedding, as shown when an O-glycosylated region was introduced into the stalk region (Schwager et al., 1999). Furthermore, basal shedding was increased, but stimulated shedding was reduced, suggesting that the glycosylation in the stalk did not abrogate shedding but modulated its regulation.

Therefore our aim was to analyse the ectodomain most proximal to the cleavage site as well as the stalk region, by testing the effect of mutating the rabbit tACE motif in human tACE. We created and analysed the following mutant cDNA tACE constructs: pcDNA tACE Ala 610-614, pcDNA tACE Ala 608-614, pcDNA tACE Ndom 608-614, pcDNA tACE Pro623Leu and pcDNA tACE N620D (figure 4.2). These constructs were made to determine whether alanine mutations in the human testis ACE would affect shedding. The latter two stalk mutants were made to address the contribution of glycosylation in shedding and whether the increase in shedding by the $P^{623}L/P^{1199}L$ polymorphism is caused by glycosylation of the potential site at N^{620}.

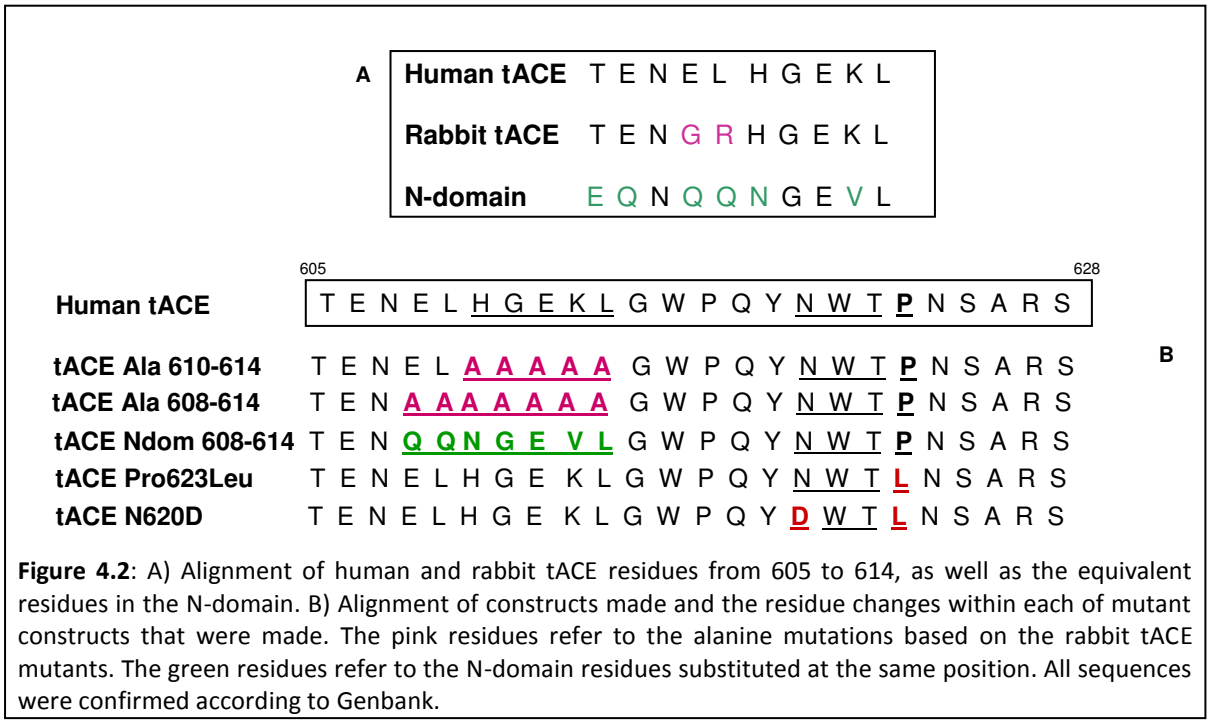

Figure 4.2: A) Alignment of human and rabbit tACE residues from 605 to 614, as well as the equivalent residues in the N-domain. B) Alignment of constructs made and the residue changes within each of mutant constructs that were made. The pink residues refer to the alanine mutations based on the rabbit tACE mutants. The green residues refer to the N-domain residues substituted at the same position. All sequences were confirmed according to Genbank.

Objectives:

1. To mutate the rabbit tACE motif H^{610}EGKL to alanines in human tACE to elucidate its role in shedding

2. To analyse the effect of a longer motif 7 residue on shedding and comparison between Ala substitutions and N-domain substitutions

3. To investigate the mechanism of shedding when a polymorphism such the Pro1199Leu is present in testis ACE ascertain whether glycosylation plays a role in the increase in the shedding when the Pro1199Leu polymorphism is present in the stalk region of tACE

4.2 Materials and Methods

4.2.1 Site-directed mutagenesis of pcDNA tACE Ala610-614, pcDNA tACE Ala 608-614, pcDNA tACE Ndom 608-614, pcDNA tACE Pro623Leu, pcDNA tACE N620D

All constructs were generated from tACE gene fragment in a pGEM -Z11f (-) vector. All primers are detailed in the appendix, table A3.4. tACE Ala610-614 was synthesised using the tACE ALA For and Rev primers. Ndom 608-614 was produced with the tACE ST _Ndom F and tACE ST _Ndom R primers and tACE Pro623Leu were synthesised with the P2LF and P2LR primers. The template DNA for these mutants were wild-type tACE. tACE Ala 608-614 was produced with the tACE ala2F and tACE ala2R primers. The DNA template used for this mutant was the pGEM tACE Ala610-614 mutant so that an additional 2 alanine residues were added upstream of residues 608 and 609. tACE N620D was produced with the primers P2LDF and P2LD R using pGEM tACE Pro623Leu as the DNA template to produce a double mutant containing leucine at position 623 and convert the asparagine 620 to aspartate to knock out the glycosylation sequon.

After confirmation of all mutant constructs by DNA sequencing, the entire tACE DNA fragment was removed from the respective pGEM –Z11f (-) construct by digesting it with BamHI and HindIII, and allowed to ligate with similarly digested mammalian expression vector pcDNA 3.1 (-). These pcDNA constructs were transformed into E.coli as previously described (Chapter 2, section 2.1.8) and prepared in bulk for CHO-K1 cell transfection by growing them in Luria broth. The DNA was extracted using the Qiagen Midi Plasmid Preparation Kit (Germany). CHO-K1 cells were transfected as previously described (chapter 2, section 2.2.3). Shedding assays, ACE activity assays and western blot analysis are detailed in chapter 2.

4.2.2 Purification of soluble pcDNA tACE Pro623Leu

The tACE Pro623Leu transfected CHO-K1 cells were propagated in 150mm^2 tissue culture flasks in growth medium (10% FCS/DMEM/HAMS). Once 100 % confluent the medium was changed to minimal medium (2% FCS/DMEM/HAMS). Soluble tACE protein was secreted

into the medium and after approximately 2 days the protein-containing medium was harvested and stored at -20°C for later use. This was repeated until approximately 350-375ml of medium was collected. Before the various harvests were pooled the activity was checked via ZPHL assays.

tACE Pro623Leu was purified via affinity chromatography using a lisinopril-sepharose column (Pantoliano et al., 1984). It was equilibrated first with wash buffer (0.5M NaCl, 20mM HEPES, pH 7.5, appendix I). All medium and reagents were passed over column with the aid of a Minipuls 3 pump (Gilson, France). The pooled medium was passed over the column and allowed to bind. The column was washed overnight with 1 litre of wash buffer to clear away unbound protein. The flow-through was retained for later analysis. Bound ACE was eluted from the column with 50 mM borate buffer, pH 9.5. The elution of ACE from the column was monitored at 280nm via a DVW-10 variable wavelength detector (Ross Recorders, USA) and fractions containing the protein were pooled and assayed for ACE activity to confirm the presence of the correct protein. Purified protein was initially dialysed at 4°C overnight in 50mM KPO_4, thereafter in 5mM KPO_4 for 1 hour to facilitate downstream analysis. The protein was concentrated in Amicon® Ultra Spin centrifugal filters (Millipore, Cork, Ireland). Protein concentrations before and after purification were determined via the Bradford method (Bradford, 1976).

4.2.3. PNGase F digest and protein preparation

Approximately 20µg of tACE Pro623Leu was incubated with 5µl of 100 units/ml PNGase F (Sigma-Aldrich) and 5µl of 5x denaturing buffer (250mM KPO_4 pH.8, 1% SDS (w/v) and 5% β-mercaptoethonal) at 37°C overnight. The entire reaction volume was loaded onto a 10% SDS PAGE alongside an undigested control. The gel was stained with Coomassie (0.2% (w/v) Coomassie Blue; 7% (v/v) glacial acetic acid; 50% (v/v) ethanol) and then destained (7% (v/v) glacial acetic acid; 50% (v/v) ethanol). The desired band was cut out with a scalpel and cut up into 1mm x 1mm x 2mm pieces.

4.2.4 MALDI MS/MS

The gel pieces were destained with 200mM NH_4HCO_3: acetonitrile 50:50 (Romill, Sigma) until clear. The gel slices then underwent dehydration and dessication before reduction in

5mM triscarboxyethyl phoshine (TCEP, Fluka) in 100mM NH_4HCO_3 for 30 minutes at 56°C. Before a further dehydration step, excess TCEP was removed. Carbamidomethylation of cysteines were done with 100mM iodoacetamide (Sigma) in 100mM NH_4HCO_3 for 30 minutes at room temperature with no light exposure. This prevents disulphide bonds from forming. The gel pieces were dehydrated, washed with 50mM NH_4HCO_3, and then dehydrated again. It was rehydrated in a 20ng/µl trypsin (Promega) solution and digested overnight at 37°C. The resultant trypsin-digested peptides were recovered with 50µl 0.1% trifluoroacetic acid (TFA) (Sigma). Thereafter they were dried down, 50µl of water was added and then concentrated to 20µl or less which removed residual NH_4HCO_3. These peptides were then ready to be spotted using the dried droplet technique (Dai et al., 1996). 0.5 µl of the sample was overlaid twice. The matrix used consisted of 10mg/ml α–cyano-4-hydroxycinmamic acid (Fluka) with 20mM $NH_4H_2PO_4$ (Fluka) in 80% acetonitrile, 0.2% TFA. The final concentrations were 5mg/ml of matrix in 40% acetronitrile, 0.1% TFA and 10mM $NH_4H_2PO_4$.

MALDI MS/MS was performed at the CPGR (Cape Town). The 4800 MALDI ToF/ToF (Applied Biosystems) was used for all mass spectrometry. The MS spectra were recorded in reflector mode, generated with 400 laser shots/spectrum, at a laser intensity of 3800 (arbitrary units) and with a grid voltage of 16kV. Internal calibration of peptide containing spots was measured against trypsin autolytic fragments.

4.3 Results

Residues within the stalk region and ectodomain have been extensively studied to determine their contribution to the regulation of ACE shedding. Recent evidence has shown that the portion of the ectodomain proximal to the stalk region is essential in the shedding of rabbit ACE (Chattopadhyay et al., 2008). Mutants were made to investigate the contribution of the residues H^{610}GEKL in the shedding of human ACE and to investigate the contribution of glycosylation to the increase in shedding of the Pro1199Leu polymorphism. In order to analyse the role of the rabbit tACE recognition motif in human testis ACE, the corresponding residues were mutated to alanines in human tACE using site-directed

mutagenesis and its effect analysed via western blot analysis and ACE activity assays. The construct tACE Ndom 608-614 provided a control for tACE Ala 608-614; the construct with 7 alanines (figure 4.2). The following results will elucidate how the alanines contribute to the changes in shedding.

4.3.1 Site-directed mutagenesis and cloning of pcDNA tACE Ala610-614, pcDNA tACE Ala 608-614, pcDNA tACE Ndom 608-614, pcDNA tACE Pro623Leu and pcDNA tACE N620D

After mutagenesis, successful incorporation/substitutions of residues were analysed by restriction endonuclease digestion and agarose gel electrophoresis (chapter 2). tACE Ala 610-614 has the 5 residues H^{610}GEKL mutated to alanines and with the mutation another NheI restriction enzyme site was introduced, due to the introduction of the new site included via the mutagenic primers. In the wild-type construct there are two present, one within the vector sequence and one within the tACE sequence. In figure 4.3, it can be seen that restriction digestion with NheI of the wild-type construct (lane 1) would yield two DNA fragments of approximately 6.5kb and 1.4kb. The addition of the third site in the mutant construct results in the emergence of three bands 5.91kb, 1.4kb, 0.59kb (lane 2) confirming the correct incorporation of the desired sequence.

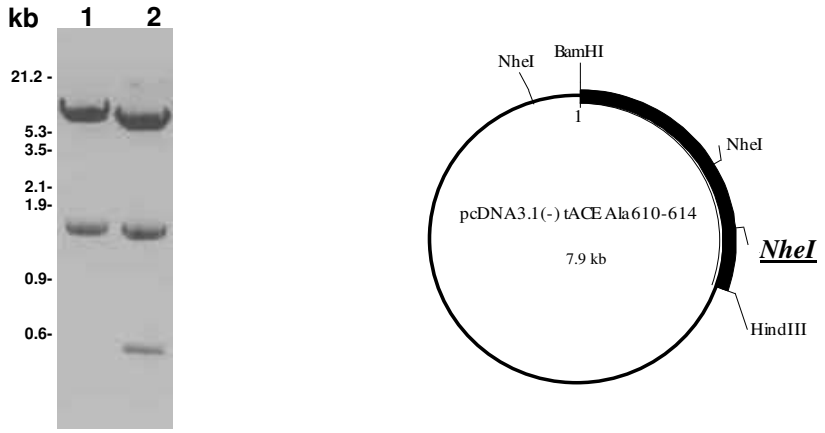

Figure 4.3: Restriction digest and plasmid map of pcDNA 3.1 (-) tACE Ala 610-614. On the left is a DNA gel of NheI digests of wild-type tACE (lane 1) and tACE Ala 610-614 (lane 2). The plasmid map highlights the endogenous restriction enzyme sites pertinent to the construct. The underlined italicised NheI site was introduced to aid in the screening of the mutation that was introduced.

Similarly, in figure 4.4, it can be seen that the addition of the BsmI site in the tACE Ala 608-614 mutant results in two DNA fragments when digested; namely a 5.1kb and a 2.8kb

fragment compared to the 7.9kb fragment for the linearised wild-type construct (lane 1), as it only has one Bsm I site in the vector sequence. tACE Ala 608-614 was produced by conducting site-directed mutagenesis on the pGEM tACE Ala 610-614 DNA template with the tACE ala 2F and 2R primers to extend the mutation to 7 alanines.

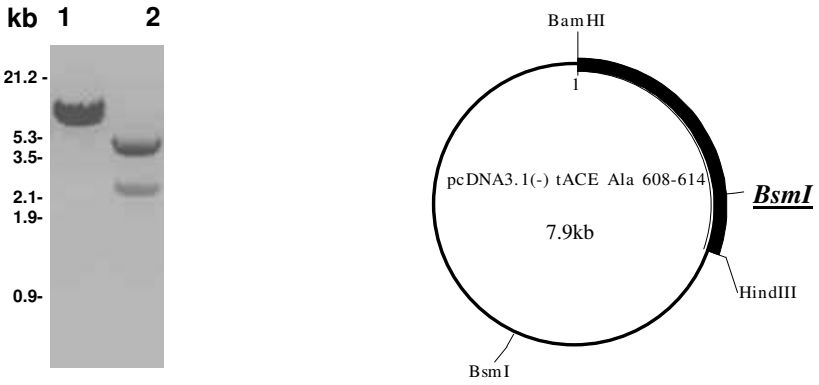

Figure 4.4: Restriction digest and plasmid map of pcDNA 3.1 (-) tACE Ala 608-614. On the left is a DNA gel of BsmI digests of wild-type tACE (lane 1) and tACE Ala 608-614 (lane 2). The plasmid map highlights the restriction enzyme sites. The underlined italicised BsmI site was introduced to aid in the screening the mutation that was introduced.

For the introduction of the N-domain residues at position 608-614, a ScaI site was included with the mutation. The two fragments that were produced after digestion with this enzyme were 4.56kb and 3.34kb in size (figure 4.5**,** lane 2), compared to the single DNA band of 7.9kb (lane 1) in size which represents the linearised form of the wild-type construct as it only had one ScaI site. These results indicate that the mutation was successfully incorporated.

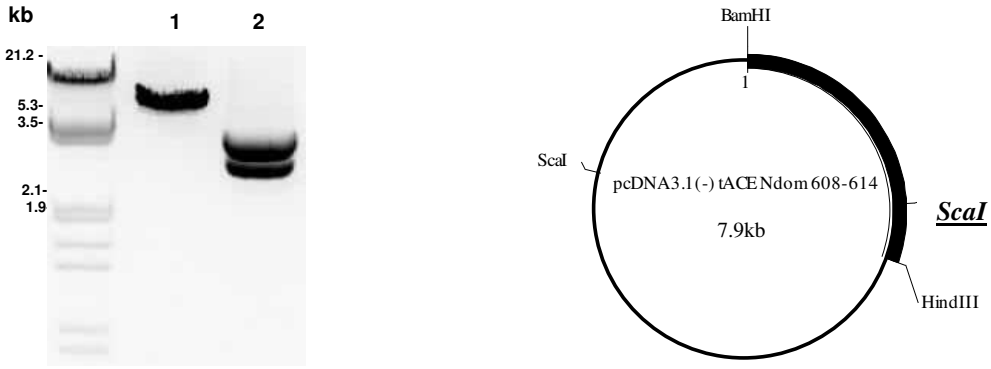

Figure 4.5: Restriction digest and plasmid map of pcDNA 3.1 (-) tACE Ndom 608-614. On the left is a DNA gel of ScaI digests of wild-type tACE (lane 1) and tACE Ndom 608-614 (lane 2). The plasmid map highlights the restriction enzyme sites pertinent to the construct. The underlined italicised ScaI site was introduced to aid in the screening of the mutation that was introduced.

The $P^{623}L$ mutation mimics the polymorphism that results in increased shedding. pcDNA 3.1 (-) tACE has two EcoRI sites, one in the vector sequence upstream of the BamHI site and one preceding the HindIII site, which are the restriction sites that flank the tACE DNA insert and were used to subclone tACE from pGEM 117 (-) f into pcDNA 3.1 (-). Therefore digestion with EcoRI yielded a 2.5kb and a 5.4kb fragment corresponding to the tACE insert and the plasmid respectively (figure 4.6, lane 1). The inclusion of another site with the substitution of P^{623} with L resulted in the 2.5kb fragment being split into 2kb and 0.5kb fragments.

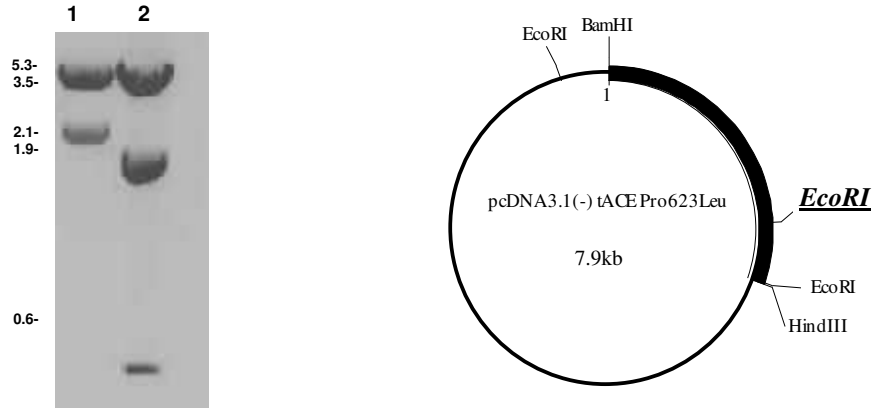

Figure 4.6: Restriction digest and plasmid map of pcDNA 3.1 (-) tACE Pro623Leu. On the left is a DNA gel of EcoRI digests of wild-type tACE (lane 1) and tACE Pro623Leu (lane 2). The plasmid map highlights the restriction enzyme sites. The underline italicised EcoRI site was introduced to aid in the screening the mutation that was introduced.

The enzyme used to screen the mutation for the conversion of N^{620} to D was Eco47III, which was present singularly in wild-type tACE. This generates a mutant that had the glycosylation site N620 knocked out. Thus digestion with this enzyme for wild-type tACE results in a single fragment of 7.9kb in size (figure 4.7, lane 1). In lane 2, the emergence of two fragments sized 6.4kb and 1.5kb compares favourably with the introduction of the correct mutation for pcDNA tACE N620D.

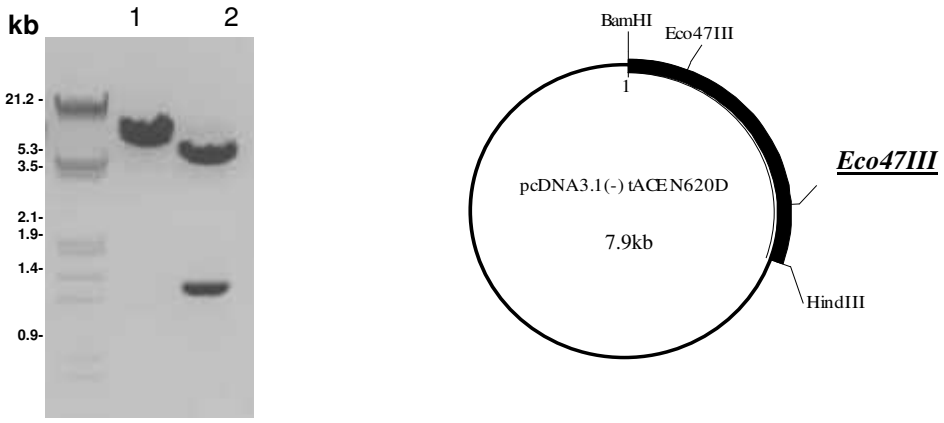

Figure 4.7: Restriction digest and plasmid map of pcDNA 3.1 (-) tACE N620D. On the left is a DNA gel of Eco47III digests of wild-type tACE (lane 1) and tACE N620D (lane 2). The plasmid map highlights the restriction enzyme sites pertinent to the construct. The underlined italicised Eco47III site was introduced to aid in the screening of the mutation that was introduced.

4.3.2 Expression and activity of stalk/proximal ectodomain mutants

The shedding behaviour of tACE and its mutant derivatives were analysed by measuring their ACE activity in the medium and cell lysates and thus the ratio of the ACE activity in the medium over the total ACE activity (i.e. medium and cell lysates) acts as an indication of how much of the cell-anchored ACE was released from the cell membrane. Western blots provided a visual representation of the shedding activity as well as to confirm the size of the protein. In addition, the total ACE activity under each condition analysed was calculated. Wild-type testis ACE was previously discussed and how it differs from previous reports (chapter 3). It was also necessary to highlight the total activity that was present for tACE and how the other mutants are affected in this regard as changes in the total activity (the mU of ACE activity per millilitre of culture medium produced in one minute) was more evident than in the rate of shedding.

With the introduction of the alanines at residues 610-614 (figure 4.9), the rate of shedding is not affected if one compares the percentage shed of tACE Ala610-614 to wild-type under basal or untreated conditions (figure 4.8). In figure 4.9 B, the shedding of tACE Ala 610-614 appears to be normal at approximately 30%. However, the western blot analysis (figure 4.9, A) shows that there are two forms of the protein, one representing the correctly processed form that migrates alongside wild-type tACE and perhaps an underglycosylated band that migrates below it. It can be seen that there is a much lower proportion of the correctly

processed form and only the shed form comes from this population. The total activity was also much lower than wild-type (figure 4.9, C), which corroborates what was seen in the western blot. Therefore the alanine mutation affects the processing greatly and reduces the amount of protein available for shedding. The basal shedding of this mutant was higher than wild-type so it would seem that what little ACE was available at the cell surface was shed quite well, in addition to having a discernible increase in shedding in response to the addition of the phorbol ester PDBu. Therefore this mutation affected processing more than shedding under the conditions set out here.

The effects of the alanines at H^{610}EGKL were exacerbated when the mutation was extended a further 2 residues upstream to residues E608 and L609. Under unstimulated conditions, the total activity of tACE Ala 608-614 (figure 4.10, C) was reduced to 1.5mU/ml/min compared to tACE Ala 610-614 (2.5mU/ml/min, figure 4.9, C) and greatly reduced compared to tACE wild-type (14mU/ml/min, figure 4.8, C)**.** Basal shedding was markedly diminished, but the phorbol response was still highly apparent (figure 4.10, B). The western blot again showed that the shed protein in the medium samples migrated with the fully processed form that also migrated alongside the wild-type ACE (figure 4.10, A). The cell lysates had two protein bands and the greater proportion of the membrane-bound form was migrating

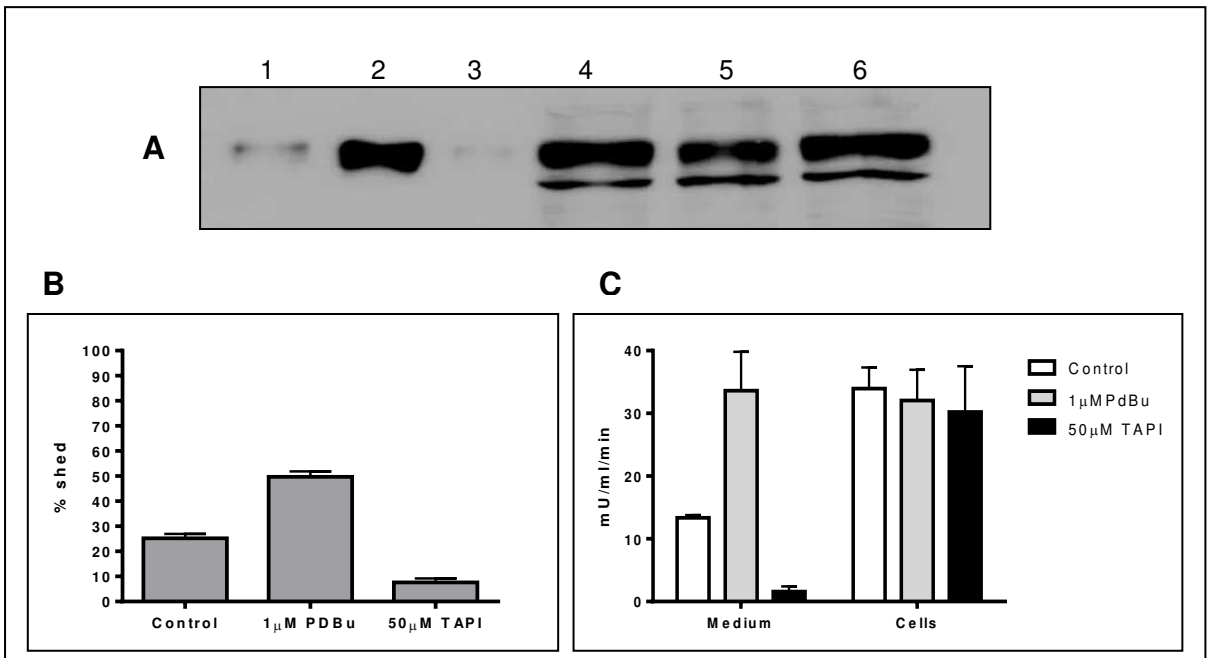

Figure 4.8: Shedding analysis of pcDNA tACE. A) Western blot: Lane 1: control, medium; lane 2: 1μM PDBu added medium; lane 3: 50μM TAPI added medium; lane 4: control, cell lysate; lane 5: 1μM PDBu, cell lysate; lane 6: 50μM TAPI, cell lysate. B) Activity assays showing percentage shed ACE of total ACE activity. C) Total activity. Data represented are mean ±SEM, n=2.

lower than the normal wild-type form.

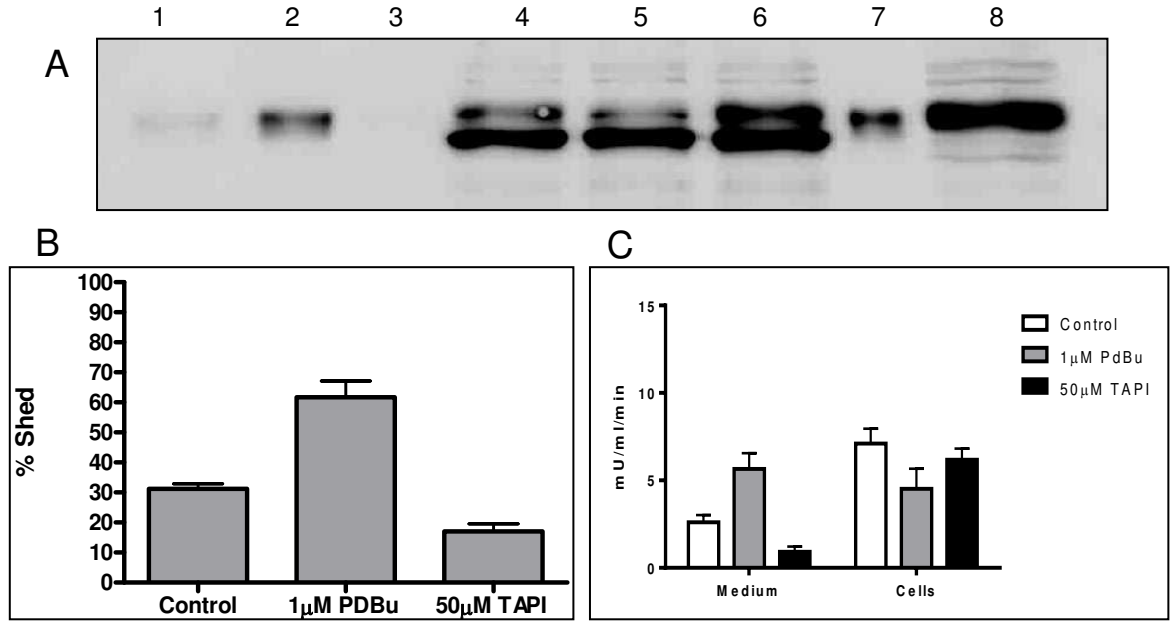

Figure 4.9: Shedding analysis of pcDNA tACE Ala610-614. A) Western blot: Lane 1: control, medium; lane 2: 1μM PDBu medium; lane 3: 50μM TAPI medium; lane 4: control, cell lysate; lane 5: 1μM PDBu, cell lysate; lane 6: 50μM TAPI, cell lysate; lane 7: w.t tACE medium; lane 8: w.t. tACE cell lysate. B) Activity assays showing percentage shed ACE of total ACE activity. C) Total activity. Data represented are mean

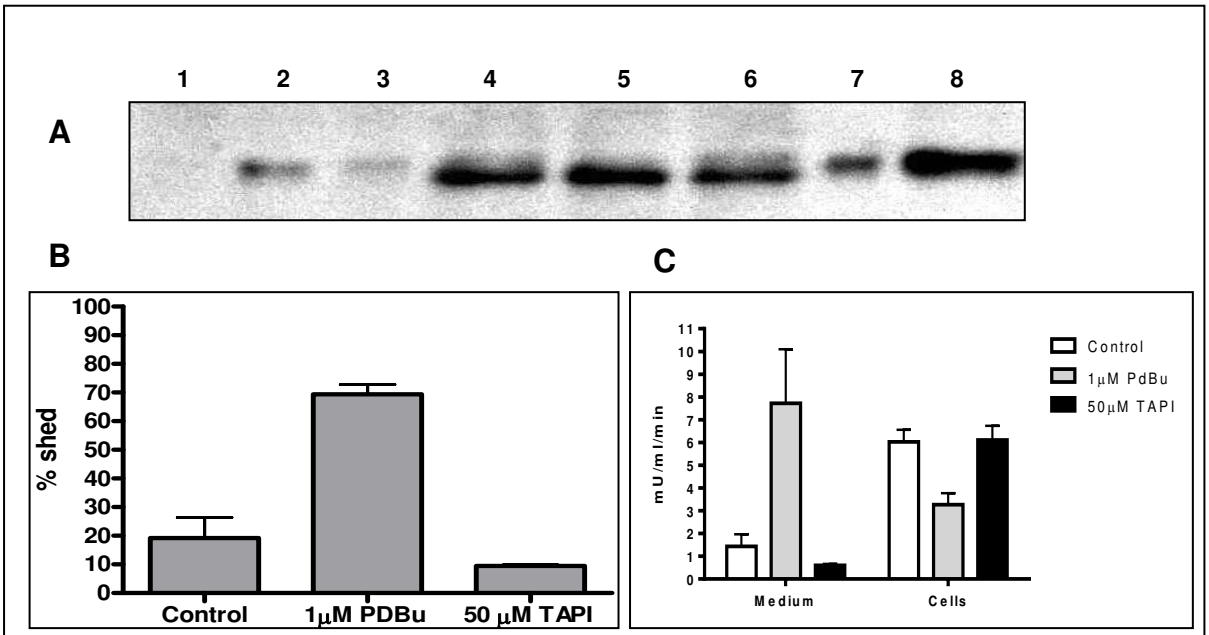

Figure 4.10: Shedding analysis of pcDNA tACE Ala 608-614. A) Western blot: Lane 1: control, medium; lane 2: 1μM PDBu added medium; lane 3: 50μM TAPI added medium; lane 4: control, cell lysate; lane 5: 1μM PDBu, cell lysate; lane 6: 50μM TAPI, cell lysate; lane 7: w.t tACE medium; lane 8: w.t. tACE cell lysate. B) Activity assays showing percentage shed ACE of total ACE activity. C) Total activity. Data represented are mean ±SEM, n=2.

The effect alanines have on shedding and processing is not replicated when the residues 608-614 are converted to the corresponding N-domain residues and not alanines. According to the western blot, expression of tACE NdomST 608-614 in CHO-K1 cells (figure 4.11, A) resulted in a greater proportion of the ACE protein that was in the correctly processed form as well as was shed normally. Overall activity and basal shedding is slightly lower than wild-type but still comparable. This would imply that the N-domain residues have the necessary molecular requirements to maintain shedding and processing as opposed to alanines.

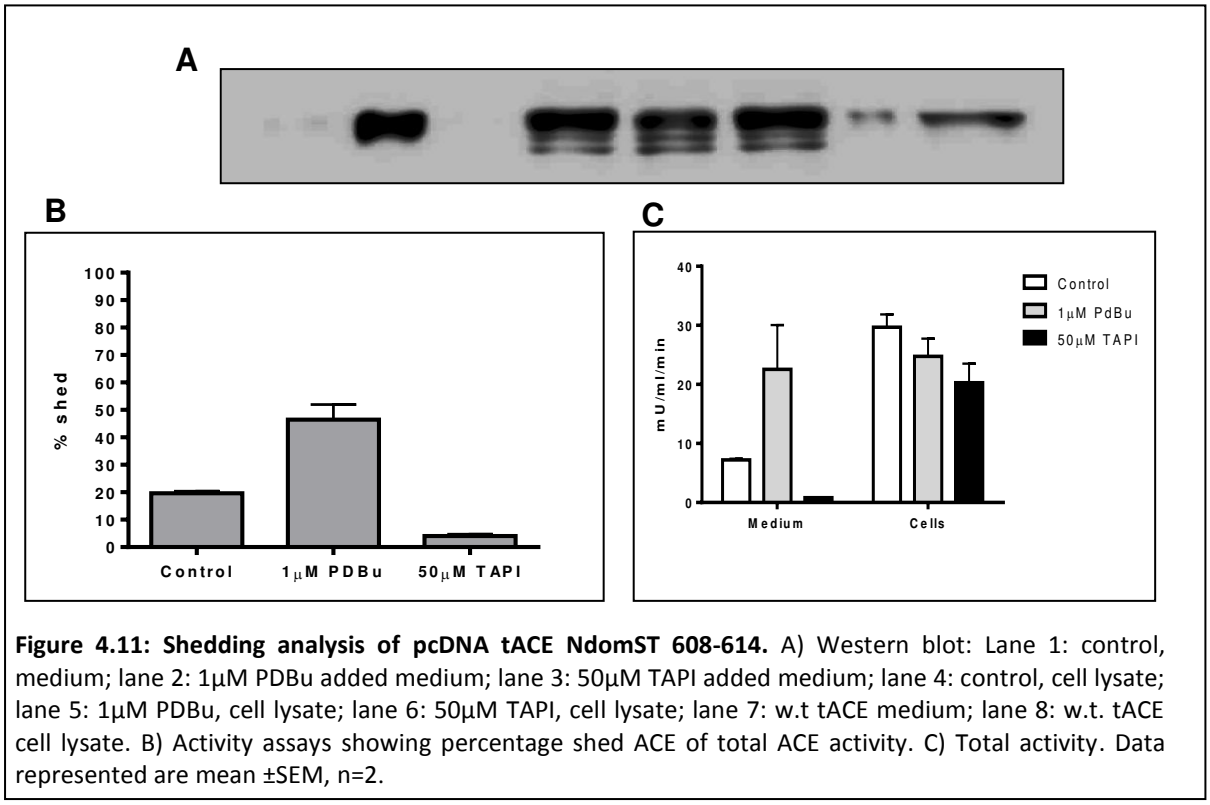

Figure 4.11: Shedding analysis of pcDNA tACE NdomST 608-614. A) Western blot: Lane 1: control, medium; lane 2: 1μM PDBu added medium; lane 3: 50μM TAPI added medium; lane 4: control, cell lysate; lane 5: 1μM PDBu, cell lysate; lane 6: 50μM TAPI, cell lysate; lane 7: w.t tACE medium; lane 8: w.t. tACE cell lysate. B) Activity assays showing percentage shed ACE of total ACE activity. C) Total activity. Data represented are mean ±SEM, n=2.

In addition, the total activity under basal conditions is somewhat restored as it is 3-fold that of the tACE Ala 610-614 and 5-fold that of tACE Ala 608-614 (figure 4.10, C). These results would suggest the residues H^{610}EGKL proposed by Chattophadhay et al., (2008) as a sheddase recognition motif has an effect on shedding in human tACE as well as processing. The 2-residue extension of this mutation upstream reduced basal shedding even more, and cellular processing was negatively affected. The presence of N-domain residues at these positions, however, allowed for the maintenance of processing and shedding occurred as

normal. This indicates that this motif is important for shedding and processing, but in relation to previous work, this is not the sole recognition motif of ACE.

4.3.3 Characterisation of pcDNA tACE Pro623Leu

Previous work has shown that the presence of L instead of P at position 1199 (sACE) or 623 (tACE) increases shedding up to 5-fold in serum and 1.5 fold in vitro (Eyries et al., 2001; Kramers et al., 2001). The explanation for this increase was that leucine creates a more flexible loop allowing access to the cleavage site by the sheddase. We made this mutation in human tACE to ascertain whether the increase in shedding was rather due to the glycosylation of the sequeon Asn-Trp-Thr (NWT) upstream of P^{623}. This motif is the final potential glysosylation site within tACE, but usually remains unglycosylated due to the P that follows the sequon (Yu et al., 1997). Mass spectral analysis of purified and de-glycosylated tACE Pro623Leu was performed to test whether the increase in shedding of the P to L polymorphism was due to glycosylation and whether the cleavage site changed.

4.3.3.1 Determination of increased shedding of tACE Pro623Leu

tACE Pro623Leu was expressed in CHO-K1 cells and the effects of this mutation on shedding were determined. The mutation increased basal shedding to 35% (figure 4.12, B). There was only a 15% increase above wild-type tACE (figure 4.6), yet within the range observed previously (Eyries et al., 2001a). Shedding of the $P^{623}L$ mutant did not display the same magnitude increase in shedding as was found in serum (Eyries et al., 2001b; Kramers et al., 2001). Western blot analysis confirmed that there was an increase in basal shedding over wild-type (figure 4.10, A). This confirmed that basal shedding was increased when this mutation was incorporated in tACE.

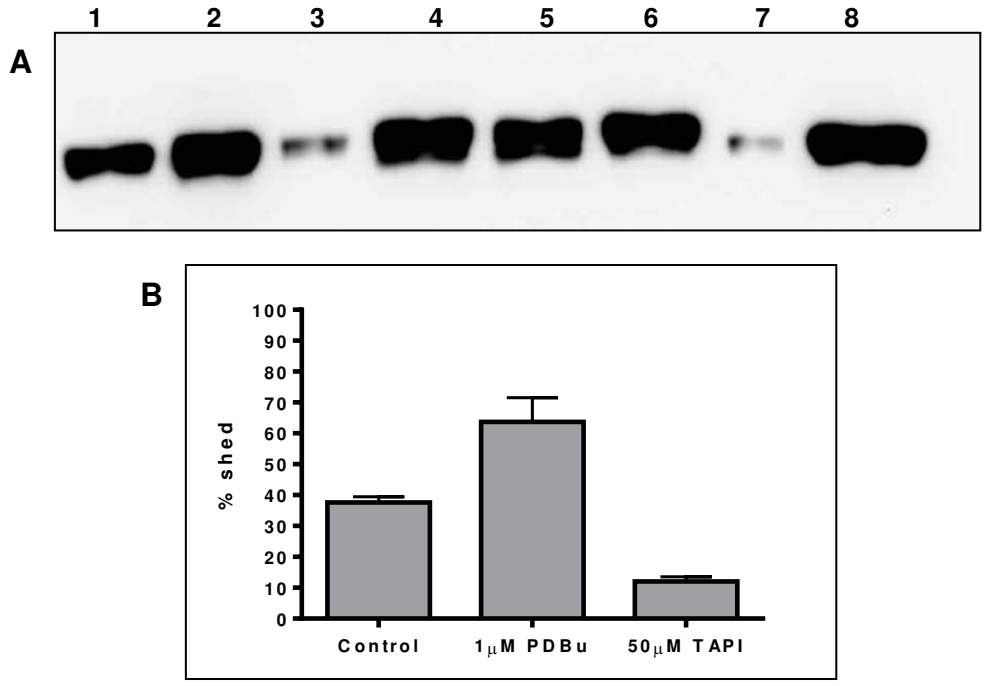

Figure 4.12: Shedding analysis of tACE Pro623Leu. A) Western blot: Lane 1: control, medium; lane 2: 1μM PDBu added medium; lane 3: 50μM TAPI added medium; lane 4: control, cell lysate; lane 5: 1μM PDBu, cell lysate; lane 6: 50μM TAPI, cell lysate; lane 7: w.t tACE medium; lane 8: w.t. tACE cell lysate. B) Activity assays showing percentage shed ACE of total ACE activity. Data represented are mean ±SEM, n=2.

4.3.3.2 Purification, treatment and preparation of soluble tACE Pro623Leu

To determine the presence of glycosylation at position N620 and to explore the role of glycosylation in the increase in shedding of the Pro^{623}Leu polymorphism, the tACE Pro623Leu protein was purified (appendix A4.1, A4.2), deglycosylated and analysed via SDS-PAGE. After a shift in size was confirmed on the gel, the protein was eluted from the gel, underwent reduction and cysteine protection, and then an in-gel trypsin digest was performed, where after it was subjected to MALDI analysis. The serine protease, trypsin, cleaved the protein after every lysine and arginine resulting in distinct peptides that were measured via mass spectrometry. Figure 4.13 illustrates the shift in migration of the protein via SDS-PAGE when the protein is deglycosylated with PNGase F.

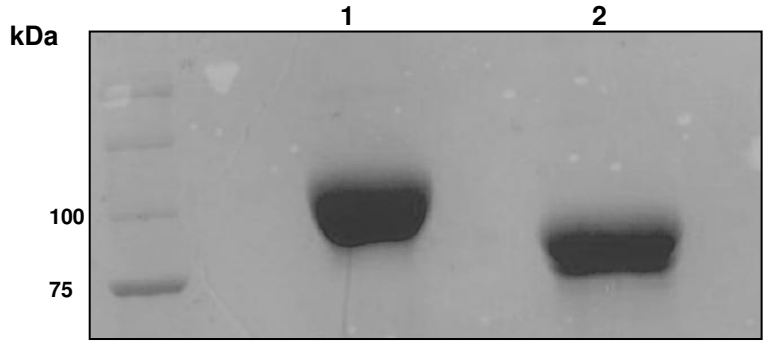

Figure 4.13: SDS PAGE of Pro623Leu tACE: Lane 1: the migration of the protein in its undigested form, lane 2: the migration of the protein after overnight digestion at 37°C with PNGase F.

Besides removing the glycan side chains and causing a change in mass, the deamidation of the asparagine at the start of the glycan "marker sequence" converts the Asn (N) to an Asp (D) when the glycans were removed and caused a gain in mass of 1Da. If no glycosylation occurred then the expected mass of the fragment in that region would have been 1705.85Da. If glycosylation occurred then the N would have been converted to a D after deglycosylation with PNGase F. The deglycosylated mass of 1706.84Da was observed in the resultant mass spectra (Figure 4.14). This confirmed glycosylation occurred at the N^{620}. The cleavage site was also determined from the mass spectrometry data.

4.3.3.3 Glycan confirmation and cleavage site determination

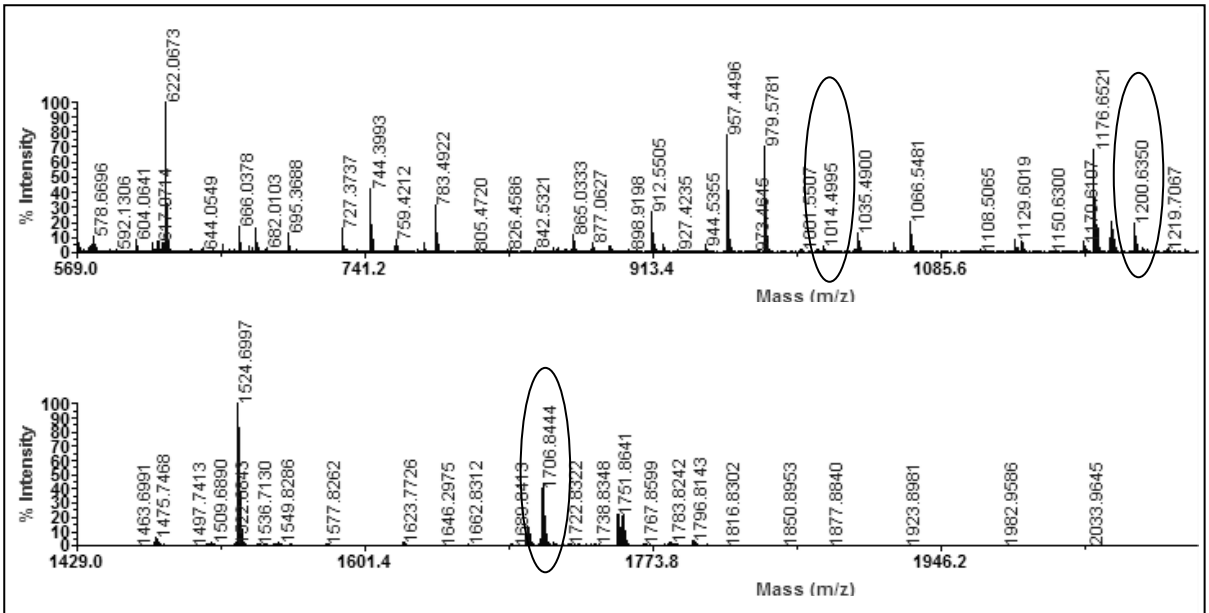

Figure 4.14: MALDI-ToF/MS spectra showing observed masses of peptides from trypsin digestion of purified tACE Pro623Leu. The encircled masses highlights the observed masses.

In table 4.1 the sequences and masses are listed. The peptide corresponding to 1014.6 (residues 628-637) was produced by the tryptic digest. The peptide which corresponded to 1200.6 was observed, which represents a fragment that consists of residues 628-639. This peptide ends at Ser639, suggesting this peptide was the result of another cleavage event other than the trypsin digests. Therefore, the cleavage site at which tACE Pro623Leu was cleaved off the membrane was between Ser639 and Phe640; a shift from the endogenous R^{627}-S^{628} (Ehlers et al., 1996).

Table: 4.1 Observed masses of peptides identified via mass spectrometry compared to expected masses based on the sequence of the fragments expected.

Observed MH^+	Expected MH^+	Sequence	AA no.	MS/MS confirmed
1706.844	1706.83	LGWPQY**D**WTLNSAR	614-627	yes
	1705.85	LGWPQY**N**WTLNSAR	614-627	no
1014.500	1014.47	SEGPLPDSGR	628-637	yes
1200.604	1200.578	SEGPLPDSGR VS	628-639	yes

Thus MALDI analysis confirmed that the putative glycosylation site became glycosylated when P^{623} was converted to L. Table 4.1 summarises the masses observed, to confirm that the N-glycosylation site 7 was glycosylated when P^{623} was mutated to L. The cleavage site also shifted from the wild-type site of R^{627} to S^{659} suggesting an alternative sheddase may be cleaving this mutant or the sheddase is recognising an alternate site because of conformational changes due to the presences of glycans (figure 4.15).

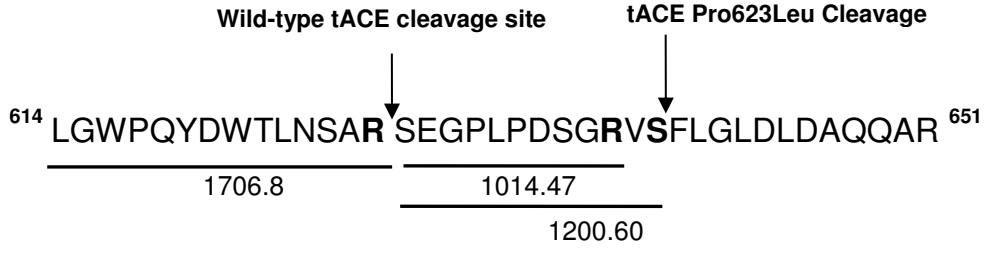

Figure 4.15: Sequence of peptides identified up till the transmembrane region. Arrows highlight the cleavage sites. The sizes of the observed masses are indicated for each peptide fragment.

4.3.4 Characterisation of pcDNA tACE N620D

4.3.4.1 Western blot and enzyme activity

To confirm that it is indeed the glycosylation of site 7 N620 which results in the increase in shedding of tACE Pro623Leu, the glycosylation site itself was knocked out. With leucine still present at position 623, N^{620} was converted to D, removing the side chain necessary for glycans to attach.

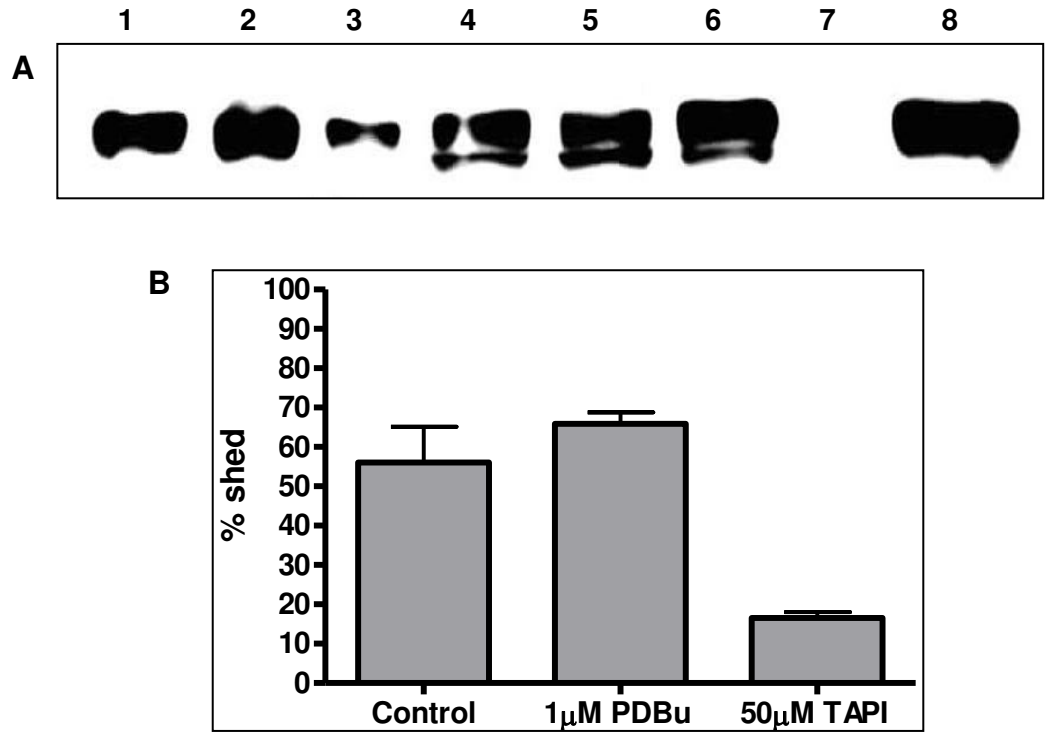

Figure 4.16: Shedding analysis of pcDNA tACE N620D. A) Western blot: Lane 1: control, medium; lane 2: 1μM PDBu added medium; lane 3: 50μM TAPI added medium; lane 4: control, cell lysate; lane 5: 1μM PDBu, cell lysate; lane 6: 50μM TAPI, cell lysate; lane 7: w.t tACE medium; lane 8: w.t. tACE cell lysate. B) Activity assays showing percentage shed ACE of total ACE activity. Data represented are mean ±SEM, n=2.

If the glycosylation was responsible for the increase in shedding of tACE Pro623Leu, then the basal shedding would have reverted to wild-type levels. However, from the shedding analysis of pcDNA tACE N620D (figure 4.16), it is evident the shedding had not reverted to wild-type levels, but shedding had increased even more to 56 %. Basal shedding was so high it was comparable to phorbol-activated shedding. This indicates the removal of the

glycosylation site does not decrease shedding and confirms that the change from proline to leucine, causes the initial increase in shedding. The removal of the glycosylation site actually promotes a further increase in basal shedding; suggesting that the glycosylation site formed down regulates the effect of the leucine in the stalk region (figure 4.17). These results highly suggest the ectodomain boundary proximal to the stalk region and the cleavage site affects the shedding of tACE.

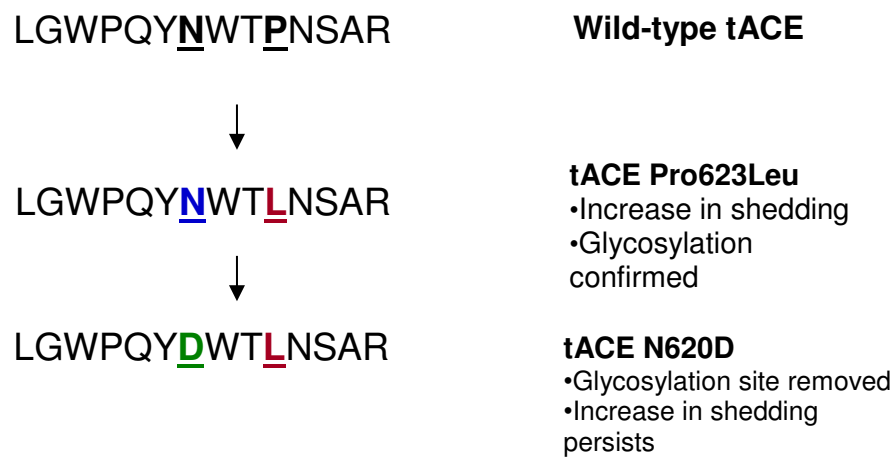

Figure 4.17: Schematic representation and summary of the mutations made in the stalk region of tACE and the resultant effect on shedding.

4.4 Discussion

The regulation of ACE shedding has been extensively studied by mutating or deleting sections of the cytoplasmic tail (Chubb et al., 2002), transmembrane region; stalk region (Schwager et al., 2001, 1999, 1998) or ectodomain (Sadhukhan et al., 1998; Woodman et al., 2006, 2005). After such exhaustive studies across the ACE protein to identify the ACE sheddase recognition motif, it was necessary to further investigate the proposed recognition motif put forward in Chattopadhay et al., (2008).

There are several other ectoproteins that contain a sheddase recognition motif in their stalk regions. Most notably a 5 residue motif (P^{161}QLQE) in CSF-1; a disulphide linked, homodimeric glycoprotein; was found through deletion studies and substitution mutants

(Deng et al., 1996). Stalk length and steric accessibility were also responsible for its ADAM 17-dependant shedding (Deng et al., 2000, 1998, 1996; Horiuchi et al., 2007). The shedding of L-selectin on the other hand was regulated more by the EGF domain (Zhao et al., 2001) than the postulated 5-residue motif K^{327}EGDY in the stalk region. Alanine mutations of these residues maintained shedding but deletion abrogated shedding, probably due to the reduction in stalk length (Migaki et al., 1995). Deletion studies of the non-collagenous domain NC-16A in the juxtamembrane of the transmembrane protein collagen XVII, implied the change in the net charge affects shedding and a negative net charge was required for optimal shedding activity (Franzke et al., 2004). It was found this region consisted of coiled-coil heptads and harboured a sheddase recognition and cleavage site. Mutagenesis of this region caused shedding to increase and was no longer ADAM-mediated, signifying its importance in shedding regulation (Nishie et al., 2012).

Previous work involved extensive investigations into the contribution of the stalk region to shedding. Most notably the stalk length was shown to be critically important and a stalk length of approximately 11 residues usually resulted in a shed protein (Ehlers et al., 1996; Schwager et al., 2001, 1998). The results presented in this chapter add weight to the proposal that this region is important for shedding. However, they were not in complete agreement with Chattopadhay et al. (2008). Substitution with the alanines has shown to affect processing of ACE greatly. The mutant tACE Ndom 608-614 (figure 4.10), strongly suggests that the N-domain residues are sufficient to maintain processing and shedding as this mutant was active and correctly processed. The western blot illustrates correct processing and shedding rates are relatively normal. Previous mutants made in this region were reported in Woodman et al., (2006), with larger N-domain substitutions into the proximal region of the tACE ectodomain. This mutant, SomNBcl (table 4.2) was still shed and correctly processed. After these investigations and other studies into deletion mutants of the stalk region of human tACE (Chubb et al., 2002; Ehlers et al., 1996; Pang et al., 2001; Schwager et al., 1999, 1998), the focus was shifted to the distal ectodomain as these numerous studies did not yield a viable sheddase recognition motif candidate as many alterations merely caused a shift in the shedding kinetics, but did not abrogate it.

The studies into the contribution of the juxtamembrane stalk have been extensive and exhaustive. A Ser/Thr rich region causing O-glycosylation modulated shedding and cleavage, but did not abolish it (Schwager et al., 1999). Likewise, the introduction of an EGF-domain causing disulphide bridges did not abolish shedding (Schwager et al., 1998). The EGF-domain from factor IX did not abolish shedding either (Schwager et al., 2001), even though disulphide bonding occurred. ACE-Δ24 and ACE-Δ17 were deletion mutants of the stalk made C-terminal to the cleavage site and did not affect shedding, as the cleavage site remained the same as wild-type (Ehlers et al., 1996). Corresponding with these results, alanine mutations from residues 651-655 (rabbit tACE) and 649-655, affected shedding and processing (Chattopadhyay et al., 2008). Deletions of the juxtamembrane stalk N-terminal to the cleavage site such as ACE-Δ6 (Schwager et al., 1999) and ACE-Δ11 (Chubb et al., 2002) resulted in shed proteins, albeit at a different rate. The ACE-Δ6 mutation introduced a glycan and this resulted in a change in cleavage site. The mutant ACE- Δ16 was a 16 residue deletion 7 residues N-terminal of the cleavage site and this resulted in an inactive and incorrectly processed protein (Chubb A., PhD thesis 2001). In light of the numerous substitution and deletion stalk mutants that were analysed, there were specific residues deleted within ACE-Δ16 resulted in such an effect, as the larger deletion in another area (ACE-Δ24) did not demonstrate a deleterious effect. The minimum stalk length required is more than adequate in this mutant, so accessibility to stalk cannot be the reason for its lack of shedding. More importantly, the residues T605-615 (table 4.2) clearly affect the processing of this mutant. It is therefore clear that the proposed rabbit tACE recognition motif forms part of this region.

The 5 residue alanine substitution mutation was made in human tACE Ala 610-614, (which corresponds to human tACE numbering) and a seven residue substitution was made to include residue E608 and L609, these two residues were different in rabbit tACE as well as the N-domain (figure 4.2). Mutation of the five residues resulted in changes in processing and western blot analysis illustrated these two forms of the protein were present in the cell lysate (figure 4.9). Only the higher molecular weight band corresponding to the correctly processed form was shed and this was present in the medium. The rate of shedding was similar to wild-type in the tACE Ala 610-614, however total activity was reduced. The tACE Ala 608-614 (figure 4.10) mutant displayed exaggerated traits of the five alanine mutant.

Shedding was greatly affected and total activity (control conditions) was 10 times lower than that of wild-type, suggesting the seven alanines in this position greatly affected processing and activity. The results produced from the current study in human tACE argue that the motif H^{610}GEKL has more of an effect on the processing and transportation of ACE.

Table 4.2: Alignment of proximal ectodomain and stalk sequences of various tACE mutants and chimeric constructs. Highlighted in blue is the rabbit tACE sheddase recognition motif, in purple are N-domain residues, highlighted in green is the P^{623}, residues in yellow are insertions from other proteins, highlighted in grey is the MDP sequence. Underlined in red are N-domain residues.

Construct	Stalk sequence	Shed	Reference
wtACE	SYFKPLLDWLRTENELHGEKLGWPQYNWTPNSARSEGPLPDSGRVSFLGLDLDAQQARVGQWLL	Y	Ehlers et al., 1996
ACE-Ndom	KYFQPVTQWLQEQNQQNGEVLGWPEYQWHPNSARSEGPLPDSGRVSFLGLDLDAQQARVGQWLL	N	Pang et al., 2001
SomNBcl	KYFQPVTQWLQEQNQQNGEVLGWPEYQWHPNSARSEGPLPDSGRVSFLGLDLDAQQARVGQWLL	Y	Woodman et. al. 2006
ACE-Δ17	SYFKPLLDWLRTENELHGEKLGWPQYNWTPNSARSEGPLPDSGR.....WLL	Y	Ehlers et al., 1996
ACE-Δ24	SYFKPLLDWLRTENELHGEKLGWPQYNWTPNSAR.....VGQWLL	Y	
ACE-Δ47	SYFKPLLDWLR.....VGQWLL	N	
ACE-Δ6	SYFKPLLDWLRTENELHGEKLGWPQYN.....RSEGPLPDSGRVSFLGLDLDAQQARVGQWLL	Y	Schwager et al., 1999
ACE-Δ11	SYFKPLLDWLRTENELHGEKLG.....RSEGPLPDSGRVSFLGLDLDAQQARVGQWLL	Y	Chubb et al., 2002
ACE-Δ16	SYFKPLLDWLR.....WTPNSARSEGPLPDSGRVSFLGLDLDAQQARVGQWLL	N?	Chubb A., PhD Thesis, 2001
ACE-ΔR627	SYFKPLLDWLRTENELHGEKLGWPQYNWTPNSA.SEGPLPDSGRVSFLGLDLDAQQARVGQWLL	Y	
ACE-JGL	SYFKPLLDWLRTENELHGEKLGWPQYNWTPNS.VTVTHGTSSQATTSSQTTTHQATARVGQWLL	Y	Schwager et al., 1999
ACE-LDL	SYFKPLLDWLRTENELHGEKLGWPQYNWTPNSHQALGDVAGRGNEKKPSSV.....RVGQWLL	Y	Ehlers et al., 1996
ACE-EGF	ELHGEKLGWPQYNWTPNSECLDNNGGCSH..VCNDLKIGYECLCPDGFQLVAQRRCERVGQWLL	Y	Schwager et al., 1998
MDP-STM	SNHAQVPGEEPIPLGQLEASCRTNYGYWTPNSARSEGPLPDSGRVSFLGLDLDAQQARVGQWLL	Y	Pang et al., 2001
MDP-TM	AELLRRQWTEAEVRGALADNLLRVFEAVEQASNHAQVPGEEPIPLGQLEASCRTNYGYWLLLFL	N	
Rabbit tACE	NYFKPLWDWLLTENGHHGEKLGWPQYTWTPNSARSEGSLPDSGRVNFLGMNLDAQQARVGQWLL	Y	
641-7A	NYFKPLWDWLLAAAAAAAEKLGWPQYTWTPNSARSEGSLPDSGRVNFLGMNLDAQQARVGQWLL	N/P	Chattopadhay etal., 2008
641-5A	NYFKPLWDWLLAAAAAHGEKLGWPQYTWTPNSARSEGSLPDSGRVNFLGMNLDAQQARVGQWLL	N/P	
651-5A	NYFKPLWDWLLTENGHHGEKLAAAAATWTPNSARSEGSLPDSGRVNFLGMNLDAQQARVGQWLL	Y	
649-7A	NYFKPLWDWLLTENGHHGEAAAAAAATWTPNSARSEGSLPDSGRVNFLGMNLDAQQARVGQWLL	Y	
646-5A	NYFKPLWDWLLTENGHAAAAAGWPQYTWTPNSARSEGSLPDSGRVNFLGMNLDAQQARVGQWLL	N	
tACE Ala 610-614	SYFKPLLDWLRTENELAAAAAGWPQYNWTPNSARSEGPLPDSGRVSFLGLDLDAQQARVGQWLL	Y?	Chapter 4
tACE Ala 608-614	SYFKPLLDWLRTENAAAAAAAGWPQYNWTPNSARSEGPLPDSGRVSFLGLDLDAQQARVGQWLL	Y?	
tACE Ndom 608-614	SYFKPLLDWLRTENQQNGEVLGWPQYNWTPNSARSEGPLPDSGRVSFLGLDLDAQQARVGQWLL	Y	

***Y and N denotes "yes" and "no" respectively.**

The block alanine mutations within the rabbit tACE region of 641-647 and 641-645, were not transported to the membrane in HeLa cells (table 4.2) (Chattopadhyay et al., 2008, rabbit tACE numbering). The 5 residue alanine mutation from residues 651-655 was transported and shed, but it was the 5 residue alanine substitution at 646 (646-5A) that caused abrogation of shedding only, while still being transported to the cell surface. Table 4.2 clearly showed that all the stalk mutants discussed where shedding was retained, had residues T^{605}-G^{615} present. Therefore, if we were to add the results of the study presented in this thesis, it would support the theory that these residues are critical for ACE processing and transportation foremost. It would appear that a deletion of this region, as in ACE-Δ16 (Chubb, PhD Thesis, 2001), disrupts the processing machinery completely and yields an inactive protein. Substitution of the HGEKL motif to alanines possibly removes the side-chains necessary to illicit correct processing interactions, but maintains sufficient structure so as to allow a proportion of active ACE to the cell surface to be shed. Substitution to N-domain residues was sufficient for correct processing and only a small reduction in the rate of shedding and activity was seen. A critique of the Chattopadhyay et al., (2008) study is that a faint band was visible in the medium after 6 hours suggesting that perhaps the rate of shedding is highly diminished but not arrested. More convincingly though is that the same mutation in the double-domain sACE caused a major reduction in shedding. This suggests that this motif regulates the same sheddase mechanisms in tACE and sACE.

A possible explanation for the seemingly contradicting evidence for the proposed shedding recognition motif between rabbit and human tACE is probably due to the initial expression of the rabbit tACE proteins in yeast (*Pichia pastoris*) instead of mammalian cells. Rabbit tACE expressed in yeast share most of the kinetic and shedding hallmarks of human tACE, but many mutants not expressed in mammalian cells are expressed in yeast. For example it was shown a rabbit tACE mutant with only one N-linked glycosylation site intact was not actively expressed in HeLa cells, yet adequately expressed in yeast (Sadhukhan and Sen, 1996). Human tACE requires at least two N-linked glycosylation sites present to be successfully expressed in CHO-K1 cells (Gordon et al., 2010). These data suggest yeast has less stringent requirements for glycosylation, processing and transport, and the rabbit tACE mutants are more likely to be successfully expressed in yeast. However, the final lead chimeric mutants

from Chattopadhyay et al., (2008) were tested in HeLa cells to guarantee adequately processing in a mammalian cell line. It could also be possible that rabbit tACE has less stringent processing requirements and may better tolerate alterations in its stalk than human tACE.

To extend the discussion further, we could ask if the motif is the substrate or target of another system. Briefly, it may be proposed that these 5-7 residues under discussion play a role in directing the transport of tACE through the ER and Golgi so as to facilitate correct glycosylation. An in vivo example of this happening in ACE is the polymorphism in the C-domain of sACE resulting in renal tubule dysgenesis, which was caused by an R substitution at Q1069, leading to absence of plasma ACE (Danilov et al., 2010). In vitro studies indicated that this mutation caused trafficking and transportation deficiencies, where proteosome inhibitors and lowered growth temperature could rescue ACE back to the cell surface by encouraging correct trafficking through the ER and Golgi.

Limitations of this study are that due to the extensive research already committed to these questions, the motif that was discussed here has been previously overlooked with respect to its importance because of the use of N-domain residue substitutions instead of alanines (table 4.2). This was done to overcome the problem caused by deletion mutants. The strengths of the study presented here explored the shedding capabilities under stimulated and inhibited conditions whereas the rabbit ACE study was confined to basal conditions only. Our study quantified the effects of the mutations on the rate of shedding, the activity of the protein as well as to illicit data about its protein processing.

The $P^{623}L$ polymorphism supports the body of evidence towards the importance of the juxtamembrane stalk in the regulation of shedding. We have shown that the conversion of P^{623} to L causes a 1.5 fold increase in shedding, glycosylation of the putative N-linked glycosylation site seven of the C-domain and a shift in the cleavage site. These results support studies done previously by Kramer et al., (2001) and Eyries et al., (2001), which demonstrated a leucine in this position caused an increase in shedding. To confirm whether the glycosylation of site seven is the direct cause of the increase in shedding, the N at 620 was knocked out to prevent attachment of the glycosaccharides. This surprisingly did not

restore shedding to wild-type levels, but instead increased shedding even more to 2.5 fold of wild-type ACE. This serves to prove that it is indeed the loss of the proline and the incorporation of leucine, directs the increase in cleavage. Eyries et al., (2001) suggested due to the fact that the stalk is now less structured and flexible, it may be more accessible to the sheddase. Moreover, we have shown that the glycans at N^{620} actually down-regulates the potential increase in shedding that the introduction of leucine causes.

Previously, studies into glycosylation in the stalk and its effect on shedding indicated the addition or removal of O-glycosylated regions modulated shedding but did not abrogate it (Schwager et al., 1999). The deletion of 6 residues in the stalk resulted in the creation of an N-linked glycosylation site, and the resultant glycan caused a shift in the cleavage site. Interestingly, the cleavage site determined for this mutant was one residue away from the cleavage site found in the $P^{623}L$ mutant (figure 4.15), suggesting an N-linked glycan in the stalk possibly interacts and directs the ACE sheddase in such a way resulting in cleavage of the stalk 12 residues C-terminal to the wild-type R^{627}-S^{628} site. To ascertain whether it is the glycan that causes the increase in shedding, we converted the N^{620}; which is necessary for glycan formation; to D. Here it was presented that deletion of the glycans promoted shedding even further (figure 4.16) and basal shedding was comparable to that of stimulated shedding. This clearly illustrate it is the presence of the L at 623 that promotes shedding and not the presence of the resultant glycan N-terminal to the site at 620. The fact such a mechanism is in place, is quite elegant, if we relate this back to the in vivo situation of the Pro1199Leu polymorphism. If there were no glycosylation site preceding the proline then a polymorphism at this site resulting in excess plasma ACE may have had a more serious clinical consequence if shedding were to occur at such a high rate without the glycan down-regulating it, as is the case in sarcoidosis (Lieberman, 1975). These residues are clearly important to the shedding and processing of ACE as a mutation of the N^{620} (residue 631 according to Alfalah et al., 2001) to Q, resulted in increased shedding. However, this occurred in the ER and was mediated by a DCI-sensitive serine protease. The sheddase involved in the cleavage of tACE N620D was inhibited by the metalloprotease inhibitor TAPI, suggesting it is the metalloprotease ACE sheddase usually responsible for shedding that is present and not the serine protease which was sequestered in the ACE NQ mutant (Alfalah

et al., 2001). It also verifies that it is not the mutation of the N itself caused the increase in shedding, but rather the removal of the glycan at N^{620} in conjunction with the L at 623.

We can thus conclude that when the rabbit tACE recognition motif (Chattopadhyay et al., 2008) is mutated to alanines in human testis ACE, it disrupts processing and transport foremost and the corresponding N-domain residues substituted at this site had no effect on the shedding of ACE. The main findings here definitely extend the body of work outlining the significance of the juxtamembrane stalk of the ectoproteins discussed. Questions still requires definitive answers are 1) whether a sheddase recognition motif still resides somewhere in the distal ectodomain; 2) whether there is communication between the distal and the proximal ectodomain; and 3) what the contribution of dimerisation, disulphide bonds and signalling is (Gordon, PhD thesis, 2011).

CHAPTER 5: The evaluation of ACE ectodomain shedding using stalk peptide mimetics

5.1 Introduction

The shedding of ACE is regulated at multiple stages and is likely to play a role in the various physiological processes in the body. We have systematically investigated the different regions of ACE and their contribution to shedding and have learnt a substantial amount about the cellular environment required for shedding to occur. We know that a requisite of shedding is a stalk of minimal length (Ehlers et al., 1997, 1996) and accessibility by the sheddase. Certain studies have also shown a requirement for ACE to be anchored in the membrane in order to be cleaved (Ehlers et al., 1997; Sadhukhan et al., 1999). For example, it was shown that for ADAM 9 to cleave ACE, it required a catalytic domain as well as being tethered to the membrane (English et al., 2012).

In this thesis, our investigations of the substrate requirements for the shedding of ACE first considered the contribution of specific ectodomain surface helices in the regulation of shedding. Precedent for a role in shedding by helical motifs distal to the cleavage site has previously been shown in the cytokine TNF-α (Zheng et al., 2004). As secondary structure alterations in ACE did not have a significant effect on its shedding (Chapter 3), we therefore studied the ectodomain proximal to the membrane, the juxtamembrane stalk region, as well as distinct residues within the stalk and those surrounding the cleavage site (Chapter 4). We found that residues in the proximal ectodomain and stalk were essential for the processing of ACE, as opposed to merely affecting its shedding.

To further investigate the role of the stalk region in ACE shedding, soluble peptides that mimic the ACE stalk were used to: 1) simulate the shedding conditions of ACE, and 2) establish an experimental system that could be used to characterise ACE shedding and its cognate sheddase. Soluble peptides consisting only of the stalk region could also be used to determine

whether the ACE sheddase requires a sheddase recognition domain within the ectodomain in addition to its interaction with the stalk cleavage site.

The knowledge we have acquired about the cleavage site and stalk region was used in the development of a continuous Fluorescence Resonance Energy Transfer (FRET) assay, to measure cleavage of the ACE stalk peptide by the, as yet, unidentified ACE sheddase. FRET technology employs a peptide containing fluorescence donor and acceptor pairs such as the ortho-aminobenzoic (Abz) group at the amide terminal and the ethylene diamine-2,4-dinitrophenyl (EDDnp) group at the carboxyl terminal. Intact peptides emit no fluorescence as the acceptor (EDDnp) group quenches fluorescence emitted by the donor (Abz), however after cleavage of the peptide, the acceptor group is no longer in close enough proximity to absorb the fluorescence, thus the resultant fluorescence emission can be measured using a fluorometer. Our peptide sequence of choice was a nine residue sequence spanning the cleavage site of ACE, flanked by these Abz and Dnp groups (figure 5.1). This technology also allows for the further characterisation of cleavage products and site(s) by high pressure liquid chromatography (HPLC) fractionation and mass spectrometry. Thus the cleavage products may be assigned sizes and the cleavage site may be determined.

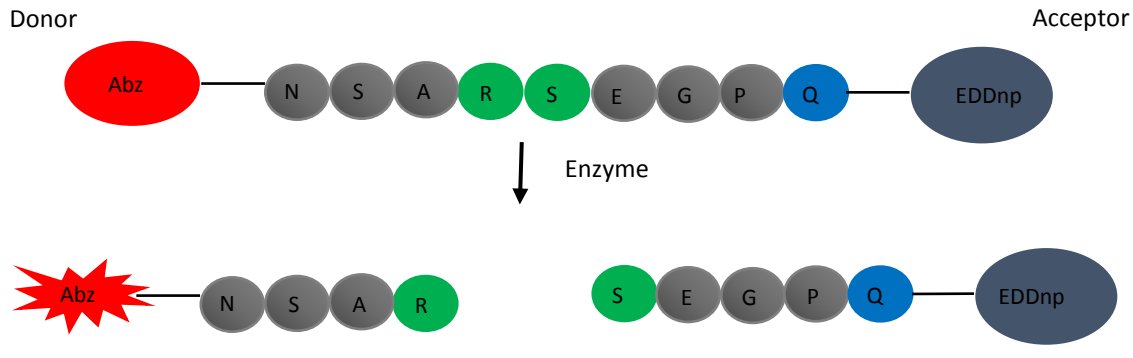

Figure 5.1: **Schematic representation of fluorescence resonance energy transfer (FRET) technology employed in the ACE sheddase assays**. The green highlighted residues of the stalk peptide represent the P1 and P1' residues Arg(R) and Ser(S), between which physiological cleavage is said to occur. No fluorescence is generated prior to cleavage as donor fluorescence is absorbed by the acceptor group. Post cleavage the groups are separated from each other and the acceptor is no longer able to absorb fluorescence emitted by donor. This is what is measured via the fluorometer.

Internally quenched peptides or FRET peptides with the Abz and EDDnp groups have been used successfully in analysing the hydrolysis of substrates by ACE (Araujo et al., 1999; Bersanetti et al., 2004; Carmona et al., 2006). While these assays were usually performed with purified ACE enzyme, ACE fluorogenic peptides have also been used in a cell culture based assay to measure ACE activity on the cell surface (Sabatini et al., 2007). This assay exploited the fact that ACE is a membrane-bound ectoprotein, whose active site is exposed to the extracellular milieu. It was possible to detect ACE activity on the cell surface of cultured cells without lysis of the cells. Aortic smooth muscle cells which had endogenous ACE as well as ACE-transfected CHO-K1 cells were grown in 12-well plates and incubated with fluorescent ACE substrate (Sabatini et al., 2007). It was important to establish the cell number and type to use so as to quantify the amount of enzyme used in the assay. Furthermore, HPLC was used to confirm cleavage products from the substrate hydrolysis. This method was shown to be a novel and effective way to study the processes involved in the activity of ACE at the cell surface with soluble peptides. It was also shown, that the activity observed was due to ACE at the cell surface and not soluble ACE as the supernatants were assayed as well. Assaying ACE *in situ* allows for deductions to be made about what other possible interactions are occurring with ACE and other molecular entities around the cell membrane (Sabatini et al., 2007).

Soluble ACE stalk peptides have been previously used to develop an assay able to monitor the purification process of the ACE sheddase from tissue or cell lysate (R. Domingo, PhD thesis, 2011). CHO-K1 cell lysates were incubated with the ACE fluorogenic stalk peptide and the cleavage site was determined by liquid chromatography-mass spectrometry (LC-MS). Interestingly, cleavage occurred at the E-G bond (figure 5.2) in this synthetic peptide, and not at the physiologically determined R-S cleavage site (Ramchandran et al., 1994; Woodman et al., 2000). The LC-MS data suggested that there might be non-specific endogenous aminopeptidases in the cell lysate hydrolysing the resultant cleavage products (R. Domingo, PhD thesis, 2011). A similar approach using a fluorogenic capped Pro-TNF-α stalk peptide was successfully used to isolate ADAM17 from tissue samples (Black et al., 1997).

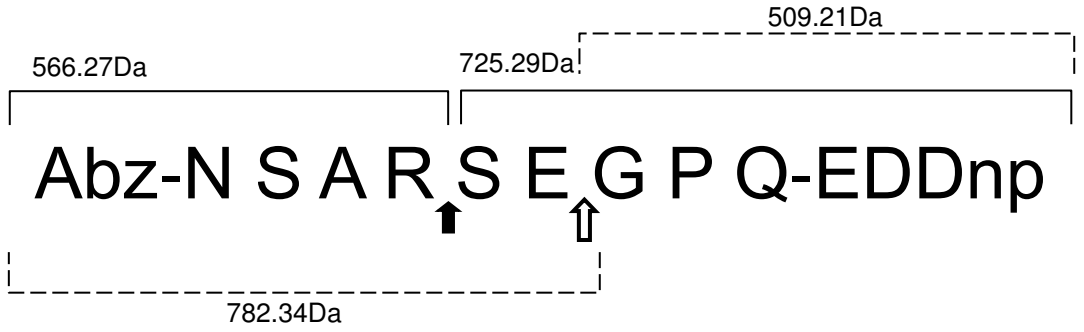

Figure 5.2: Wild-type ACE stalk FRET peptide. Arrows indicate the expected physiological cleavage site (black) and the synthetic cleavage site (white) determined by cleavage with CHO-K1 lysates. The expected sizes are indicated for each cleavage event (Domingo, PhD thesis, 2011).

Based on the success of the ACE stalk fluorogenic assay using cell lysates, we decided to adapt it to be used with cell cultures. There is a requirement for ACE and its sheddase to be anchored in the membrane (Parvathy et al., 1997; Sadhukhan et al., 1999), making such a cell-based assay more physiologically relevant, while circumventing lysis of the cells and exposure of the peptide substrates to proteases released from the intracellular milieu. Furthermore, a cell-based assay facilitates downstream analyses such as HPLC and MALDI by simplifying the sample preparation and eliminating the need to remove cellular debris from the lysate.

To further characterise the endogenous ACE sheddase, a set of ACE stalk analogues were designed with various substitutions in the P1 and P1' positions. While the ACE sheddase does not have a preferential cleavage site sequence that drives shedding (Beldent et al., 1993), the sheddase may be influenced by particular residues available to it within the stalk region (Ehlers et al., 1996). The cell assay was also used to analyse different peptides and the enzyme's S1 and S1' subsite preferences. Similar peptide studies were performed with ADAM17 and ADAM 10 to ascertain which residues conferred selectivity (Caescu et al., 2009). The authors proposed that changes in the P1' position might influence substrate recognition (Caescu et al., 2009), and found that ADAM 17 prefers aliphatic hydrophobic residues (Jin et al., 2002), whereas ADAM 10 prefers larger residues such as leucine (Krstenansky et al., 2004).

Over and above the impact of varying assay conditions, the possibility of non-specific aminopeptidase activity and amino acid preferences at the cleavage site, we also needed to investigate whether the fluorophores could affect cleavage at the endogenous ACE cleavage site. For example Jin et al., (2002) proposed that with the cleavage of Pro-TNF-α peptides, specificity of the candidate protease might be affected by steric hindrance of the capping groups. Cleavage of the capped and uncapped peptides of the Pro-TNFα stalk peptide produced the same cleavage site, but the stalk peptides were cleaved at different rates by recombinant ADAM 17 protein.

Therefore, the aim of this chapter was to further evaluate the ectodomain shedding of ACE using a cell-based assay and synthetic peptides that mimic the juxtamembrane stalk region of ACE.

The objectives of this section were:

1. To establish a cell-based assay for the cleavage of the synthetic ACE stalk FRET peptides.
2. To investigate the involvement of aminopeptidases in the cleavage of ACE stalk peptides.
3. To determine the cleavage site of the various stalk peptides in the cell-based assay.
4. To determine the effect of P1 and P1' substitutions on the proteolytic cleavage of the various ACE stalk peptides.
5. To determine the effect of peptide capping on cleavage.
6. To investigate the hydrolysis of longer uncapped peptides that may include potential/putative secondary sheddase binding sites.

5.2 Materials and Methods

5.2.1 Cell culture

CHO-K1 cells were used as they have been previously shown to have ACE sheddase activity (Ehlers et al., 1991a) and to cleave synthetic ACE stalk peptides (Domingo, PhD thesis, 2011). Cells were grown and maintained as previously described in Chapter 2.

5.2.2 Peptides

Peptides (gift from A. Carmona) were made by the solid-phase methodology using Fmoc-Lys(Dnp)-OH, with details described previously (Hirata et al., 1995). Peptides were dissolved in 100% DMSO and diluted to a stock solution of 5 mM and stored at 4°C. Working stock solutions were diluted in a buffer of choice to 100 µM (Domingo, PhD thesis, 2011).

5.2.3 Cell-based fluorogenic assay

This method was conducted in accordance to Sabatini et al. (2007). CHO-K1 cells were plated in 6, 24 or 48-well plates and cells were grown overnight to confluence in 10% FSC/DMEM/HAMS. Cells were washed twice with Hank's Balanced Salt Solution (HBSS) buffer (140mM NaCl, 0.1M $CaCl_2$, 0.63mM $MgSO_4$, 1mM Na_2HPO_4, 6.1mM glucose, 10µM $ZnCl_2$, pH7.4) and assays were conducted in this buffer, in duplicate. Unless otherwise stated, 10µM of fluorogenic substrate was used. Peptides were diluted appropriately in HBSS buffer and added to cells. The uncapped peptides were diluted to 100µM in HBSS buffer. 600µl of the dilution was incubated for 6 or 18 hours on CHO-K1 cells in 6-well plates. Uncapped peptides were diluted in Optimem®(Gibco) for the 18 hour incubation to prevent cells undergoing stress. The cell culture plates were incubated at 37°C with 85% humidity and 5% carbon dioxide (CO_2) at variable intervals. After the appropriate incubation time, 125-250µl of the cell culture supernatants were transferred to a 96-well microtitre plate (Nunc Corp). Fluorescence was read on a Cary ECLIPSE Fluorescence Spectrophotometer (Varian, Walnut Creek, CA) at excitation and emission wavelengths (λ) of

320 and 420nm respectively, using 10 nm wide entrance and exit slits and a photomultiplier tube (PMT) voltage of 800 (V). Peptides from the cell culture were resolved via HPLC.

5.2.4. Continuous fluorogenic stalk peptide assay

The continuous fluorogenic assays were conducted in 96-well plates. Cells were harvested in Triton lysis buffer (1 % Triton X-100, 50mM HEPES pH 7.5, 0.5M NaCl, 1mM phenylmethylsulphonyl fluoride (PMSF)) and centrifuged at high speed in a microfuge to sediment cell debris. The protein content was quantitated using the Bradford method via the Bio-Rad Protein Assay Dye Reagent Concentrate (Bio-Rad Laboratories, USA) (Bradford, 1976) according to manufacturer's instructions. Lysates were also heat inactivated at 72°C for 15 minutes and included as negative controls with all assays. Ten µg of CHO-K1 cell lysate was added to 2.5-5µM of substrate in 50 mM Tris, 5 µM $ZnCl_2$, 0.01% Brij 35, pH 9.0. Brij was used as a substitute for glycerol as it reduces the background fluorescence. Reactions were monitored over 12-18 hours at room temperature and fluorescence read continuously on a Cary ECLIPSE Fluorescence Spectrophotometer (Varian, Walnut Creek, CA) at excitation and emission wavelengths (λ) of 320 and 420 nm respectively, using 10nm wide entrance and exit slits and a PMT voltage of 800 (V). Fluorogenic stalk peptides (Table 5.2) were incubated with CHO-K1 cell lysates in a 96-well plate and the assay was conducted according to the protocol detailed above (section 5.2.4). The increase in fluorescence was measured continuously in a fluorometer, and a graph of fluorescence emitted versus time was generated. The change in fluorescence was calculated over one hour from time points taken within the linear region of the graph, representing the initial velocity of the hydrolysis of the peptide (Cornish-Bowden, 1995).

5.2.5 Chromatography of peptides using HPLC

Cleavage products from the various assays were separated by HPLC. A 250 x 4.6mm Jupiter 5µM C18 reverse-phase column (Phenomenex, CA) was used with a SpectraSERIES P200 Gradient Pump. An elution gradient of 0.1% trifluoroacetic acid (TFA) to 0.1% TFA / 75% acetonitrile was used. Products were detected at wavelengths 215nm and 354nm via Spectrasystem UV/VIS Detector (Spectra-Physics, Freemont, CA) and data were analysed using

the EX Chrom™ Chromatography Data System. The wavelength of 354nm was used to detect carboxyl-terminal products containing the 2, 4-dinitrophenol ethylenediamine (DNP) moiety. The uncapped peptides were analysed on the Agilent 1260 Infinity system using a 50 x 4.6mm Poroshell 120, 2.7µM C18 reverse-phase column (Agilent, USA). An elution gradient of 0.1% trifluoroacetic acid (TFA) to 0.1% TFA / 75% acetonitrile was used. Products were detected at a wavelength of 214nm and data were analysed using the Agilent ChemStation Software (2004).

5.2.6 MALDI mass spectrometry (MS)

Cleavage products were prepared for MALDI by purification and desalting using ZipTip® Pipette Tips (Millipore, USA) containing C_{18} resin. Samples (0.5µl) were spotted onto MALDI plates twice. The matrix used consisted of 10mg/ml α –cyano-4-hydroxycinmamic acid (Fluka) with 20mM $NH_4H_2PO_4$ (Fluka) in 80% acetonitrile, 0.2% TFA. The final concentrations were 5mg/ml of matrix in 40% acetronitrile, 0.1% TFA and 10mM $NH_4H_2PO_4$. MALDI MS/MS was performed at the Centre for Proteomics and Genomics Research (CPGR, Cape Town) on a 4800 MALDI ToF/ToF (Applied Biosystems). The MS spectra were recorded in reflector mode, generated with 400 laser shots/spectrum at a laser intensity of 3800 (arbitrary units) and with a grid voltage of 16 kV. Internal calibration of peptide containing spots was measured against trypsin autolytic fragments.

5.3 Results

5.3.1. Development of a cell-based ACE sheddase assay

All previous attempts to use solubilised endogenous ACE sheddase from cell lines and tissue have failed to cleave membrane-bound ACE (Sadhukhan et al., 1999). This indicates that there is a requirement for the sheddase to be anchored in the membrane for effective ACE cleavage. It was thus hypothesised that a cell-based assay similar to that used by Sabatini et al., (2007) would circumvent this problem and a cell-based ACE sheddase assay was developed to evaluate the activity of the sheddase in the presence of inhibitors and stimulators.

The ACE stalk peptide (Abz-NSARSEGPQ-EDDnp) was incubated with CHO-K1 cells in culture and change in fluorescence was measured. Preliminary results were promising as they indicated an increase in fluorescence units (FU) with an increase in substrate concentration (figure 5.3, A) and time (figure 5.3, B). Interestingly, a measurable change in fluorescence was observed within a 6-hour period compared to that of the continuous assay (cell lysates), which required 10-18 hours for similar observations (R.Domingo, PhD thesis, 2011).

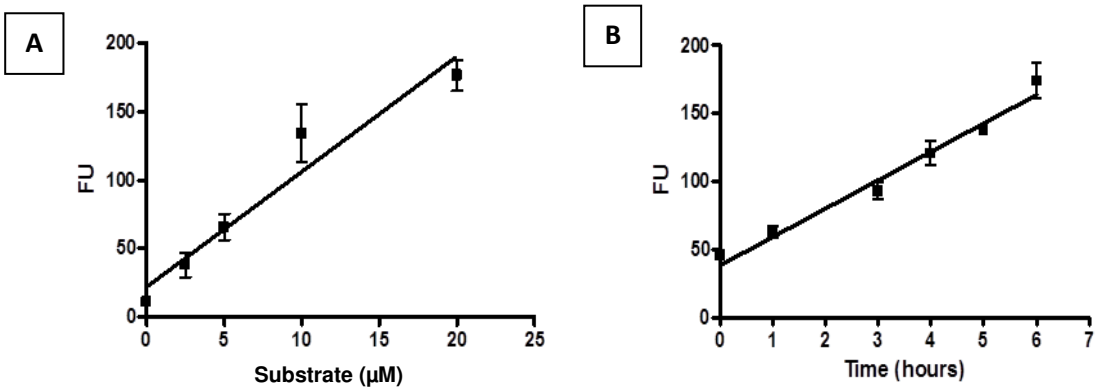

Figure 5.3: **Cleavage of ACE wild-type fluorogenic stalk peptide (Abz-NSARSEGPQ-EDDnp) in CHO-K1 cells**. A) Increasing concentrations of the ACE wild-type fluorogenic stalk peptide were incubated on the cell surface of CHO-K1 cells in HBSS buffer for 6 hours, and resulting fluorescent units (FU) were measured. B) 10μM of ACE stalk peptide was incubated for increasing time periods. Assay was conducted in a 24-well plate. Supernatants were transferred to 96-well plate and fluorescence measured on fluorometer. Data represented are the mean ±SEM, n=3.

ACE shedding is characteristically inhibited by the the hydroxamate inhibitor, TAPI, and stimulated by the phorbol ester PDBu (Chubb et al., 2004; Ehlers et al., 1997, 1995). To investigate if Abz-NSARSEGPQ-EDDnp exhibited similar inhibition and stimulation profiles within the cell-based assay, cells were incubated with the ACE stalk peptide in the presence of TAPI or PDBu and resulting fluorescence was monitored. There was a small, but not significant, increase in mean fluorescence units in the presence of PDBu, however incubation with 100 μM TAPI had no effect on substrate hydrolysis (figure 5.4, A). Incubation of CHO-K1 cells with the Pro-TNF-α stalk peptide resulted in a 3-fold increase in mean fluorescence compared to the ACE stalk peptide, however TAPI and PDBu also had no effect on the Pro-TNF-α stalk peptide (figure 5.4, B). This implies that the mechanisms involved in cleaving the fluorogenic ACE stalk peptide may

have some differences compared to that of the cleavage of the wild-type membrane-bound ectoprotein.

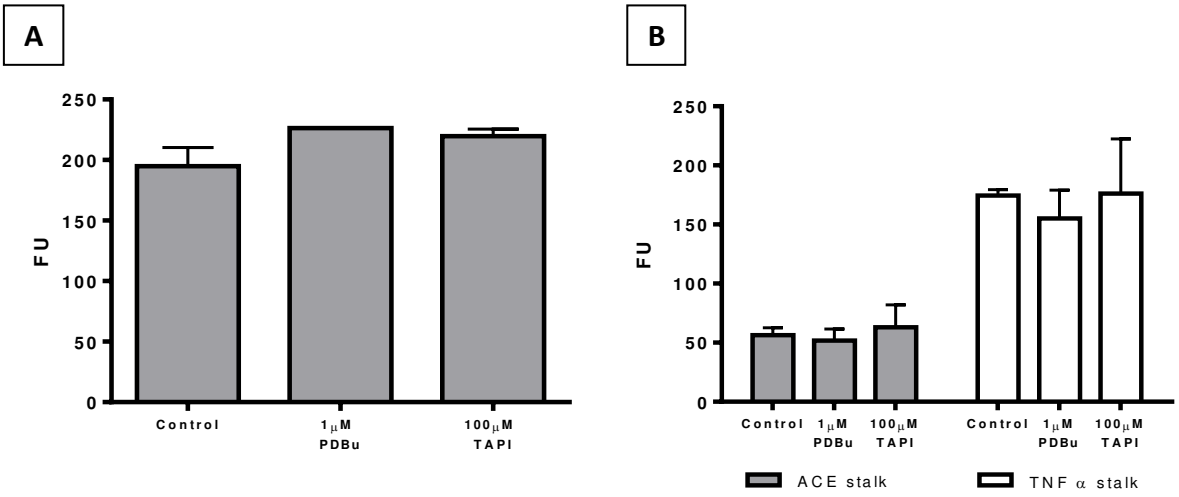

Figure 5.4: Cleavage of stalk peptides with regulators of shedding. A) 1μM PDBu or 100μM TAPI were added to 5μM ACE stalk peptide and incubated on the surface of CHO cells for 6 hours in a 24-well plate. B) Same conditions as in A, except assay was performed in a 48-well plate and included the TNF-α stalk peptide. Data represented are mean ±SEM, n=3.

To further validate the cell-based assay, the inhibition of ACE activity in the CHO-K1 cell assay was investigated. Figure 5.5 shows a 2-fold reduction in tACE activity in the presence of lisinopril as described previously (Sabatini et al., 2007). Hydrolysis of the ACE stalk peptide in

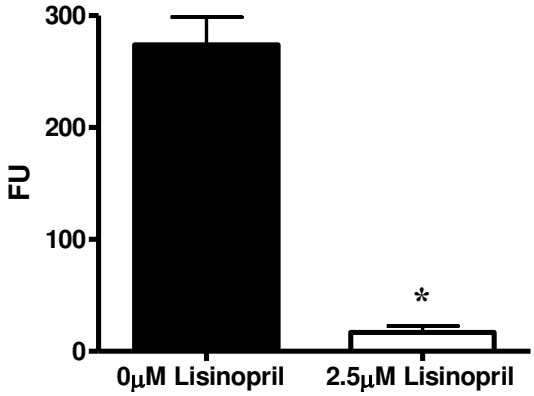

Figure 5.5: The effect of lisinopril on ACE activity in the cell assay. The ACE inhibitor lisinopril was pre-incubated on tACE-expressing CHO-K1 cells for 5 minutes and ACE subtsrate Abz-LFK-Dnp was added and incubated for 10 minutes at 37°C. One ml of the supernatant was removed and fluorescence measured. Data represented are the mean ±SEM, n=2, *p*=0.05.

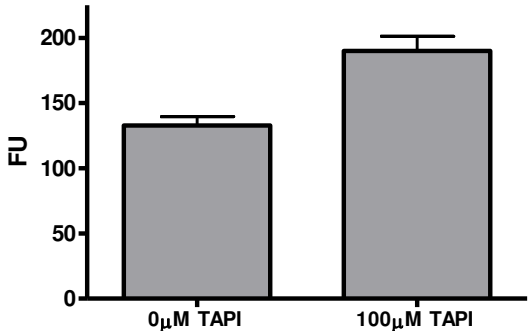

Figure 5.6: Pre-incubation of the sheddase inhibitor TAPI with CHO-K1 cells. 100μM of TAPI was pre-incubated with CHO-K1 for 1 hour. 5μM of fluorescent ACE stalk peptide was added and supernatants were collected and fluorescence read after 6 hours. Assay was performed in a 24-well plate. Data represented are the mean ±SEM, n=3.

cell culture in the presence of the hydroxamate inhibitor TAPI, revealed no significant decrease in the cleavage of fluorogenic substrate (figure 5.6).

To determine the involvement of metallo- or serine proteases in the hydrolysis of the ACE stalk peptide, cells were incubated with the metalloprotease inhibitor EDTA or the serine protease inhibitor PMSF. The graph in figure 5.7 represents the effect of increasing concentrations of EDTA or PMSF on the cleavage of the ACE stalk peptide. A 58% decrease can be seen with the

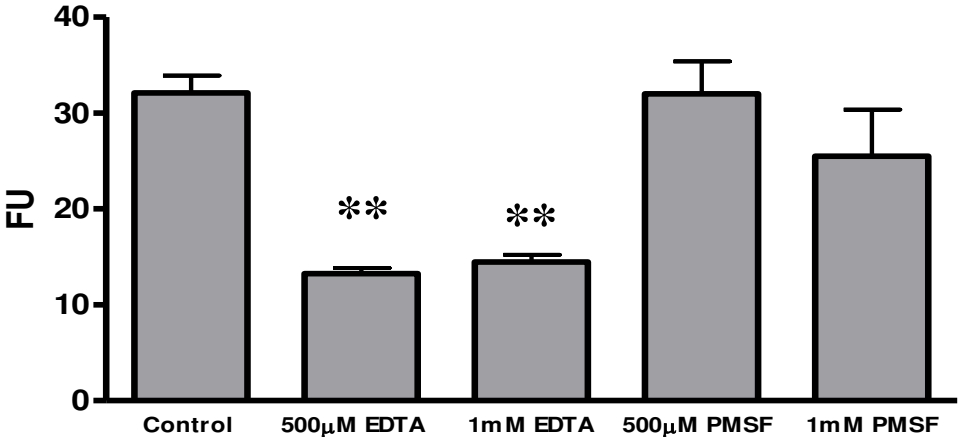

Figure 5.7: Inhibition of cleavage of the fluorescent stalk peptide by broad-range inhibitors. Fluorescent units (FU) of stalk peptide cleavage in presence of …Inhibition of hydrolysis of ACE stalk peptide (2.5μM) by EDTA (metalloprotease inhibitor) and PMSF (serine protease inhibitor). Assay was conducted in 48-well plate. Data represented are the mean ±SEM, n=3, *p*=0.05**

addition of 500μM of EDTA, with no further decrease observed at 1mM EDTA, while the serine protease inhibitor PMSF had no effect on substrate hydrolysis. This confirms that

metalloprotease activity is involved in the stalk peptide cleavage, while serine protease activity does not play a role. Interestingly, even at a low concentration of stalk peptide (2.5µM), the addition of EDTA did not completely abolish the cleavage, indicating that some of the hydrolysis must be due to non-metalloprotease cleavage. This could also explain why the hydroxamate inhibitor, TAPI, had no effect, suggesting that the protease responsible for cleaving the peptide may be a metalloprotease but does not respond specifically to the hydroxamate class of inhibitors. Thus, the protease responsible for cleaving the stalk peptides under these cell assay conditions is likely to be different to the ACE sheddase responsible for cleaving membrane-anchored ACE, or alternatively, there could potentially be additional proteases involved in the cleavage of the fluorogenic stalk peptide.

5.3.2 The evaluation of aminopeptidase hydrolysis of the ACE stalk peptide

Cleavage of the wild-type ACE stalk peptide exposed to CHO-K1 cells in culture did not display the same characteristics of shedding as transfected ACE. To determine which other proteases may be responsible for the cleavage of the ACE stalk peptides in the cell assay, the effect of the aminopeptidase inhibitor, bestatin, on peptide hydrolysis was investigated. The cell assay was performed in the presence of 100 µM bestatin (figure 5.8). Eventhough there seems to be a decrease in fluorescence, bestatin had no significant effect on peptide cleavage (even at 500µM (results not shown)), indicating that aminopeptidase activity was not involved in the cleavage of the ACE stalk peptide.

To determine the cleavage site of the ACE stalk peptide under cell assay conditions, HPLC and MS were employed as described in sections 5.2.5 and 5.2.6 (Appendix figure A5.1 illustrates the workflow for the experiments used to determine the cleavage site of the stalk peptides). The ACE stalk peptide at t_0 eluted from the HPLC column as a single peak corresponding to that of the uncleaved peptide (figure 5.9A). In figure 5.9B, the incubation of stalk peptide with CHO-K1 cells for 6 hours resulted in the formation of a second peak, representing a cleavage product eluting at 23 minutes. It is also clear from this figure that there is a large proportion of uncleaved peptide still present in the sample. These products could be visualised as product

peaks on the HPLC as the spectrophotometer was able to detect the EDDnp C-terminal moiety at 354nm. Fractions eluted from the column were collected in 1 ml aliquots, and their fluorescence measured on a fluorometer at excitation and emission wavelengths of 320nm and 420nm, to detect the presence of the Abz group. One fraction, corresponding to the approximate 15-minute elution, displayed fluorescence at this wavelength, and this fraction as well as fractions corresponding to the cleaved (24 minutes) and uncleaved (23 minutes) products were stored for MS analysis. Similarly, samples from the bestatin time course were subjected to HPLC to ascertain the resultant cleavage products. Results indicate that the

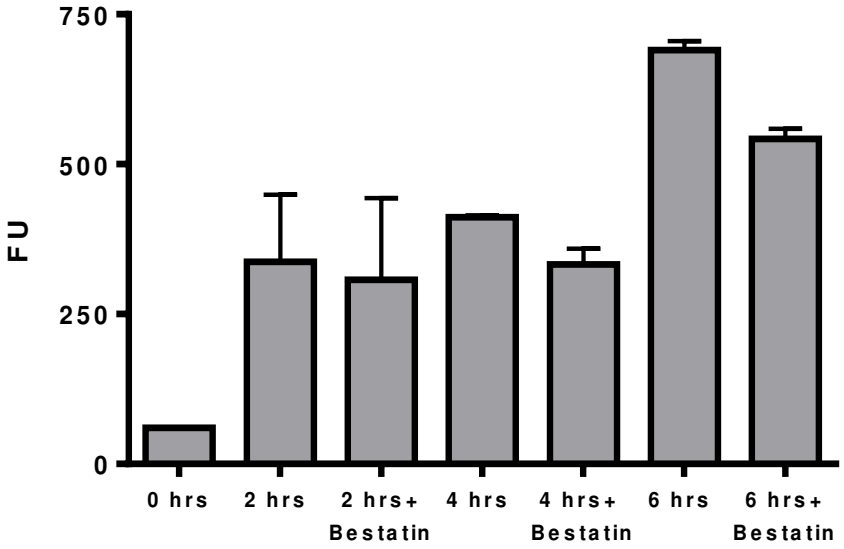

Figure 5.8: Effect of aminopeptidase inhibitor bestatin on the cleavage of the fluorogenic ACE stalk peptide. Assay was conducted in a 6-well plate, using 5µM of substrate and 100µM over 6 hours, in duplicate.

presence of bestatin does not change the product profile (figure A5.3, appendix).

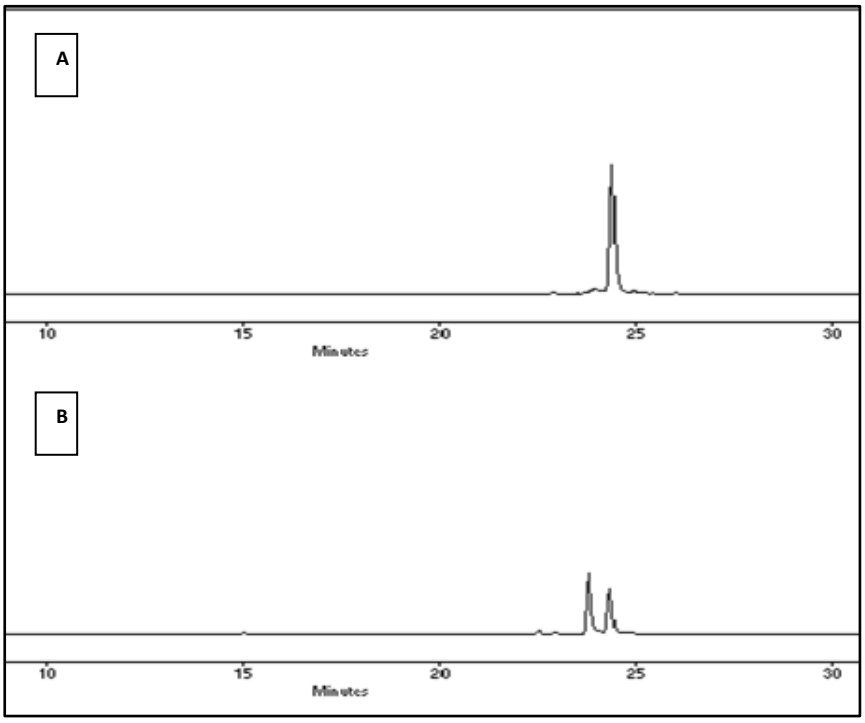

Figure 5.9: HPLC chromatogram of 10µM of wild-type fluorogenic ACE stalk peptide incubated on the surface of CHO-K1 cells in a 6-well plate for 6 hours. A) uncleaved stalk peptide at t_0 incubation with CHO-K1 cells B) stalk peptide after 6 hours incubation with CHO-K1 cells. Chromatogram of 354nm wavelength to monitor the C-terminal EDDnp acceptor group.

The cleavage site at 6 hours (no bestatin) was determined by analysing the HPLC fractions using mass spectrometry. The $[M+H]^+$ ion corresponding to the uncleaved peptide was identified as 1272.54 (figure 5.10). The masses that were found for the cleaved products were m/z 782.36, corresponding to Abz-NSARSE (eluted at 15 minutes) and m/z 509.21, corresponding to GPQ-EDDnp (eluted at 23 minutes; figure 5.11). These masses compare well with the calculated masses (figure 5.10 and table 5.1), and indicate that the primary cleavage occurs between the E and G and not the expected R and S, and that that no secondary trimming of cleavage products occurs.

N-terminal ladder:	C-terminal ladder:
1272.54Da. Abz-NSARSEGPQ-EDDnp	1272.54Da. Abz- NSARSEGPQ-EDDnp
1064.48Da Abz-NSARSEGPQ	1153.50Da. NSARSEGPQ-EDDnp
936.42Da. Abz-NSARSEGP	1039.46Da. SARSEGPQ-EDDnp
839.36Da. Abz-NSARSEG	952.42Da ARSEGPQ-EDDnp
782.34Da. Abz-NSARSE	881.39Da. RSEGPQ-EDDnp
653.30Da. Abz-NSARS	**725.29Da** **SEGPQ-EDDnp**
566.27Da. Abz-NSAR	638.25Da EGPQ-EDDnp
410.17Da. Abz-NSA	509.21Da. GPQ-EDDnp
339.13Da. Abz-NS	452.19Da. PQ-EDDnp

Figure 5.10: The theoretical m/z masses of potential cleavage products of the wild-type ACE fluorogenic stalk peptide. The N-terminal ladder represents all b-ions that may be detected and the C-terminal ladder represents the all the y-ions that may be detected via MALDI.

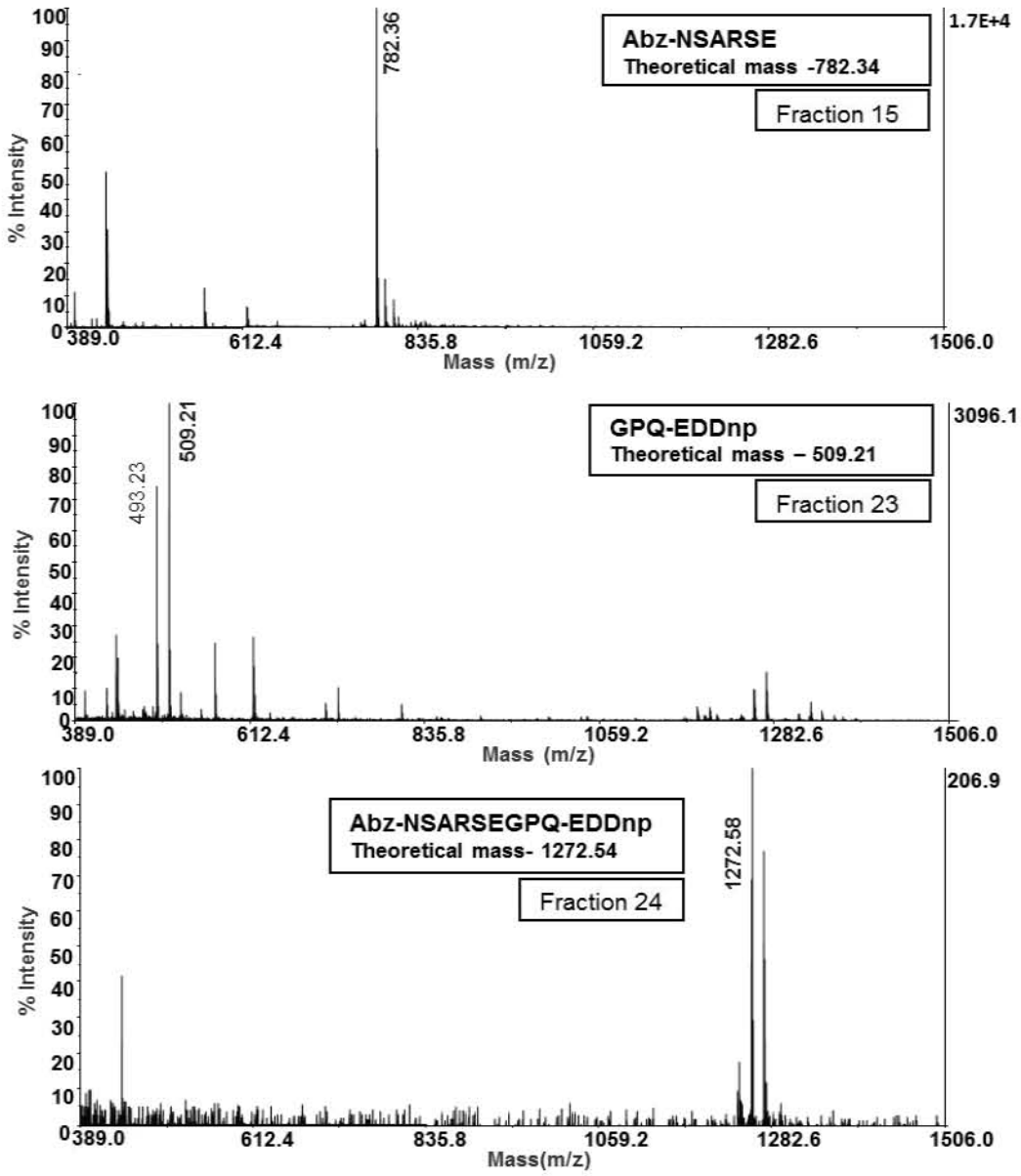

Figure 5.11: MALDI-ToF spectra of 3 fractions purified from the HPLC of the cleaved wild-type ACE stalk peptide. The major product peaks have been highlighted. Calculated masses are indicated for fraction 15 minutes, 23 minutes and 24 minutes.

The fractions from the time course experiment which aimed to describe the contribution of aminopeptidases to the cleavage of the wild-type fluorogenic ACE stalk peptides, were also submitted for mass spectrometric analysis. From these data we can identify all peptide products that emerge over the incubation period. The molecular ions at m/z 725.29 and 509.21

identified in the product peak collected at 24 minutes (table 5.1 and figure 5.12) correspond to the C-terminal fragments SEGPQ-EDDnp and GPQ-EDDnp, respectively. The molecular ion at m/z 725.29 corresponds to the SEGPQ-EDDnp product detected at 4 hours (no bestatin), 4 hours (100µM bestatin) and 6 hours (500µM bestatin) (table 5.1). In addition, the molecular ion at m/z 782.34 corresponding to the N-terminal fragment (Abz-NSARSE) was observed at every time point.

Table 5.1: Observed m/z ions of peptides generated from cell based assay with wild-type ACE soluble peptide.

		$[M+H]^+$ calculated				
		Abz-NSARSEGPQEDDnp	**GPQ-EDDnp**	**Abz-NSARSE**	**Abz-NSAR**	**SEGPQ-EDDnp**
		1272.54	**509.21**	**782.34**	**566.27**	**725.29**
Sample	**Fraction**			**$[M+H]^+$ observed**		
4hour	14 min			782.34		
	23 min	1272.51				
	24-25min	1272.51	509.19			725.27
4hour 100µM bestatin	14 min			782.35		
	23 min					
	24-25min		509.19			725.28
6hour	14 min			782.35 (very low)		
	23 min					
	24-25min	1272.48	509.19			
6hour 100µM bestatin	14 min			782.34		
	23 min		509.21			
	24-25min	1272.49				
6hour 500µM bestatin	14 min			782.34		
	23 min		509.22			725.25
	24-25min	1272				725.27

These results confirm that even in the presence of an excess of the aminopeptidase inhibitor bestatin, there is specific cleavage at the E-G bond and not the expected R-S bond, and that the GPQ-EDDnp product is not the result of secondary aminopeptidase activity. Therefore, even with an excess of bestatin (500µM), the products with m/z of 509.21 and 782.34 were observed, providing further evidence that the E-G bond is the favoured cleavage site of the ACE

stalk peptide. A secondary minor cleavage site at the R-S bond was also observed (as evidence by the presence of the m/z of 509.21 ion), which agrees with the physiological cleavage of ACE.

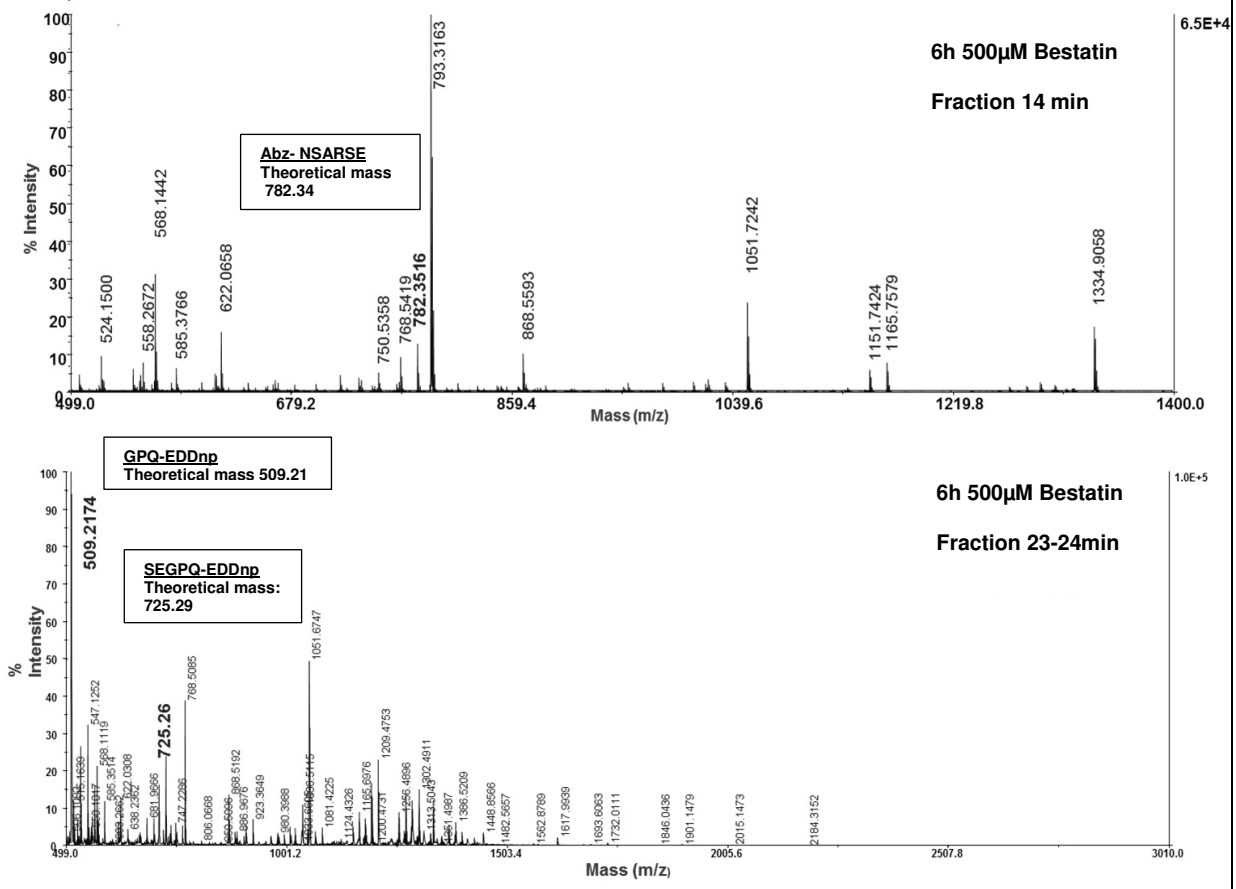

Figure 5.12: MALDI-ToF/ MS of fractions from cell based assay with wild-type fluorogenic ACE peptide and the aminopeptidase inhibitor bestatin. These represent the 6 hour time point with the highest concentration of bestatin. Masses of cleavage peptides are indicated in bold.

5.3.3 The effect of the P1 and P1' residues on the cleavage of the ACE stalk peptide

We next investigated the effect of the P1 or P1' residues in the ACE stalk peptides on cleavage. A range of peptides were made where the P1 (R) or P1' (S) residue positions of the endogenous stalk peptide, or both, were substituted with the hydrophobic residues Y, W or F, to examine the impact of these specific residues in the cleavage of the stalk peptides (Table 5.2). The

peptides are referred to by the single-letter amino acid residues present in the predicted P1 and P1' groups, for example RS represents the wild-type peptide Abz-NSA**RS**EGPQ-EDDnp.

Table 5.2: **Fluorogenic ACE stalk peptide mimetics.**

Peptide	Name	Alteration
Abz-NSA**RS**EGPQ-EDDnp	Wild-type stalk peptide	
Abz-NSA**FS**EGPQ-EDDnp		F in P1 position
Abz-NSA**RF**EGPQ-EDDnp		F in P1' position
Abz-NSA**FF**EGPQ-EDDnp		F in P1 and P1' position
Abz-NSA**RW**EGPQ-EDDnp		W in P1' position
Abz-NSA**WS**EGPQ-EDDnp		W in P1 position
Abz-NSA**YS**EGPQ-EDDnp		Y in P1
Abz-ESNIKVLPQ-EDDnp	CD 4	CD4 stalk sequence
Abz-LAQ**AV**RSSSQ-EDDnp	Pro-TNFα	Pro-TNFα stalk sequence

*Peptides werer designed based on predicted on or theoretical P1 and P1' sites i.e R-S bond. This occurred before the cleavage site was determined to be at E-G. The P1 and P1' postions will still be dicussed based on the predicted position.

The fluorogenic peptides were incubated with CHO-K1 cell lysate in the 96-well plate continuous assay (section 5.2.4). Flourogenic peptides with hydrophobic groups in the theoretical P1' position, such as RW and RF, were cleaved more efficiently than the wild-type RS peptide (figure 5.13). FF, YS and FS all displayed negligible increases above the background fluorescence of the uncleaved peptide, while CD4 and WS peptides were not cleaved at all. These data support the suggestion that an R residue at the P1 position is favoured in ACE shedding (Ehlers et al., 1996). However, the requirements of the P1' residue seem to be less rigid and bulky W and F residues seem to facilitate cleavage at this position.

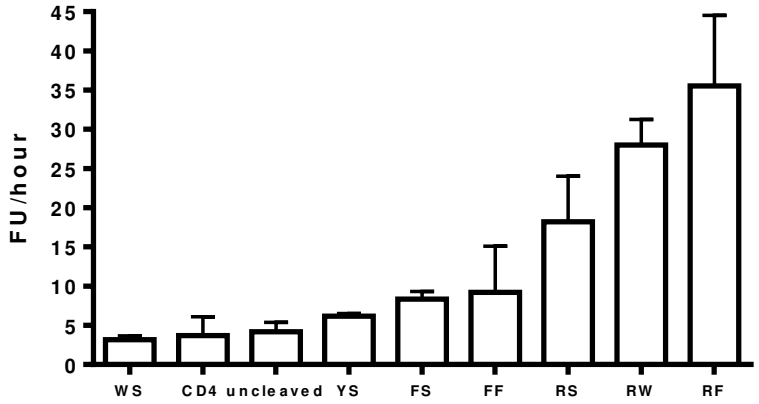

Figure 5.13: Cleavage site mutants of the fluorogenic ACE stalk peptides in a 96-well plate assay. Stalk peptide mutants were incubated with CHO-K1 cell lysates in a 96-well and analysed continuously as detailed previously in 5.2.3. FU/hour were calculated from the linear region of the fluorescence curve. WS, YS, FS, FF, RS, RW and RF represent the theoretical P1 and P1` sites based on the endogenous ACE stalk cleavage site peptides. The CD4 peptide represents the stalk sequence of the cytokine CD4. Data represents mean±SEM, assays were conducted in duplicate and experiments were repeated twice.

The peptides were then analysed using the cell-based assay. It was immediately evident that the cell assay produces a very different cleavage pattern to the CHO-K1 lysate assay (figure 5.14). In the cell assay; the peptides that showed the lowest cleavage in the cell lysate 96-well plate continuous assay, such as WS, YS, FS and FF; have much higher fluorescence than RS, RW, RF and even TNF-α (included as positive control).

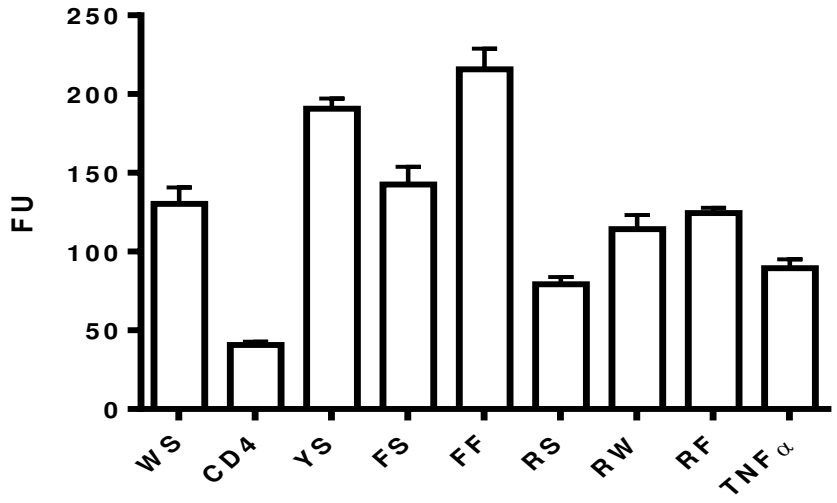

Figure 5.14: Cleavage site mutants of the fluorogenic ACE stalk peptide in a cell-based fluorogenic assay. The graph represents the fluorescence after 6 hours when the fluorogenic peptides were incubated with intact CHO-K1 cells at 37°C. Assays were conducted in a 48-well plate with 5µM peptide. WS, YS, FS, FF, RS, RW, RF represent the theoretical P1 and P1` sites of the ACE peptides. The CD4 and TNFα peptides represent the stalk sequences of cytokine CD4 and Pro-TNFα respectively. Fluorescence was normalised against background fluorescence of uncleaved peptide. Data represents mean±SEM, assays were conducted in triplicate, experiments repeated twice.

To characterise the cleavage sites of the different peptides incubated in the cell-based assay, cleavage products were subjected to MS analysis. Data from the MALDI-ToF M/S were analysed for the presence of specific masses corresponding to the calculated masses of potential products for each peptide (table 5.3).

The C- and N-terminal cleavage products of the wild-type RS peptide were identified as the molecular ions at m/z 509.17 and m/z 782.28, which correspond to the GPQ-EDDnp and Abz-NSARSE fragment, respectively (table 5.3). Similarly, RF was cleaved to produce the C- and N-terminal fragments GPQ-EDDnp (m/z 509.17) and Abz-NSARFE (m/z 842.33). The RW peptide produced two sets of fragments indicating that cleavage occurred between both the theoretical P2' - P3' (E/G) and P1' - P2' (W/E) residues; producing the fragments GPQ-EDDnp (m/z 509.18) and Abz-NSARWE (m/z 881.34) as well as EGPQ-EDDnp (m/z 638.21) and Abz-NSARW (m/z 752.38). These results demonstrate that the main cleavage site for all of these three peptides occurs between the E and G (theoretical P2' - P3') residues.

The four remaining peptides, FF, FS, WS and YS, all produced a prominent cleavage product corresponding to GPQ-EDDnp (m/z 509.21), again designating the P1 and P1' residues as E and G. It is important to note that these four peptides also had observable masses in the uncleaved control samples (m/z 509.18 and 725.25) matching the cleavage products. These results indicate some level of degradation, however, the wild-type (RS) and two P1' mutant stalk peptides RF and RW displayed no degradation products in the uncleaved samples and the observed masses compared well to their calculated masses (table 5.3).

Table 5.3: Cleavage products obtained from the various stalk peptides. Calculated and observed masses determined via MALDI-ToF M/S for uncleaved (control) and cleaved samples (6 hour exposure to CHO-K1 cells). Samples were prepared according to the outline (appendix, figure A5.2). Masses corresponding to peptides FF, FS, WS and YS are underlined and have potassium (K) adducts (+38).

	Uncleaved	Uncleaved	Cleaved	Cleaved
	MH^+ calculated	MH^+ **observed**	MH^+ calculated	MH^+ **observed**
Abz-NSARSEGPQ-EDDnp	1272.54	1272.45		
GPQ-EDDnp			509.21	509.17
Abz-NSARSE			782.34	782.28
Abz-NSARFEGPQ-EDDnp	1332.56	1332.49		
GPQ-EDDnp			509.21	509.17
Abz-NSARFE			842.38	842.33
Abz-NSARWEGPQ-EDDnp	1371.58	1371.49		
GPQ-EDDnp			509.21	509.18
EGPQ-EDDnp			638.25	638.21
Abz-NSARWE			881.39	881.34
Abz-NSARW			752.35	752.30
Abz-NSAFSEGPQ-EDDnp	1263.51	**1301.38**		
GPQ-EDDnp		509.17		509.19
SEGPQ-EDDnp		725.25		725.27
Abz-NSAFFEGPQ-EDDnp	1323.54	**1362.41**		
GPQ-EDDnp	509.21	509.1779		509.189
Abz-NSAWSEGPQ-EDDnp	1302.52	**1340.45**		
GPQ-EDDnp	509.21	509.19		509.18
SEGPQ-EDDnp		725.28		
Abz-NSAYSEGPQ-EDDnp	1279.50	**1317.41**		
GPQ-EDDnp		509.187		509.19
SEGPQ-EDDnp		725.27		
Abz-ESNIKVLPQ-EDDnp (CD4 stalk)	1354.68	1354.63		
Abz-LAQAVRSSSQ-EDDnp (Pro-TNF-α stalk)	1373.6	1373.62		
Abz-LAQAVR			776.44	776.42
SSQ-EDDnp			529.20	529.99

The CD4 peptide incubated on CHO-K1 cells (figure 5.14) displayed no distinct products with molecular ions corresponding to any of the calculated masses, indicating that no specific cleavage of this peptide occurred (table 5.3). However, an increase in fluorescence after 6 hours of incubation with cells was observed (figure 5.14) illustrating that there may be cleavage due to non-specific protease activity.

Incubation of CHO-K1 cells with the Pro-TNF-α peptide (figure 5.14) produced two fragments identified as SSQ-EDDnp (m/z 529.99) and Abz-LAQAVR (m/z 776.42) (table 5.3), with a similar cleavage site to that of the ACE stalk peptides where primary cleavage occurs 3 residues from the C-terminus. Interestingly, there were no molecular ions denoting cleavage at the physiological A-V cleavage site. Therefore, cleavage of all the fluorogenic stalk peptides, including those in the cell-based assay does not appear to be sequence-specific.

5.3.4 The effect of peptide capping on cleavage

5.3.4.1 Cleavage of a non-capped stalk peptide

To determine whether the presence of the fluorogenic capping groups altered the cleavage position of the stalk peptides, we analysed peptides lacking these fluorogenic groups using the same cell assay as was used for the capped peptides (table 5.4). Interestingly, HPLC revealed no cleavage products were present with only a single peak eluting at 10.6 minutes corresponding to the intact peptide NSARSEGPQ (figure 5.15).

Table 5.4: Uncapped ACE stalk peptides

Sequence	Length	Abbreviation	Rationale
NSA**RS**EGPQ	9	WT	Fluorophores omitted only, same length
EL<u>HGEKL</u>GWPQYNWT*P*NSA**RS**EGPQ	25	RM	Peptide sequence extended at the N-terminus to include putative stalk/ectodomain recognition motif (underlined).

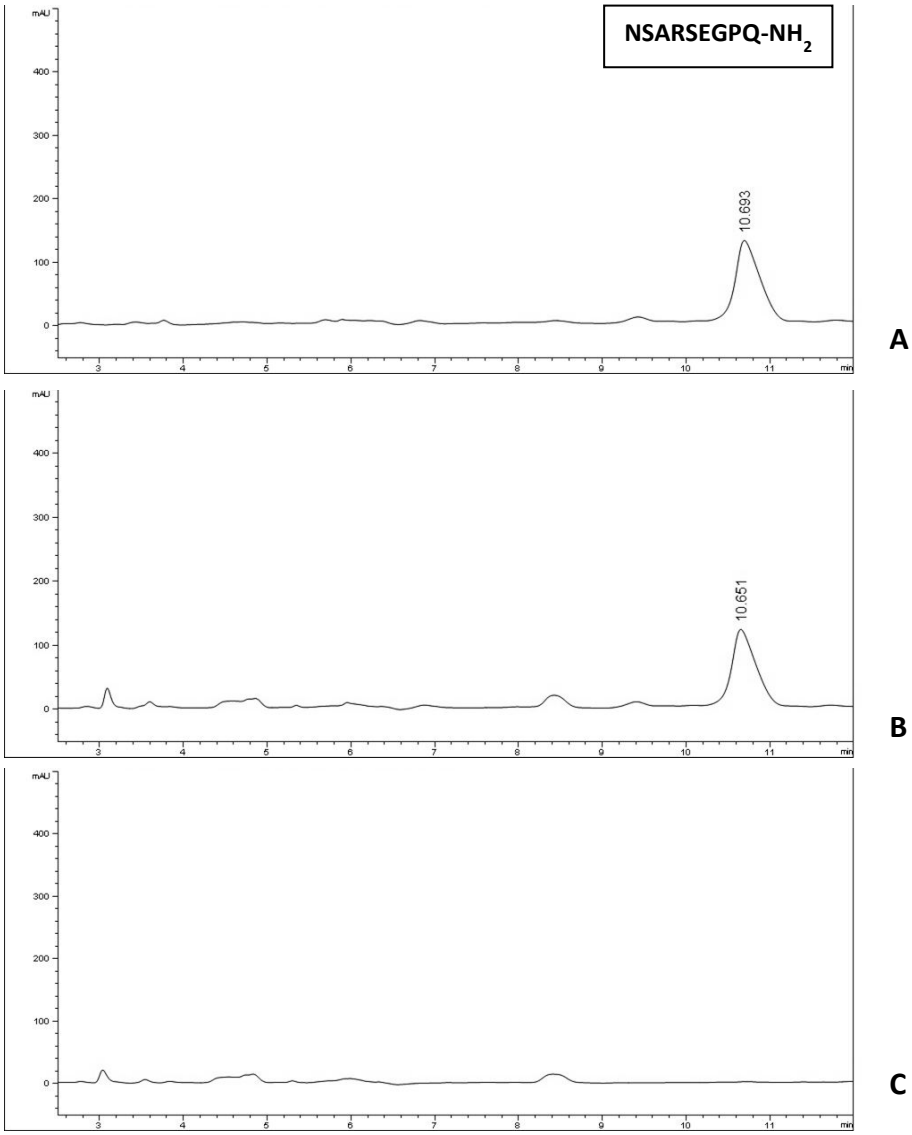

Figure 5.15: HPLC chromatograms of the uncapped NSARSEGPQ ACE stalk peptide. 100µM of peptide (in HBSS buffer) was incubated on the surface of CHO-K1 for 6 hours, and resulting fluorescence measured. A) WT uncapped ACE stalk peptide incubated for 0 hours on cells B) WT uncapped ACE stalk peptide incubated for 6 hours on cells C) HBSS buffer alone incubated for 6 hours. Fluorescence was monitored at wavelength was at 214nm.

5.3.4.2 Analysis of cleavage of longer peptides incorporating putative secondary sheddase recognition motifs

To probe whether a longer stalk peptide may be more susceptible to specific cleavage by the ACE sheddase, we extended the peptide N-terminally by 9 residues to include the entire juxtamembrane stalk as well as part of the proximal ectodomain. This ectodomain region has previously been shown to play a role in directing the cleavage of rabbit ACE (chapter 4,

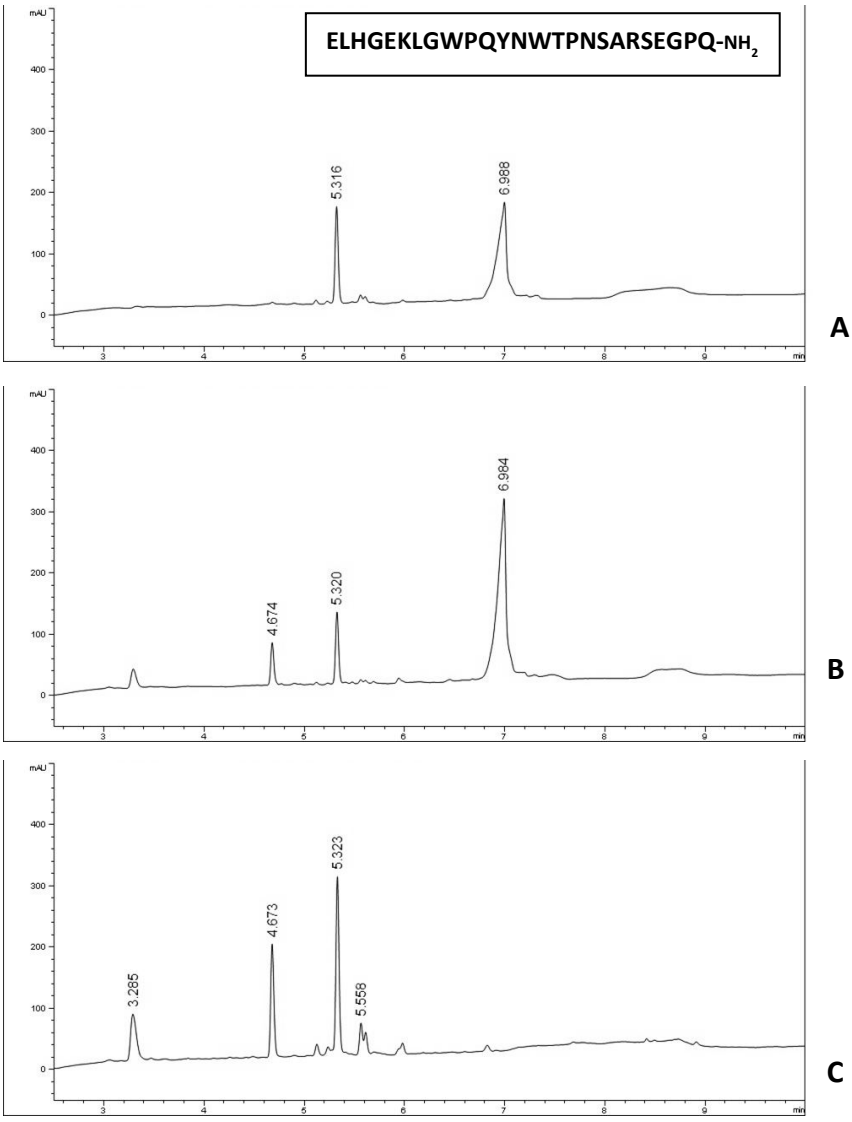

Figure 5.16: HPLC chromatograms of the 25 residue long uncapped ACE stalk peptide. 100µM of peptide was incubated on the surface of CHO-K1 for 6 hours, diluted in HBSS buffer A) RM uncapped ACE stalk peptide incubated for 0 hours on cells B) RM uncapped ACE stalk peptide incubated for 6 hours on cells C) HBSS buffer only incubated for 6 hours. Recorded wavelength was at 214nm.

Chattopadhyay et al., 2008). The resulting 25-residue peptide (RM) (table 5.4) was incubated for 6 hours with CHO-K1 cells in the cell assay and resolved using HPLC. The unlceaved RM peptide eluted at 6.98 minutes, however no new product peaks were observed when the reaction was analysed with HPLC (figure 5.16) implying that the fluorohpore groups have some sort of impact on the cleavage of the fluorogenic stalk peptides. Similar results were obtained for both of the 9- and 25-residue uncapped peptides even after an extended incubation period of 18 hours (Table 5.5).

Table 5.5: Cleavage of uncapped peptides. Peptides were incubated for 6 and 18 hours on CHO-K1 in the minimal media Optimem®. Percentage of substrate remaining is indicated where cleavage was observed**.**

Peptide	**Cleavage**	**% substrate remaining**	
		6 hours	**18 hours**
NSARSEGPQ	No	100%	100%
ELHGEKLGWPQYNWTPNSARSEGPQ	No	100%	100%
Abz-NSARSEGPQ-EDDnp	Yes	89 %	52%

The 18-hour incubations in the cell assay were prepared for mass spectrometry as previously described and a representative figure of the MALDI-ToF results is shown in figure 5.17. It is clear that after 18 hours of incubation, the m/z ions of the 9- (944.41) and 25- (2880.12) residue uncapped stalk peptides are in agreement with the calculated values of the intact peptides.

Thus, the fluorogenic capping groups seem to have a marked influence on the cleavage of the stalk peptides. While no cleavage was observed in the uncapped peptides even after an extensive incubation of 18 hours, the fluorescently capped peptides were cleaved efficiently under similar conditions, albeit at unexpected positions. We see a mass of m/z 509.15 that corresponds to the C-terminal cleavage product of GPQ-EDDnp.

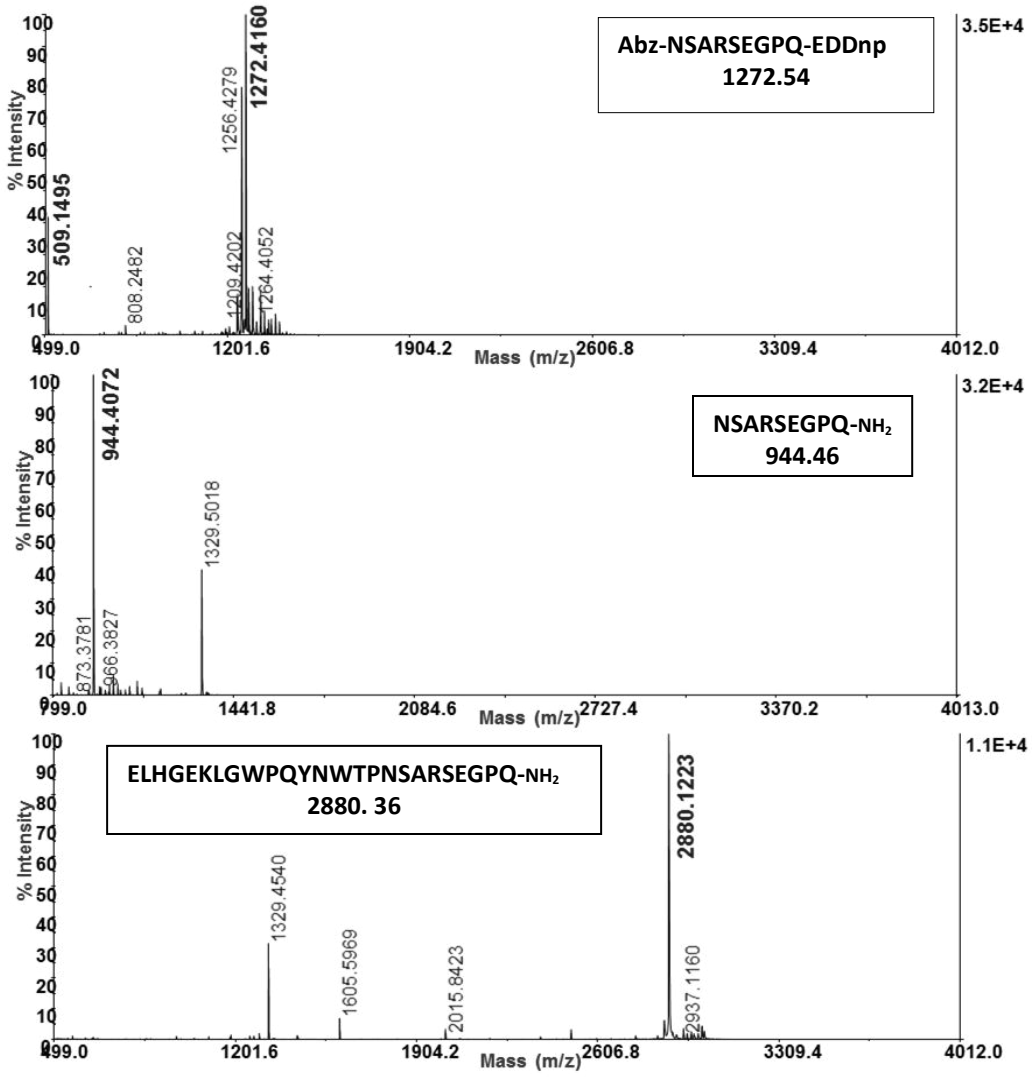

Figure 5.17: MALDI-ToF spectra of the 18-hour incubation of peptides with CHO-K1 cells. Calculated masses are indicated for each peptide. The top panel shows the 9-residue wild-type fluorogenic peptide. In bold the dominant cleavage product corresponding to m/z 509.15 is shown and the intact peptide corresponding to m/z 1272.4242. The second panel represents the 9-residue uncapped peptide and an observed m/z mass of 944.41 is seen which corresponds to the intact peptide. The lower panel represents the 25-residue uncapped peptide, with an observed mass (2880. 12) corresponding to that of the uncleaved species (2880.3).

5.4 Discussion

This study set out to define the minimal requirements needed to direct the shedding of ACE by investigating the role of its stalk region in this process. The original analysis of fluorogenic ACE

stalk peptides demonstrated that they were cleaved by CHO-K1 cell lysate, but at a very slow rate (R. Domingo, PhD thesis, 2011).

A cell-based assay initially used to evaluate ACE substrates in cell culture (Sabatini et al., 2007) was adapted to investigate the hydrolysis of the ACE stalk peptide. While the rate of shedding of full-length ACE expressed in different cell lines is increased via the addition of the phorbol ester, PDBu, and inhibited by the hydroxamate inhibitor, TAPI, the addition of these effectors made no change to the cleavage of the wild-type fluorogenic ACE stalk peptide (figure 5.4A). Moreover, pre-incubation with TAPI, still did not inhibit cleavage of the ACE stalk peptide (figure 5.6). However, under the conditions described by Sabatini et al. (2007), the activity of ACE in the cell-based assay could be inhibited by lisinopril. The reason for the discrepancy between inhibition of ACE activity and inhibition of sheddase activity could be that with using tACE transfected cell lines the protein is being overexpressed at a high rate. CHO-K1 cells, on the other hand, generate an endogenous sheddase/protease with an unknown level proteolytic? activity (Ehlers et al., 1996, 1995, 1991b). Alternatively, the peptides might be cleaved by proteases other than metalloproteases. .

Soluble ACE hydrolyses its substrates with similar efficiency to full-length ACE that includes the transmembrane and cytoplasmic domains. Studies carried out with the sheddase, ADAM 17, and a soluble peptide representing the TNF-α stalk (Dnp-SPLAQAVRSSSR-$NH_{2)}$ (Caescu et al., 2009; Doedens et al., 2003; Jin et al., 2002) showed that this peptide was cleaved by recombinant ADAM 17 as well as cell lysates. Moreover, the cleavage products generated when using cell lysate expressing endogenous levels of protein were considerably lower than when purified recombinant ADAM 17 was used. Studies done with TNF-α stalk peptides showed that there was no difference in cleavage site when a capped versus an uncapped peptide was analysed using recombinant ADAM 17 (Jin et al., 2002). However, when untransfected cell lines with endogenous ADAM 17 levels were used, the peptide (Dabcyl- SPLAQAVRSSSR –Edans) was not cleaved (Becker et al., 2002). Similarly cleavage of a TNF-α stalk peptide (Dnp-SPLAQAVRSSSR) by untransfected monocytic cells (DRM) was limited compared to cleavage by

recombinant purified ADAM 17 (Doedens et al., 2003). This indicates that peptide hydrolysis by recombinant proteins are more specific than using untransfected cell lines expressing endogenous levels of the protein of interest.

To determine if the cleavage of stalk peptides was the result of a specific class of protease, we incubated the peptides with EDTA, known to inhibit metalloproteases and previously shown to inhibit the solubilisation of ACE from tissue, as well as the serine protease inhibitor, PMSF (Naim, 1996; Oppong and Hooper, 1993). PMSF had no effect on cleavage and EDTA resulted in 50 % inhibition (figure 5.6), suggesting that proteases other than metalloproteases were also contributing to the cleavage of the peptide.

Mass spectral data revealed that the same cleavage site was observed with all the ACE stalk peptides tested. Becker et al., (2002) have previously shown that cleavage of both fluorogenic and non-fluorogenic TNF-α stalk peptides by recombinant human ADAM 17 resulted in hydrolysis of the expected Ala-Val bond (the observed cleavage site in full-length TNF-α). However, incubation with HUVEC cells, HMC-1, and peripheral blood lymphocytes (PBL) resulted in no identifiable cleavage products. No stimulation was seen and no inhibition by the hydroxamate inhibitor TAPI-2 occurred. These assays relied on untransfected cells and endogenous levels of proteins, leading to inconclusive results. The important difference between the Becker et al. (2002) study and the results presented here is that they observed complete degradation of their peptide using cell lysates and their starting material disappeared completely and the cleavage site was not determined, while the ACE stalk peptides were not completely degraded and that a defined and consistent cleavage site was observed.

The cleavage site resulting from both the cell lysate (R. Domingo, PhD thesis, 2011) and cell assay methods (figure 5.11) did not agree with the physiological cleavage site. This initial characterisation of the cell-assay showed that the cleavage of the ACE stalk peptide was not susceptible to stimulation and inhibition (by phorbol esters or hydroxamate inhibitors respectively) (figure 5.4 and 5.6). Moreover, fractionation of the supernatant from the cell

assay resulted in the identification of, not only the C-terminal fragment found before (R.Domingo, PhD thesis, 2011), but also the corresponding N-terminal fragment. This was the first unequivocal evidence that specific cleavage of ACE stalk peptides occurs at the E-G bond (figure 5.11) irrespective of system used i.e. the cell-based or cell lysate assay.

In the presence of the aminopeptidase inhibitor, bestatin, the ACE stalk peptide was still preferentially cleaved at the E-G bond, however; there was also a secondary minor cleavage at the R-S bond (figure 5.7). These data confirmed that aminopeptidases do not play a role in the cleavage of the fluorogenic ACE stalk peptide. Numerous studies have revealed multiple cleavage sites for specific substrates that undergo ectodomain shedding. For example, the cleavage site of an ectoprotein such as ACE or L-selectin may vary depending on the sheddase recruited under basal or stimulated conditions (Schwager et al., 1998; Zhao et al., 2001). ACE 2 is another excellent example of a sheddase substrate that produces differing cleavage products, under different conditions (Iwata et al., 2009).

The mutations in the theoretical P1 and P1' positions of the ACE stalk peptide showed that irrespective of changes in the residues targeted by the sheddase, the peptides were cleaved at the same position (table 5.3) i.e. three as opposed to five residues from the C-terminus. When the P1' serine was mutated to a tryptophan or phenylalanine, cleavage was enhanced in the cell lysate assay. However, when the P1 arginine was mutated to W, Y and F, cleavage was no longer observed. This indicates that the R in the theoretical P1 position is favoured and the P1' position modulates cleavage rates. Interestingly, previous work has shown that mutation of the R^{627} in the stalk of full-length tACE does not knock out shedding completely, but modulates the shedding and cleavage site. In this case, the cleavage site shifted 10 and 13 residues C-terminal to R^{627} and was cleaved at R-V and F-L, respectively (Chubb, PhD thesis, 2001). Results from the stalk peptide mutants assayed with cell lysates agree with what has been established in membrane-bound ACE. The peptide with a double mutation at both the P1 and P1' positions, was cleaved much less efficiently than peptides with P1' mutations alone. Most notably, the

TNF-α stalk peptide was cleaved at the same position as the ACE stalk peptides (3 residues from the C-terminus, table 5.3) and not at the previously reported A-V site (Jin et. al. 2002).

Work by Domingo (2011) used a TNF-α stalk peptide capped with the Abz fluorescent donor and the EDDnp quenching groups (table 5.5) which differs from the peptide analysed by Jin et al. (2002), which had a 9,10-diphenylanthracene (Dpa) quenching group at the C-terminus. Using recombinant ADAM 17 it was found that the k_{cat}/k_{prime} (a measure of the enzyme's catalytic efficiency) of ADAM17 with this EDDnp-peptide was 35-fold lower than that with the Dpa groups. It was suggested that the EDDnp quenching group lowered the affinity of the substrate by 4-fold and that the chemistry of the Dpa group allowed for increased hydrogen bonding within the catalytic site (Jin et al., 2002). Another study using the acceptor/ donor groups FAM (6- carboxyfluorescein) and TAMRA (6-carboxytetramethylrhodamine) respectively (Alvarez-Iglesias et al., 2005), reported real-time measurements on the surface of live cells. The advantage of these peptides were validated using recombinant ADAM 17 and ADAM 10 in conjunction with peptides utilizing other fluorophores to compare specificity and efficiency of each capping pair. The K_{cat}/K_m was higher for FAM-TAMRA groups than the MCA-Dnp groups, indicating that FAM-TAMRA peptides are cleaved more efficiently (table 5.5). This implies that other fluorophores are not as sensitive and specific as FAM-TAMRA.

Table 5.5: Kinetic analysis of TNF-α peptides with various capping groups.

Peptide	Cleavage site(s)	Capping pair	k_{cat}	k_{cat}/K_M	Reference
Abz- LAQAVRSSSR -Dpa	A-V	Abz –Dpa	21.6 s^{-1}		Jin et.al., 2002
LAQAVRSSSR			0.34 s^{-1}		Jin et.al., 2002
FAM– SPLAQAVRSSSRK-TAMRA		FAM-TAMRA		0.99 $\mu M^{-1}s^{-1}$	Alvarez-Iglasias et.al., 2005
Mca- SPLAQAVRSSSRK-Dnp		Mca-Dnp		0.13 $\mu M^{-1}s^{-1}$	Amour et.al., 1998
Abz- LAQAVRSSSRQ-EDDnp		Abz-EDDnp	2.28s^{-1}	6.27 $\mu M^{-1}s^{-1}$	R. Domingo, PhD thesis, 2011
SPLAQAVRSSSR	A-V (rhADAM17)				Becker et.al., 2002
Dabcyl- SPLAQAVRSSSR -Edans	A-V (rhADAM 17)	Dabcyl-Edans			Becker et.al., 2002

The use of soluble peptides to determine cleavage site preferences has been well studied over the years. Jin et al., 2002 showed the consistency of TACE cleaving at the A-V bond, while a screen of a peptide library with ADAM 8, known to cleave myelin basic protein (MBP) showed that basic residues at the P1 and P2' positions increased cleavage efficiency (Naus et al., 2006; Schlomann et al., 2002). Cleavage by ADAM 33 was shown to favour an APP substrate with V, A and Q at the P3, P2 and P1' positions respectively (Zou et al., 2005). It was found that a minimum of nine specific residues were necessary for recognition as well as cleavage. Another extensive study was conducted to determine amino acid preferences for cleavage sites and to use these preferences as a means to differentiate between putative sheddases (Caescu et al., 2009). It was found that hydrophobic residues such as L and V were common in the P1' site for ADAM 17 specific peptides and the preference of a valine residue at the P1' position distinguishes ADAM 17 from ADAM 10 substrates. These studies all suggest that sheddases are constrained to cleave at preferred sites within the juxtamembrane region.

Unlike ACE, the CD4 protein has been shown to not be cleaved from the cell membrane. Interestingly, Sadhukhan et al. (1998) have shown that a construct containing the CD4 stalk region with an ACE ectodomain was in fact cleaved, alluding to the potential presence of a sheddase recognition motif within the ectodomain of ACE. We therefore also included the peptide Abz-ESNIKVLPQ-EDDnp, based on the sequence for the CD4 stalk region, in our assays, but found no cleavage (table 5.3). The results confirmed that the CD4 stalk sequence was not sufficient for cleavage to occur and illustrates that the small amount of fluorescence observed from the CD4 peptide was due to undefined proteases (figure 5.14). This is in line with our results that both TAPI and phorbol esters had no effect on the cleavage of the ACE stalk peptide (figure 5.4) and that EDTA does not knock out shedding completely (figure 5.7). This suggests that the proteases/sheddases responsible for cleaving the ACE stalk peptides in our assays, probably require certain minimal sequence specificities to direct cleavage, but without adhering to the physiological cleavage site. Furthermore, they are not fully inhibited by broad range metalloprotease inhibitors that inhibit the shedding of ACE in CHO-KI cells, again reiterating the role of non-metalloproteases in the cleavage of the peptides.

A limitation of this study is that the fluorogenic ACE stalk peptide was cleaved at an alternative site compared to the expected endogenous cleavage site. This emphasises that our experimental model is not optimised to target the correct protease in CHO-K1 cells, which is a sheddase that is sensitive to TAPI inhibition and stimulated by phorbol esters. Furthermore, the use of uncapped peptides with no fluorogenic groups revealed no cleavage, suggesting that these shortened soluble sequences are not sufficient for hydrolysis by the ACE sheddase. The uncapped peptides also has no fluorogenic groups with which to monitor the cleavage and there is a reliance on HPLC and MALDI/MS to analyse cleavage products. This reduces the ability to make the assay amenable to high throughput usage. From these results, we can see that the cell-based assay may not be the optimal way to study the shedding activities that are specifically responsible for the cleavage of membrane-bound ACE in CHO-K1 cells.

Removal of the fluorogenic capping groups rendered the 9-residue ACE stalk peptide uncleavable under the 6-hour cell assay conditions. Extending the N-terminus by 16 residues did not result in cleavage, suggesting that the additional sequence from the juxtamembrane stalk and proximal ectodomain does not help facilitate hydrolysis of the peptide. Even after 18 hours incubation, neither of the uncapped peptides were cleaved and the capped fluorogenic peptide was cleaved, albeit not at the expected physiological site. This reemphasises the need for the ACE sheddase substrate to be anchored in the lipid bilayer of the cell membrane In contrast, 20 amino acid long mimetic peptides of the ACE2 (ACE homologue) juxtamembrane region provided soluble substrates of sufficient length to create secondary structures necessary for efficient cleavage by the ACE2 sheddase, ADAM 17. These were successfully used to determine the cleavage site of the ACE2 cognate sheddase, ADAM 17, in cell culture (Iwata et al., 2009; Lai et al., 2009).

A critical finding from this study is that the protease present in CHO-K1 cells cleaving the fluorogenic wild-type ACE stalk peptide favours the E-G site, and not the expected R-S site favoured by the ACE sheddase in endogenous ACE cleavage. An encouraging feature of the cell-based assay developed for this study is that it can be used to study proteolysis using soluble peptides where the cleavage sites of peptides incubated on the cell surface can be investigated by either purifying products via HPLC or conducting a manual clean up with Zip–tip C18 reverse phase resins. With the latter method, we were able to perform conventional MALDI-ToF to analyse the resulting peptide products. This method also circumvented the requirements to ultracentrifuge samples and analyse samples with LC-MS, as was necessary with the CHO-K1 lysate samples.

In summary, the fluorogenic ACE stalk peptides were cleaved 3 residues from the C-terminus and the fluorogenic groups present influenced how the peptide was cleaved. There was also a preference for certain residues in the P1 and P1' positions, with the protease cleaving these peptides and favouring hydrophobic residues within the P1' position, while not tolerating such residues in the P1 position. The cleavage of these fluorogenic peptides was not regulated by known stimulators or inhibitors of ACE shedding, making it more difficult to identify the cognate sheddase. It was examined whether it was sufficient for the sheddase only to be anchored in the membrane and cleave a soluble peptide substrate, but in the case of an ACE sheddase, there is a requirement for the substrate to be tethered to the membrane as well. In all likelihood, the ACE sheddase requires more stringent conditions in order to cleave the ACE stalk as well as the ACE stalk peptide used in this study.

The requirement of having the substrate and ACE sheddase attached to the membrane, ties in with the premise that there exists a complex interplay of regulatory proteins involved in shedding, suggesting that other proteins might participate in the shedding process. A key example of such a multifactorial shedding machinery is the annexins, which have been shown to interact with ADAM 17 to modulate the shedding of the ProAREG, an EGFR ligand precursor (Nakayama et al., 2012). Another well-documented example is the tyrosine receptor Eph, shed

by ADAM 10, which needs to be bound by its ligand that is expressed by an adjacent cell. This complex creates a favourable conformation to expose an ADAM 10 recognition site (Janes et al., 2009, 2005). The shedding of L-selectin is negatively controlled by calmodulin bound to its cytoplasmic domain (Gifford et al., 2012), and interestingly, ACE has been shown to be associated with calmodulin via its cytoplasmic tail and this association is another measure of shedding control (Chattopadhyay et al., 2005). More recently it was discovered that a member of the rhomboid family of proteins, iRhom2, is responsible for controlling the maturation of ADAM 17 ensuring it reaches the cell surface in its correct form (Adrain et al., 2012; Issuree et al., 2013; McIlwain et al., 2012). This demonstrates that there is another tier of regulation at the sheddase maturation or processing level, adding further complexity to the shedding process.

In conclusion, the use of soluble peptides of varying lengths for the characterisation of the ACE sheddase in CHO-K1 cells is not ideal. This is likely due to the requirement for the substrate of the ACE sheddase to be attached to the membrane. Other systems that present the substrate in its appropriate environment and conformation for the ACE sheddase need to be explored and adapted for further analysis of the shedding of this enzyme. These alternatives will be discussed in the concluding chapter of this thesis.

CHAPTER 6: Conclusions and Future work

Testis and somatic ACE both play vital roles throughout the body, with the most commonly described being in fertility and blood pressure regulation, respectively. Both isoforms of ACE are subject to ectodomain shedding, but we have very little knowledge about the physiological role for this process. This dissertation aimed to characterise the conformational structures inherent to ACE which direct cleavage secretion by the as yet unidentified ACE sheddase.

Firstly, the D^{164}-V^{416} region in the distal ectodomain of tACE, which was initially thought to possess the secondary binding site or recognition motif (Woodman et al., 2006), was investigated using the 3D structure of ACE to predict potential protein-protein interaction sites. The structural boundaries of ACE was adhered to so as to maintain active and correctly processed proteins. The swop-over mutants of three ectodomain surface regions were made and shown to be catalytically active (chapter3). However, none of these mutations abolished shedding completely, suggesting that a single controlling recognition motif was not harboured within these regions. This indicated that shedding is rarely coordinated by a single region or interaction. This result confirmed that alterations made to surface helices and motifs near the cleavage site affected cleavage subtly and that ACE is part of a sophisticated shedding mechanism. Furthermore, the sheddase exosite, might consist of non-consecutive residues of the distal and proximal ectodomain as is the case for KitL2 (Kawaguchi et al., 2007).

Secondly, possible secondary binding of the sheddase to the proximal ectodomain was studied. A 5-residue motif H^{610}-L^{614} was replaced with alanines in human tACE and found to cause a reduction in tACE activity, processing as well as shedding. When the mutation was extended by two residues on the N-terminal side, a more pronounced disruptive effect on the cellular processing in terms of processing and activity was observed. This illustrates that the alanines caused a change in conformation of the proximal ectodomain and did not directly affect a secondary binding site of the sheddase with the substrate. A key result was

obtained when these 7 residues were converted to the corresponding ones from the N-domain. Eventhough there was a slight decrease in shedding, the processing was not affected, demonstrating that N-domain residues were able to maintain shedding and activity in contrast to alanines.

Thirdly, the mechanism by which the $P^{623}L$ polymorphism affected ACE shedding was investigated. Our initial hypothesis proposed that the loss of proline allowed the preceding N^{620}WT glycosylation sequon to be glycosylated. This resulted in a change in stalk conformation and improved access by the sheddase and an increase in shedding. However, on the contrary, when the glycosylation was removed by mutating N^{620}, even higher shedding was observed. This established that the flexibility that the leucine provides the stalk, is made more prominent by the lack of glycans and is the first indication that the reduction in glycosylation around the cleavage site may increase access to the sheddase. Therefore, the ACE sheddase needs a membrane-bound substrate to cleave at its preferred site. The correct conformation of the substrate provide and assemble the requisite secondary binding sites it needs to identify it as being a substrate requiring proteolytic release from the membrane.

In light of these findings, further analysis of the CC-domain mutant (Woodman et al., 2005) is needed as this mutant was cleaved in the linker region as well as in the stalk. This could be due to a decrease in the extent of glycosylation of the residues surrounding the linker, leading to better access by the sheddase. In addition, there is ongoing work being conducted in our laboratory on minimally glycosylated sACE mutants for crystallization trials and structure-function studies (Anthony et al., 2012). Shedding assays on these minimally glycosylated sACE mutants will help elucidate the effect of glycosylation on shedding.

The dimerisation of ACE might also play an integral part in shedding, which is affected by the conformational changes triggered by the disulphide-linked dimerisation between C-domains and non-covalent interactions (e.g. glycosylation) between N-domains (K. Gordan, PhD thesis, 2011). Therefore, the role of disulphide bonding has to be further investigated. The redox environment has proved to be highly influential in shedding regulation and PDI inhibitors have demonstrated to modulate shedding (Borroto et al., 2003; Willems et al.,

2010). In addition, the HVR of ADAMs, regarded to be the candidate exosite, is prone to disulphide bonding (Takeda et al., 2012) as well. Therefore, future shedding analysis should include investigations into the roles of disulphide bonding and the redox environment.

Sheddase recognition sites on substrates (Deng et al., 1996; Iwata et al., 2009; Nishie et al., 2012; Zhao et al., 2001) as well as exosites on sheddases have been identified (Stawikowska et al., 2013; Takeda et al., 2012, 2006). In addition to the redox environment and secondary binding sites of sheddases, other forms of regulation have been identified. Recently, an ADAM 17 specific regulatory protein was discovered which was responsible for its trafficking and activity (Adrain et al., 2012; Issuree et al., 2013; McIlwain et al., 2012). Considering that the 5-residue motif in the stalk of ACE had such an impact on its processing, it would be interesting to determine if ACE-specific regulatory proteins exist that play a similar role to the one identified and characterized by Adrain et al. (2012).

Finally, shedding conditions of ACE were simulated in a cell-based assay (Chapter 5). The soluble fluorogenic ACE stalk peptides utilised were cleaved at the E-G bond, and not at the physiological R-S site. Cleavage site mutants showed that the peptide was cleaved at the same site (E-G bond) irrespective of sequence, but in order to be cleaved the peptide had to mimic a stalk sequence that is cleaved physiologically. . This result prompted the analysis of non-fluorogenic peptides, which proved that the fluorogenic groups directed cleavage of the peptide, since uncapped peptides were not cleaved. Lengthening the peptide to include part of the proximal ectodomain did not render the substrate cleavable. This investigation proved that the ACE sheddase requires a substrate which is membrane-bound.

Even though we have shown that soluble peptides are not an ideal substrate for the endogenously expressed ACE sheddase, the cell-based assay has benefits over the cell lysate assay. Cleavage of the substrates are easily identifiable by HPLC, samples require minimal clean-up for follow-on procedures and require more accessible equipment as opposed to the lysate assay which required ultracentrifugation and LC-MS.

Above all, suggested future work, the ACE sheddase has to be identified. A spectrum of ADAMs may be overexpressed alongside ACE to determine if they are involved in the

shedding of ACE, with the exclusion of ADAM 17, 10 and 9, since they have been shown not be involved in basal or phorbol ester stimulated shedding (English et al., 2012; Hooper and Turner, 2000; Parvathy et al., 1998; Sadhukhan et al., 1999). If the cell assay is to be used with the cell lines overexpressing various ADAM proteins, stalk peptides with alternative fluorogenic capping groups should be used that do not promote cleavage at non-physiological sites.

One of the aims of establishing a cell-based assay was so it could be used in the purification of the ACE sheddase. Unfortunately, the ACE sheddase is not amenable to cleaving a soluble stalk peptide and it was not possible to reproduce the cleavage site and shedding inhibition conditions of cell-bound ACE. Innovative proteomic techniques could be attempted to circumvent these issues. For example, ACE may be expressed with a biotin tag at its C-terminus so that it may be immobilized on a streptavidin-coated plate. Thereafter fractions from ACE sheddase containing tissue homogenate may be passed-over, which should be able to cleave immobilized ACE. The biotin may be positioned at varying distances to replicate the membrane environment.

In conclusion, this thesis has demonstrated that ACE undergoes regulated proteolytic release from the membrane and is influenced by the structural binding sites in the ectodomain as well as stalk, with the stalk requiring a defined level of flexibility and accessibility. In addition, the stalk sequence in the form of a soluble synthetic peptide of varying lengths is not sufficient to be cleaved by a membrane-anchored ACE sheddase. These insights provide an invaluable foundation for future investigations into the determination of the ACE sheddase as well as mechanisms of interactions with ACE.

APPENDIX

A1 Reagents

A1.1 ACE activity reagents

3M NaCl:
Dissolve 17.53g NaCl in 100ml distilled water. Autoclave to sterilise.
0.28 M NaOH
Dissolve 2.8g NaOH in 250ml of distilled water. Autoclave to sterilise.

o-phthaldialdehyde
Dissolve 24mg in 1ml methanol. Make up fresh each time and cover in foil to protect from light.

3N HCl
Add 24.8ml 37% HCl to 75.2ml distilled water.

5X $KHPO_4$ buffer (with NaCl)/0.5M $KHPO_4$ buffer, pH 8.3, 1.5M NaCl
1.03g KH_2PO_4
16.09g K_2HPO_4
17.53g NaCl
pH 8.3
Dissolve in distilled water of which the final volume should be 200ml.

20mM Z-FHL stock solution
Dissolve 220mg Z-FHL (Sigma) dissolved in 2ml 0.28M NaOH and made up to a 20ml final volume with distilled water. Divided aliquots were stored at -20°C.

1mM Z-FHL working solution
15ml of distilled water was added to 4ml of 5X $KHPO_4$ buffer, to which 20µl of 10mM $ZnSO_4$ was added as well as 1ml of 20mM Z-FHL. Solution was stored at 4°C.

A1.2. Reagents for protein purification

Wash buffer

20ml	1M HEPES pH 7.5	(20mM)
250ml	2M NaCl	(500mM)

Make up to 1L with distilled water.

Elution buffer

1.55g	Boric acid	(50mM)

pH to 9.5
Make up to 500ml with distilled water.

Dialysis solution (specifically for PNGase digest)
First solution

20ml	0.5M KPO_4 pH 8	(5mM)
2ml	100mM PMSF (in EtOH)	

Make up to 2L with distilled water.

Second solution

200ml	0.5M KPO_4 pH 8	(50mM)
2ml	100mM PMSF (in EtOH)	

Make up to 2L with distilled water.

A2 Standard curves

A2.1 HL standard curve

A 5mM HL (Sigma, USA) stock solution in distilled water was prepared and diluted to a 0.5mM working solution in 1X potassium phosphate buffer. 30µl aliquots of HL in increasing concentrations were prepared and placed in a 96-well plate in triplicate. Assay conditions was described in Chapter 2, section 2.6, beginning with the addition of 0.4M NaOH. The curve was determined by linear regression analysis using GraphPad Prism 4.0 software.

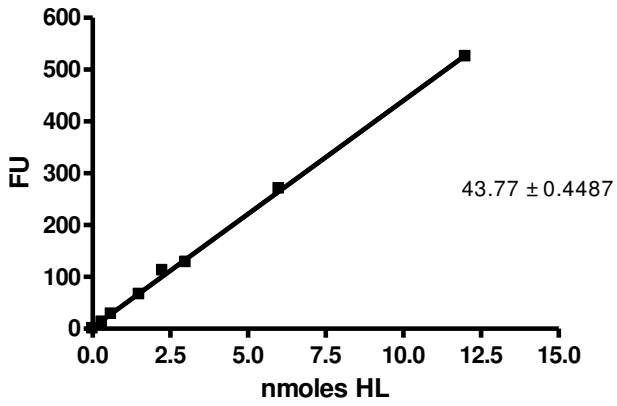

Figure A2.1: Standard curve of HL (nmoles) versus fluorescence intensity.

A.2.2 Protein Concentration

Protein concentrations of purified ACE or cell lysates were determined using a standard curve of increasing IgG concentrations.

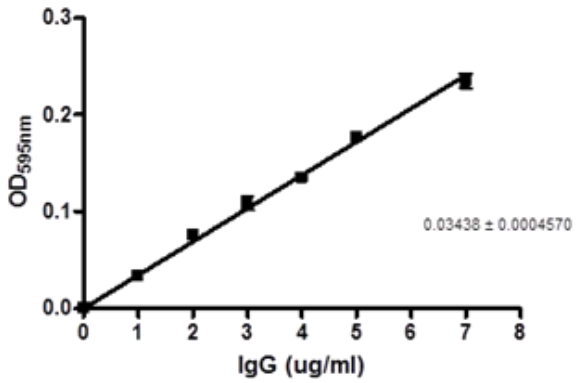

Figure A2.2: Standard curve for Bio-Rad protein assay of IgG (μg/ml) versus OD_{595nm}

A3: Mutagenic Primers

Table A3.1: Primers used in the overlap PCR mutagenesis of the α-helix 7 of tACE. Underlined letters are indicative of the restriction enzyme site created and bold letters represent the bases changed in order to create the restriction site and/or to minimize self-complementarity of the primer.

Primer name	RE site	Nucleotide Sequence
Mid For	EheI	5'-GACACGGG**C**GCCTACTGGCG**A**TCCTGGTACAACACACCATCCCTGGAGC-3'
Mid Rev	EheI	5'-GTTGTACCAGGATCGCCAGTAGGCGCCCGTGTCTACATAGCCATTGAGCCG-3'
BglII For		5'-CCAGATCTGACGAATGTGATGG-3'
NheI Rev		5'-GGGCTAGCACGTCCCCAATGG-3'

Table A3.2: Primers used in the overlap PCR mutagenesis of the α-helix 8 of tACE. Underlined letters are indicative of the restriction enzyme site created and bold letters represent the bases changed in order to create the restriction site and/or to minimize self-complementarity of the primer.

Primer name	RE site	Nucleotide Sequence
H8 For	SphI	5'-TGTACGAGACACCATCCTTCGAGGACGATCTGGAACACC-3'
H8 Rev	SphI	5'-GGTTGATGTGCTGGGCTCCGTATCGGCGATGC-3'

Table A3.3: Primers used in the site-directed mutagenesis of A^{261}-H^{263} to D^{261}-Y^{263}

Primer name	RE site	Nucleotide Sequence
AQH For	AgeI	5'-CACTACGGGG**A**CC**G**G**T**ACATCAACCTG-3'
AQH Rev	AgeI	5'-CAGGTTGATGTACCGGTCCCCGTAGTG-3'

Table A3.4: Primers used in site-directed mutagenesis of the proximal ectodomain and stalk region of tACE. Underlined letters are indicative of the restriction enzyme site created and bold letters represent the bases changed in order to create the restriction site and/or to minimize self-complementarity of the primer.

Primer name	Nucleotide sequence	RE site	Tm	Primer length
tACE ALA For tACE ALA Rev	5'-GAGAACGAGCT***AGC***TG***C***GG***C***G***GC***GGCGGGCTGGCC-3' 5'-GGCCAGCCCGCCGCCGCCGCAGCTAGCTCGTTCTC-3'	NheI	82.5	35
tACE ala2F tACE ala2R	5'-CTCCGCACGGAGAA***TG******CTGC***AGCTGCGGCGGCGGCG-3' 5'-CGCCGCCGCCGCAGCTGCAGCATTCTCCGTGCGGAG-3'	BsmI	81.7	36
tACE ST _Ndom F tACE ST _Ndom R	5'-CTCCGCACGGAGAAC***C******A******A***C***A***G***A***ATGGGGAAGTACTGGGCTGGCCGC-3' 5'-GCGGCCAGCCCAGTACTTCCCCATTCTGTTGGTTCTCCGTGCGGAG-3'	ScaI	79.8	46
P2LF P2LR	5'-GCAGTACAACTGGACGC***T***GAAT***T***CCGCTCGCTCC-3' 5'-GGAGCGAGCGGAATTCAGCGTCCAGTTGTACTGC-3'	Eco RI	74.3	34
P2LD F P2LD R	5'-CCGCAGTAC***G***ACTGGACGCTGAAT***AG***CGCTCGCTCAG-3' 5'-CTGAGCGAGCGCTATTCAGCGTCCAGTCGTACTGCGG-3'	Eco 457III	76.8	37

A4. Protein purification

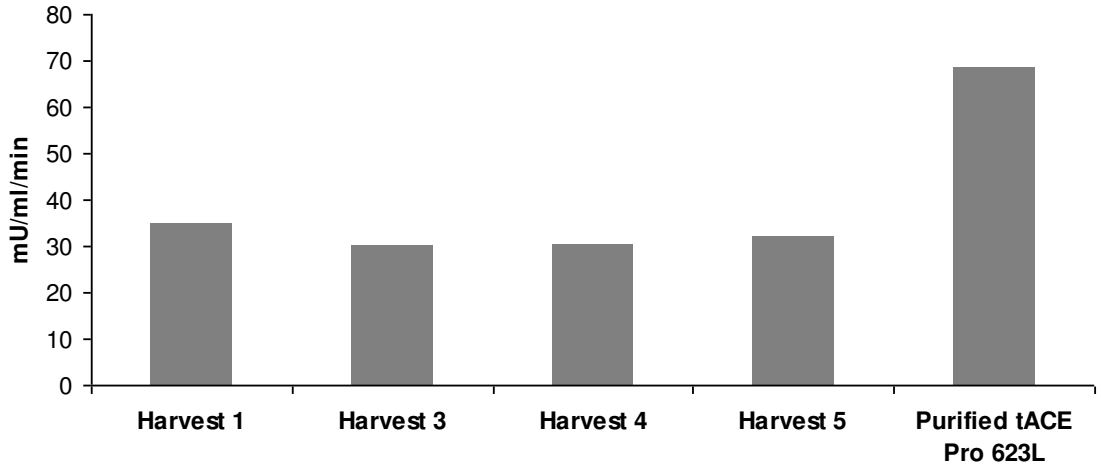

Figure A4.1: ZFHL activity assays of tACE Pro623Leu. The first 4 bars represent activity of the medium harvested from bulk growth flasks. The medium was pooled and purified using the Lisinopril-sepharose column. The most active fractions were subsequently pooled and concentrated on an Amicon filter. The final concentration of purified and concentrated protein is shown in the last bar.

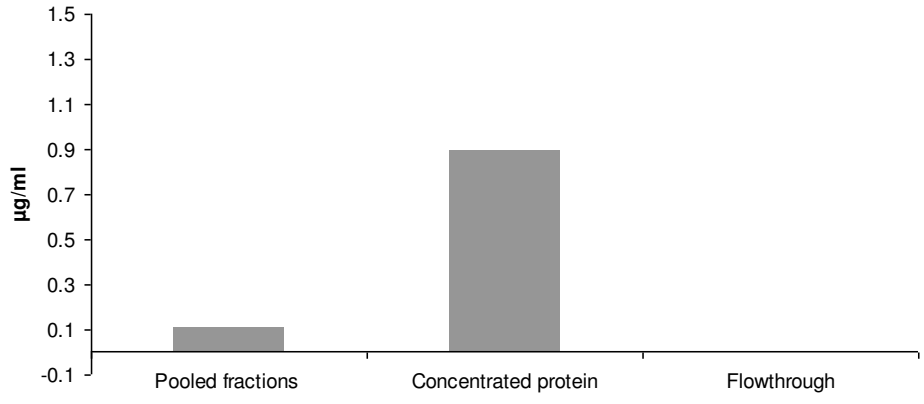

Figure A4.2: Protein concentrations of purified tACE Pro623Leu.

A5: ACE stalk peptides

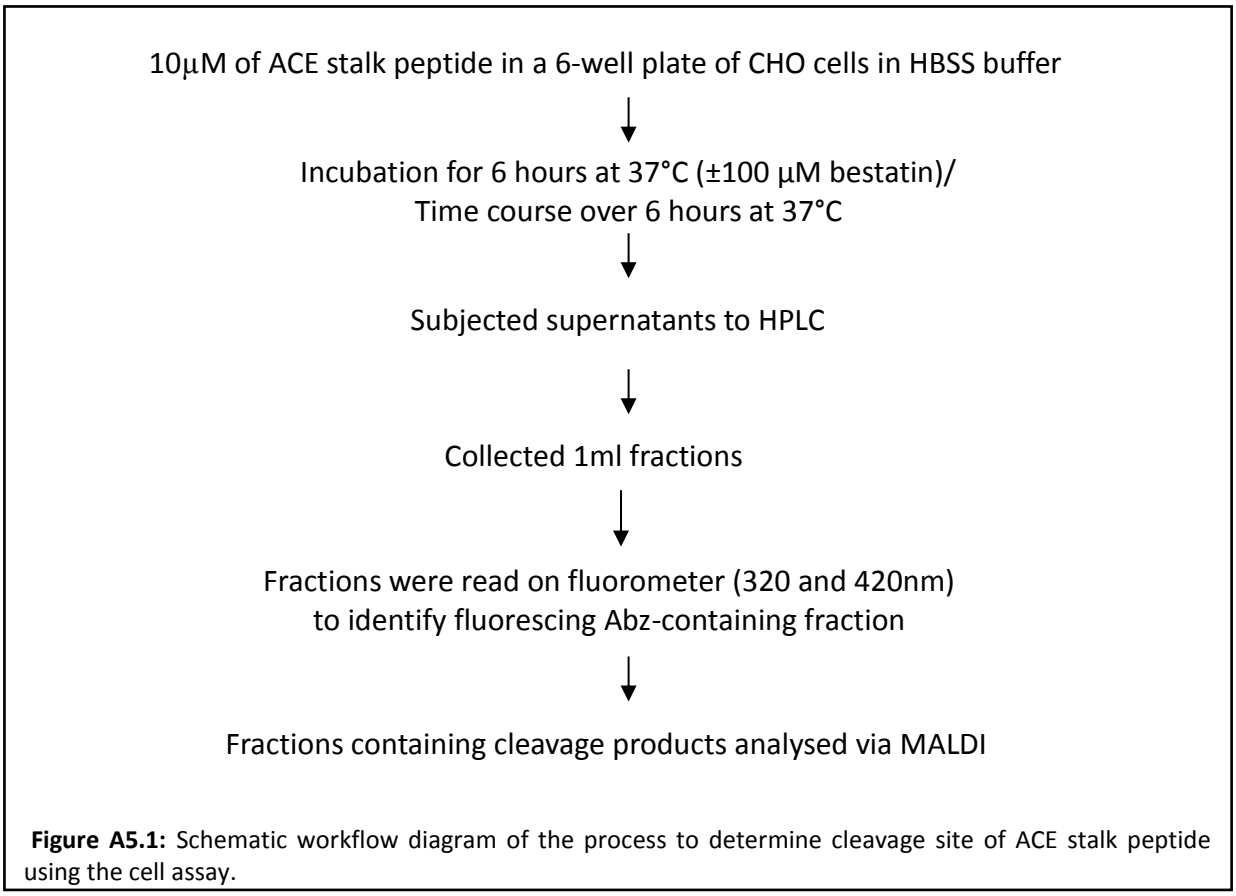

Figure A5.1: Schematic workflow diagram of the process to determine cleavage site of ACE stalk peptide using the cell assay.

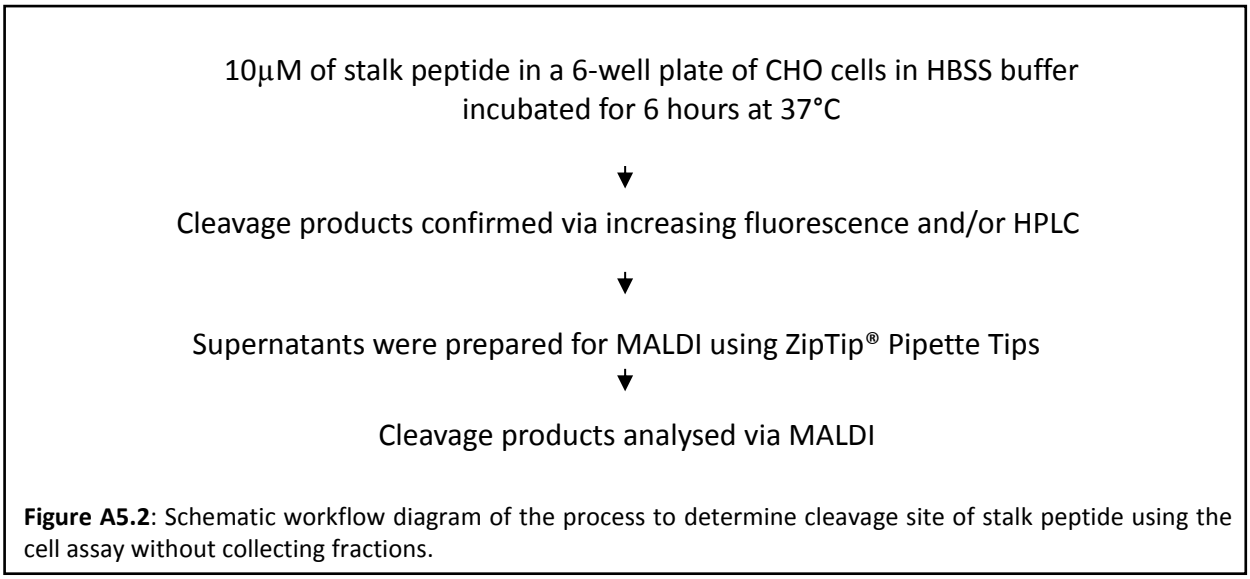

Figure A5.2: Schematic workflow diagram of the process to determine cleavage site of stalk peptide using the cell assay without collecting fractions.

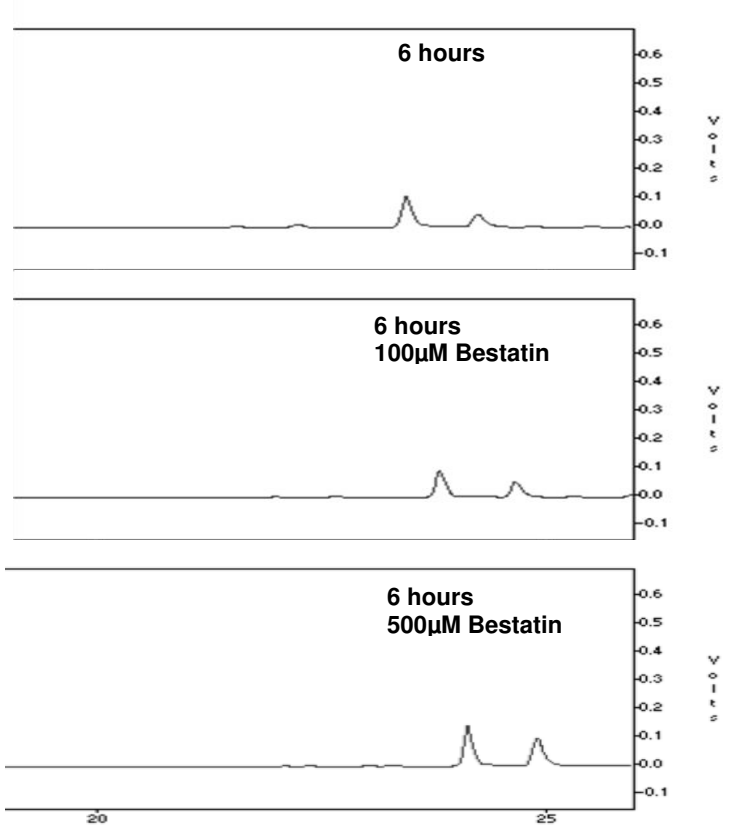

Figure A5.3: The HPLC chromatograms monitored at 354nm of the ACE sheddase cell assay using the wild-type stalk peptide over at 6 hours, with 100µM and 500µM bestatin.

The cleavage of the fluorogenically capped 9-residue peptide was investigated under the same conditions as the uncapped peptides. The sample represented in figure A5.4A, was sampled after 15 minutes of adding peptide and therefore we can see the presence of a cleavage product by this time. The uncleaved peptide elutes at 6.690 minutes and the cleavage product elutes at 6.315 minutes. In figure A5.4B, after 6 hours the peak area of the product peak at 6.315 minutes had increased by approximately 6-fold. Figure A5.4C represents the buffer control, which accounts for the other peaks present that were not generated by peptide hydrolysis.

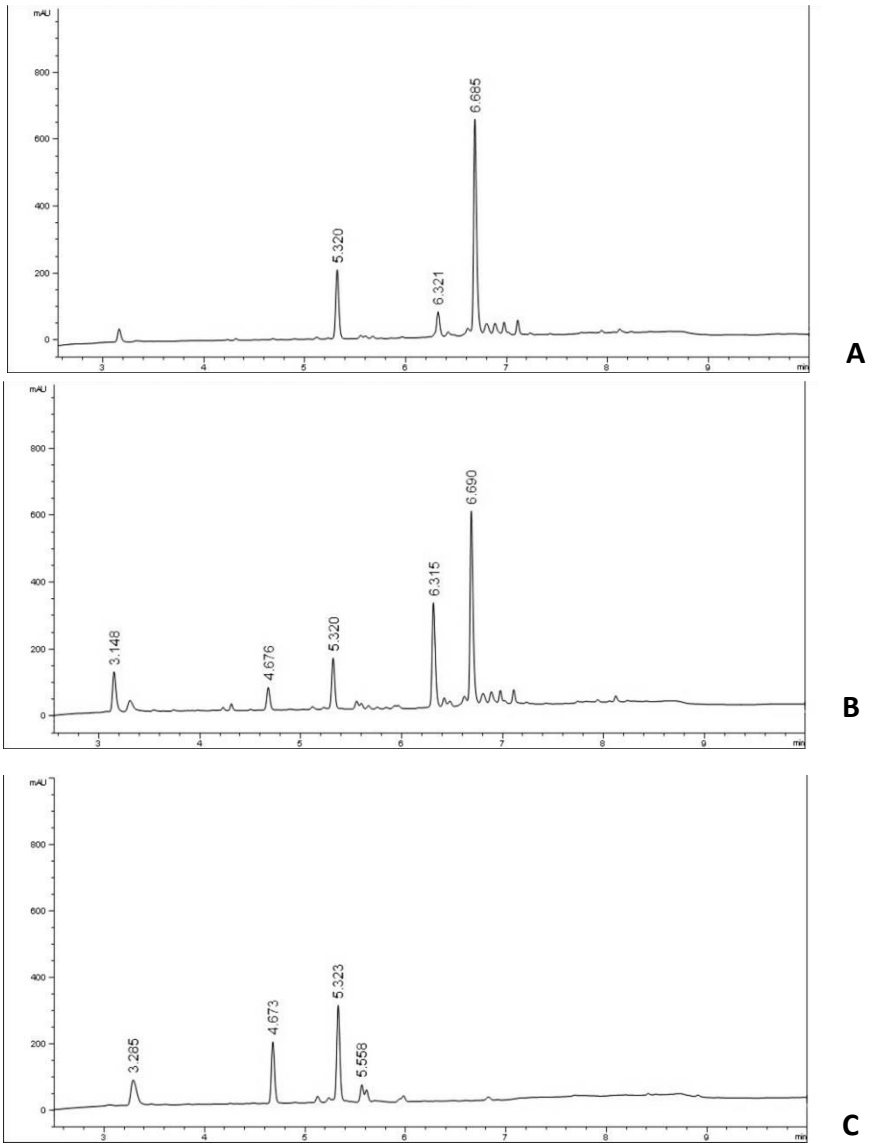

Figure A5.4: HPLC chromatograms of the fluorescent 9 residue ACE stalk peptide. 100µM of peptide was incubated on the surface of CHOKI for 6 hours, diluted in HBSS buffer A) Fluorescent ACE stalk peptide incubated for 0 hours on cells B) Fluorescent ACE stalk peptide incubated for 6 hours on cells C) HBSS buffer only incubated for 6 hours. Recorded wavelength was at 214nm.

REFERENCES

Adrain, C., Zettl, M., Christova, Y., Taylor, N., Freeman, M., 2012. Tumor necrosis factor signaling requires iRhom2 to promote trafficking and activation of TACE. Science 335, 225–228.

Akiyama, M., Takeda, S., Kokame, K., Takagi, J., Miyata, T., 2009. Crystal structures of the noncatalytic domains of ADAMTS13 reveal multiple discontinuous exosites for von Willebrand factor. Proc. Natl. Acad. Sci. U. S. A. 106, 19274–19279.

Alfalah, M., Parkin, E.T., Jacob, R., Sturrock, E.D., Mentele, R., Turner, A.J., Hooper, N.M., Naim, H.Y., 2001. A point mutation in the juxtamembrane stalk of human angiotensin I-converting enzyme invokes the action of a distinct secretase. J. Biol. Chem. 276, 21105–21109.

Alhenc-Gélas, F., Soubrier, F., Hubert, C., Allegrini, J., Corvol, P., 1989. The peculiar characteristics of the amino acid sequence of angiotensin I-converting enzyme, as determined by cDNA cloning of the human endothelial enzyme. J. Cardiovasc. Pharmacol. 14 Suppl 4, S6–9.

Allinson, T.M.J., Parkin, E.T., Condon, T.P., Schwager, S.L.U., Sturrock, E.D., Turner, A.J., 2004. The role of ADAM10 and ADAM17 in the ectodomain shedding of angiotensin converting enzyme and the amyloid precursor protein. Eur. J. Biochem. FEBS 271, 2539–2547.

Althoff, K., Müllberg, J., Aasland, D., Voltz, N., Kallen, K., Grötzinger, J., Rose-John, S., 2001. Recognition sequences and structural elements contribute to shedding susceptibility of membrane proteins. Biochem. J. 353, 663–672.

Althoff, K., Reddy, P., Voltz, N., Rose-John, S., Müllberg, J., 2000. Shedding of interleukin-6 receptor and tumor necrosis factor alpha. Contribution of the stalk sequence to the cleavage pattern of transmembrane proteins. Eur. J. Biochem. FEBS 267, 2624–2631.

Altmeppen, H.C., Prox, J., Puig, B., Kluth, M.A., Bernreuther, C., Thurm, D., Jorissen, E., Petrowitz, B., Bartsch, U., De Strooper, B., Saftig, P., Glatzel, M., 2011. Lack of a-disintegrin-and-metalloproteinase ADAM10 leads to intracellular accumulation and loss of shedding of the cellular prion protein in vivo. Mol. Neurodegener. 6, 36.

Alvarez-Iglesias, M., Wayne, G., O'Dea, K.P., Amour, A., Takata, M., 2005. Continuous real-time measurement of tumor necrosis factor-alpha converting enzyme activity on live cells. Lab. Investig. J. Tech. Methods Pathol. 85, 1440–1448.

Anthony, C.S., Corradi, H.R., Schwager, S.L.U., Redelinghuys, P., Georgiadis, D., Dive, V., Acharya, K.R., Sturrock, E.D., 2010. The N domain of human angiotensin-I-converting enzyme: the role of N-

glycosylation and the crystal structure in complex with an N domain-specific phosphinic inhibitor, RXP407. J. Biol. Chem. 285, 35685–35693.

Anthony, C.S., Masuyer, G., Sturrock, E.D., Acharya, K.R., 2012. Structure based drug design of angiotensin-I converting enzyme inhibitors. Curr. Med. Chem. 19, 845–855.

Anthony, C.S. 2011. The importance of N-linked glycosylation on the N-domain of Angiotensin-L Converrting Enzyme. PhD thesis.

Araujo, M.C., Melo, R.I., Del Nery, E., Alves, M.F., Juliano, M.A., Casarini, D.E., Juliano, L., Carmona, A.K., 1999. Internally quenched fluorogenic substrates for angiotensin I-converting enzyme. J. Hypertens. 17, 665–672.

Arribas, J., Coodly, L., Vollmer, P., Kishimoto, T.K., Rose-John, S., Massagué, J., 1996. Diverse cell surface protein ectodomains are shed by a system sensitive to metalloprotease inhibitors. J. Biol. Chem. 271, 11376–11382.

Balyasnikova, I V, Metzger, R., Sun, Z.-L., Berestetskaya, Y.V., Albrecht, R.F., Danilov, S.M., 2005. Development and characterization of rat monoclonal antibodies to denatured mouse angiotensin-converting enzyme. Tissue Antigens 65, 240–251.

Balyasnikova, I.V., Karran, E.H., Albrecht, R.F., 2nd, Danilov, S.M., 2002. Epitope-specific antibody-induced cleavage of angiotensin-converting enzyme from the cell surface. Biochem. J. 362, 585–595.

Balyasnikova, I.V., Metzger, R., Franke, F.E., Danilov, S.M., 2003. Monoclonal antibodies to denatured human ACE (CD 143), broad species specificity, reactivity on paraffin sections, and detection of subtle conformational changes in the C-terminal domain of ACE. Tissue Antigens 61, 49–62.

Balyasnikova, Irina V, Sun, Z.-L., Franke, F.E., Berestetskaya, Y.V., Chubb, A.J., Albrecht, R.F., Sturrock, E.D., Danilov, S.M., 2005. Monoclonal antibodies 1B3 and 5C8 as probes for monitoring the integrity of the C-terminal end of soluble angiotensin-converting enzyme. Hybrid. 2005 24, 14–26.

Balyasnikova, Irina V, Woodman, Z.L., Albrecht, R.F., 2nd, Natesh, R., Acharya, K.R., Sturrock, E.D., Danilov, S.M., 2005b. Localization of an N-domain region of angiotensin-converting enzyme involved in the regulation of ectodomain shedding using monoclonal antibodies. J. Proteome Res. 4, 258–267.

Bause, E., 1983. Structural requirements of N-glycosylation of proteins. Studies with proline peptides as conformational probes. Biochem. J. 209, 331–336.

Bause, E., Legler, G., 1981. The role of the hydroxy amino acid in the triplet sequence Asn-Xaa-Thr(Ser) for the N-glycosylation step during glycoprotein biosynthesis. Biochem. J. 195, 639–644.

Bech-Serra, J.J., Santiago-Josefat, B., Esselens, C., Saftig, P., Baselga, J., Arribas, J., Canals, F., 2006. Proteomic identification of desmoglein 2 and activated leukocyte cell adhesion molecule as substrates of ADAM17 and ADAM10 by difference gel electrophoresis. Mol. Cell. Biol. 26, 5086–5095.

Becker, B.F., Gilles, S., Sommerhoff, C.P., Zahler, S., 2002. Application of peptides containing the cleavage sequence of pro-TNFalpha in assessing TACE activity of whole cells. Biol. Chem. 383, 1821–1826.

Bennett, T.A., Edwards, B.S., Sklar, L.A., Rogelj, S., 2000. Sulfhydryl regulation of L-selectin shedding: phenylarsine oxide promotes activation-independent L-selectin shedding from leukocytes. J. Immunol. Baltim. Md 1950 164, 4120–4129.

Bersanetti, P.A., Andrade, M.C.C., Casarini, D.E., Juliano, M.A., Nchinda, A.T., Sturrock, E.D., Juliano, L., Carmona, A.K., 2004. Positional-scanning combinatorial libraries of fluorescence resonance energy transfer peptides for defining substrate specificity of the angiotensin I-converting enzyme and development of selective C-domain substrates. Biochemistry (Mosc.) 43, 15729–15736.

Black, R.A., Rauch, C.T., Kozlosky, C.J., Peschon, J.J., Slack, J.L., Wolfson, M.F., Castner, B.J., Stocking, K.L., Reddy, P., Srinivasan, S., Nelson, N., Boiani, N., Schooley, K.A., Gerhart, M., Davis, R., Fitzner, J.N., Johnson, R.S., Paxton, R.J., March, C.J., Cerretti, D.P., 1997. A metalloproteinase disintegrin that releases tumour-necrosis factor-alpha from cells. Nature 385, 729–733.

Blobel, C.P., 2002. Functional and biochemical characterization of ADAMs and their predicted role in protein ectodomain shedding. Inflamm. Res. Off. J. Eur. Histamine Res. Soc. Al 51, 83–84.

Borroto, A., Ruiz-Paz, S., de la Torre, T.V., Borrell-Pages, M., Merlos-Suarez, A., Pandiella, A., Blobel, C.P., Baselga, J., Arribas, J., 2003. Impaired trafficking and activation of tumor necrosis factor-alpha-converting enzyme in cell mutants defective in protein ectodomain shedding. J. Biol. Chem. 278, 25933–25939.

Bradford, M.M., 1976. A rapid and sensitive method for the quantitation of microgram quantities of protein utilizing the principle of protein-dye binding. Anal. Biochem. 72, 248–254.

Caescu, C.I., Jeschke, G.R., Turk, B.E., 2009. Active-site determinants of substrate recognition by the metalloproteinases TACE and ADAM10. Biochem. J. 424, 79–88.

Carmona, A.K., Schwager, S.L., Juliano, M.A., Juliano, L., Sturrock, E.D., 2006. A continuous fluorescence resonance energy transfer angiotensin I-converting enzyme assay. Nat. Protoc. 1, 1971–1976.

Chattopadhyay, S., Karan, G., Sen, I., Sen, G.C., 2008. A small region in the Angiotensin-Converting Enzyme distal ectodomain is required for cleavage-secretion of the protein at the plasma membrane. Biochemistry (Mosc.) 47, 8335–8341.

Chattopadhyay, S., Santhamma, K.R., Sengupta, S., McCue, B., Kinter, M., Sen, G.C., Sen, I., 2005. Calmodulin Binds to the Cytoplasmic Domain of Angiotensin-converting Enzyme and Regulates Its Phosphorylation and Cleavage Secretion. J. Biol. Chem. 280, 33847–33855.

Chesneau, V., Becherer, J.D., Zheng, Y., Erdjument-Bromage, H., Tempst, P., Blobel, C.P., 2003. Catalytic properties of ADAM19. J. Biol. Chem. 278, 22331–22340.

Chubb, A.J., 2001. The search for the angiotensin converting enzyme sheddase recognition domain. Phd thesis.

Chubb, A.J., Schwager, S.L.U., van der Merwe, E., Ehlers, M.R.W., Sturrock, E.D., 2004. Deletion of the cytoplasmic domain increases basal shedding of angiotensin-converting enzyme. Biochem. Biophys. Res. Commun. 314, 971–975.

Chubb, A.J., Schwager, S.L.U., Woodman, Z.L., Ehlers, M.R.W., Sturrock, E.D., 2002. Defining the boundaries of the testis angiotensin I-converting enzyme ectodomain. Biochem. Biophys. Res. Commun. 297, 1225–1230.

Cornish-Bowden, A., 1995. Fundamentals of Enzyme Kinetics, Rev Sub edition. ed. Portland Press Limited.

Dai, Y., Whittal, R.M., Li, L., 1996. Confocal Fluorescence Microscopic Imaging for Investigating the Analyte Distribution in MALDI Matrices. Anal. Chem. 68, 2494–2500.

Danilov, S.M., Gordon, K., Nesterovitch, A.B., Lünsdorf, H., Chen, Z., Castellon, M., Popova, I.A., Kalinin, S., Mendonca, E., Petukhov, P.A., Schwartz, D.E., Minshall, R.D., Sturrock, E.D., 2011. An angiotensin I-converting enzyme mutation (Y465D) causes a dramatic increase in blood ACE via accelerated ACE shedding. PloS One 6, e25952.

Danilov, S.M., Kalinin, S., Chen, Z., Vinokour, E.I., Nesterovitch, A.B., Schwartz, D.E., Gribouval, O., Gubler, M.-C., Minshall, R.D., 2010. Angiotensin I-converting enzyme Gln1069Arg mutation impairs trafficking to the cell surface resulting in selective denaturation of the C-domain. PloS One 5, e10438.

Deng, P., Rettenmier, C.W., Pattengale, P.K., 1996. Structural requirements for the ectodomain cleavage of human cell surface macrophage colony-stimulating factor. J. Biol. Chem. 271, 16338–16343.

Deng, P., Wang, Y.L., Haga, Y., Pattengale, P.K., 1998. Multiple factors determine the selection of the ectodomain cleavage site of human cell surface macrophage colony-stimulating factor. Biochemistry (Mosc.) 37, 17898–17904.

Deng, P., Wang, Y.L., Shahbazian, V.L., Pattengale, P.K., 2000. Biological characterization of uncleavable plasma membrane-anchored human macrophage colony-stimulating factor. Biochem. Biophys. Res. Commun. 276, 304–311.

Deng, W., Putkey, J.A., Li, R., 2013. Calmodulin adopts an extended conformation when interacting with L-selectin in membranes. PloS One 8, e62861.

Depierre, D., Roth, M., 1975. Fluorimetric determination of dipeptidyl carboxypeptidase. (angiotensin-I-converting enzyme). Enzyme 19, 65–70.

Deuss, M., Reiss, K., Hartmann, D., 2008. Part-time alpha-secretases: the functional biology of ADAM 9, 10 and 17. Curr. Alzheimer Res. 5, 187–201.

Doedens, J.R., Mahimkar, R.M., Black, R.A., 2003. TACE/ADAM-17 enzymatic activity is increased in response to cellular stimulation. Biochem. Biophys. Res. Commun. 308, 331–338.

Domingo, R., 2011. Characterization of the angiotensin-converting enzyme sheddase and synthesis of peptidomimetic inhibitors. Phd thesis.

Donoghue, M., Hsieh, F., Baronas, E., Godbout, K., Gosselin, M., Stagliano, N., Donovan, M., Woolf, B., Robison, K., Jeyaseelan, R., Breitbart, R.E., Acton, S., 2000. A novel angiotensin-converting enzyme-related carboxypeptidase (ACE2) converts angiotensin I to angiotensin 1-9. Circ. Res. 87, E1–9.

Douglas, R.G., Ehlers, M.R., Sturrock, E.D., 2013. Antifibrotic peptide N-acetyl-Ser-Asp-Lys-Pro (Ac-SDKP): Opportunities for angiotensin-converting enzyme inhibitor design. Clin. Exp. Pharmacol. Physiol. 40, 535–541.

Ehlers, M.R., Chen, Y.N., Riordan, J.F., 1991a. Purification and characterization of recombinant human testis angiotensin-converting enzyme expressed in Chinese hamster ovary cells. Protein Expr. Purif. 2, 1–9.

Ehlers, M.R., Chen, Y.N., Riordan, J.F., 1991b. Spontaneous solubilization of membrane-bound human testis angiotensin-converting enzyme expressed in Chinese hamster ovary cells. Proc. Natl. Acad. Sci. U. S. A. 88, 1009–1013.

Ehlers, M.R., Chen, Y.N., Riordan, J.F., 1992. The unique N-terminal sequence of testis angiotensin-converting enzyme is heavily O-glycosylated and unessential for activity or stability. Biochem. Biophys. Res. Commun. 183, 199–205.

Ehlers, M.R., Scholle, R.R., Riordan, J.F., 1995. Proteolytic release of human angiotensin-converting enzyme expressed in Chinese hamster ovary cells is enhanced by phorbol ester. Biochem. Biophys. Res. Commun. 206, 541–547.

Ehlers, M.R., Schwager, S.L., Chubb, A.J., Scholle, R.R., Brandt, W.F., Riordan, J.F., 1997. Proteolytic release of membrane proteins: studies on a membrane-protein-solubilizing activity in CHO cells. Immunopharmacology 36, 271–278.

Ehlers, M.R., Schwager, S.L., Scholle, R.R., Manji, G.A., Brandt, W.F., Riordan, J.F., 1996. Proteolytic release of membrane-bound angiotensin-converting enzyme: role of the juxtamembrane stalk sequence. Biochemistry (Mosc.) 35, 9549–9559.

Endres, K., Anders, A., Kojro, E., Gilbert, S., Fahrenholz, F., Postina, R., 2003. Tumor necrosis factor-alpha converting enzyme is processed by proprotein-convertases to its mature form which is degraded upon phorbol ester stimulation. Eur. J. Biochem. FEBS 270, 2386–2393.

English, W.R., Corvol, P., Murphy, G., 2012. LPS activates ADAM9 dependent shedding of ACE from endothelial cells. Biochem. Biophys. Res. Commun. 421, 70–75.

Eyries, M., Michaud, A., Deinum, J., Agrapart, M., Chomilier, J., Kramers, C., Soubrier, F., 2001. Increased shedding of angiotensin-converting enzyme by a mutation identified in the stalk region. J. Biol. Chem. 276, 5525–5532.

Fleming, I., 2006. Signaling by the angiotensin-converting enzyme. Circ. Res. 98, 887–896.

Fleming, I., Kohlstedt, K., Busse, R., 2005. New fACEs to the renin-angiotensin system. Physiol. Bethesda Md 20, 91–95.

Franzke, C.-W., Tasanen, K., Borradori, L., Huotari, V., Bruckner-Tuderman, L., 2004. Shedding of collagen XVII/BP180: structural motifs influence cleavage from cell surface. J. Biol. Chem. 279, 24521–24529.

Friedland, J., Silverstein, E., 1976. A sensitive fluorimetric assay for serum angiotensin-converting enzyme. Am. J. Clin. Pathol. 66, 416–424.

Fuchs, S., Frenzel, K., Hubert, C., Lyng, R., Muller, L., Michaud, A., Xiao, H.D., Adams, J.W., Capecchi, M.R., Corvol, P., Shur, B.D., Bernstein, K.E., 2005. Male fertility is dependent on dipeptidase activity of testis ACE. Nat. Med. 11, 1140–1142; author reply 1142–1143.

Fujihara, Y., Tokuhiro, K., Muro, Y., Kondoh, G., Araki, Y., Ikawa, M., Okabe, M., 2013. Expression of TEX101, regulated by ACE, is essential for the production of fertile mouse spermatozoa. Proc. Natl. Acad. Sci. U. S. A. 110, 8111–8116.

Gifford, J.L., Ishida, H., Vogel, H.J., 2012. Structural Insights into Calmodulin-Regulated L-Selectin Ectodomain Shedding. J. Biol. Chem. 287, 26513–26527.

Gordon, K., 2011. Protein-protein interactions of human somatic angiotensin-converting enzyme. PhD thesis

Gordon, K., Balyasnikova, I.V., Nesterovitch, A.B., Schwartz, D.E., Sturrock, E.D., Danilov, S.M., 2010. Fine epitope mapping of monoclonal antibodies 9B9 and 3G8 to the N domain of angiotensin-converting enzyme (CD143) defines a region involved in regulating angiotensin-converting enzyme dimerization and shedding. Tissue Antigens 75, 136–150.

Guy, J.L., Lambert, D.W., Warner, F.J., Hooper, N.M., Turner, A.J., 2005. Membrane-associated zinc peptidase families: comparing ACE and ACE2. Biochim. Biophys. Acta 1751, 2–8.

Hayashida, K., Bartlett, A.H., Chen, Y., Park, P.W., 2010. Molecular and Cellular Mechanisms of Ectodomain Shedding. Anat. Rec. Adv. Integr. Anat. Evol. Biol. 293, 925–937.

Hemming, M.L., Selkoe, D.J., 2005. Amyloid beta-protein is degraded by cellular angiotensin-converting enzyme (ACE) and elevated by an ACE inhibitor. J. Biol. Chem. 280, 37644–37650.

Hinkle, C.L., Mohan, M.J., Lin, P., Yeung, N., Rasmussen, F., Milla, M.E., Moss, M.L., 2003. Multiple metalloproteinases process protransforming growth factor-alpha (proTGF-alpha). Biochemistry (Mosc.) 42, 2127–2136.

Hirata, I.Y., Cezari, M.H.S., Nakaie, C.R., Boschcov, P., Ito, A.S., Juliano, M.A., Juliano, L., 1995. Internally quenched fluorogenic protease substrates: Solid-phase synthesis and fluorescence spectroscopy of peptides containing ortho-aminobenzoyl/dinitrophenyl groups as donor-acceptor pairs. Lett. Pept. Sci. 1, 299–308.

Hooper, N.M., Turner, A.J., 2000. Protein processing mechanisms: from angiotensin-converting enzyme to Alzheimer's disease. Biochem. Soc. Trans. 28, 441–446.

Horiuchi, K., Le Gall, S., Schulte, M., Yamaguchi, T., Reiss, K., Murphy, G., Toyama, Y., Hartmann, D., Saftig, P., Blobel, C.P., 2007. Substrate selectivity of epidermal growth factor-receptor ligand sheddases and their regulation by phorbol esters and calcium influx. Mol. Biol. Cell 18, 176–188.

Hubert, C., Houot, A.M., Corvol, P., Soubrier, F., 1991. Structure of the angiotensin I-converting enzyme gene. Two alternate promoters correspond to evolutionary steps of a duplicated gene. J. Biol. Chem. 266, 15377–15383.

Issuree, P.D.A., Maretzky, T., McIlwain, D.R., Monette, S., Qing, X., Lang, P.A., Swendeman, S.L., Park-Min, K.-H., Binder, N., Kalliolias, G.D., Yarilina, A., Horiuchi, K., Ivashkiv, L.B., Mak, T.W., Salmon, J.E., Blobel, C.P., 2013. iRHOM2 is a critical pathogenic mediator of inflammatory arthritis. J. Clin. Invest. 123, 928–932.

Iwata, M., Silva Enciso, J.E., Greenberg, B.H., 2009. Selective and specific regulation of ectodomain shedding of angiotensin-converting enzyme 2 by tumor necrosis factor alpha-converting enzyme. Am. J. Physiol. Cell Physiol. 297, C1318–1329.

Janes, P.W., Saha, N., Barton, W.A., Kolev, M.V., Wimmer-Kleikamp, S.H., Nievergall, E., Blobel, C.P., Himanen, J.-P., Lackmann, M., Nikolov, D.B., 2005. Adam meets Eph: an ADAM substrate recognition module acts as a molecular switch for ephrin cleavage in trans. Cell 123, 291–304.

Janes, P.W., Wimmer-Kleikamp, S.H., Frangakis, A.S., Treble, K., Griesshaber, B., Sabet, O., Grabenbauer, M., Ting, A.Y., Saftig, P., Bastiaens, P.I., Lackmann, M., 2009. Cytoplasmic relaxation of active Eph controls ephrin shedding by ADAM10. PLoS Biol. 7, e1000215.

Jia, H.P., Look, D.C., Tan, P., Shi, L., Hickey, M., Gakhar, L., Chappell, M.C., Wohlford-Lenane, C., McCray, P.B., Jr, 2009. Ectodomain shedding of angiotensin converting enzyme 2 in human airway epithelia. Am. J. Physiol. Lung Cell. Mol. Physiol. 297, L84–96.

Jin, G., Huang, X., Black, R., Wolfson, M., Rauch, C., McGregor, H., Ellestad, G., Cowling, R., 2002. A continuous fluorimetric assay for tumor necrosis factor-alpha converting enzyme. Anal. Biochem. 302, 269–275.

Kawaguchi, N., Horiuchi, K., Becherer, J.D., Toyama, Y., Besmer, P., Blobel, C.P., 2007. Different ADAMs have distinct influences on Kit ligand processing: phorbol-ester-stimulated ectodomain shedding of Kitl1 by ADAM17 is reduced by ADAM19. J. Cell Sci. 120, 943–952.

Killock, D.J., Ivetić, A., 2010. The cytoplasmic domains of TNFalpha-converting enzyme (TACE/ADAM17) and L-selectin are regulated differently by p38 MAPK and PKC to promote ectodomain shedding. Biochem. J. 428, 293–304.

Kohlstedt, K., Brandes, R.P., Müller-Esterl, W., Busse, R., Fleming, I., 2004. Angiotensin-converting enzyme is involved in outside-in signaling in endothelial cells. Circ. Res. 94, 60–67.

Kohlstedt, K., Gershome, C., Friedrich, M., Müller-Esterl, W., Alhenc-Gelas, F., Busse, R., Fleming, I., 2006a. Angiotensin-converting enzyme (ACE) dimerization is the initial step in the ACE inhibitor-induced ACE signaling cascade in endothelial cells. Mol. Pharmacol. 69, 1725–1732.

Kohlstedt, K., Kellner, R., Busse, R., Fleming, I., 2006b. Signaling via the angiotensin-converting enzyme results in the phosphorylation of the nonmuscle myosin heavy chain IIA. Mol. Pharmacol. 69, 19–26.

Kohlstedt, K., Shoghi, F., Müller-Esterl, W., Busse, R., Fleming, I., 2002. CK2 phosphorylates the angiotensin-converting enzyme and regulates its retention in the endothelial cell plasma membrane. Circ. Res. 91, 749–756.

Kondoh, G., Tojo, H., Nakatani, Y., Komazawa, N., Murata, C., Yamagata, K., Maeda, Y., Kinoshita, T., Okabe, M., Taguchi, R., Takeda, J., 2005. Angiotensin-converting enzyme is a GPI-anchored protein releasing factor crucial for fertilization. Nat. Med. 11, 160–166.

Kondoh, G., Watanabe, H., Tashima, Y., Maeda, Y., Kinoshita, T., 2009. Testicular Angiotensin-converting enzyme with different glycan modification: characterization on glycosylphosphatidylinositol-anchored protein releasing and dipeptidase activities. J. Biochem. (Tokyo) 145, 115–121.

Kost, O.A., Balyasnikova, I.V., Chemodanova, E.E., Nikolskaya, I.I., Albrecht, R.F., 2nd, Danilov, S.M., 2003. Epitope-dependent blocking of the angiotensin-converting enzyme dimerization by monoclonal antibodies to the N-terminal domain of ACE: possible link of ACE dimerization and shedding from the cell surface. Biochemistry (Mosc.) 42, 6965–6976.

Kramers, C., Danilov, S.M., Deinum, J., Balyasnikova, I.V., Scharenborg, N., Looman, M., Boomsma, F., de Keijzer, M.H., van Duijn, C., Martin, S., Soubrier, F., Adema, G.J., 2001. Point mutation in the stalk of angiotensin-converting enzyme causes a dramatic increase in serum angiotensin-converting enzyme but no cardiovascular disease. Circulation 104, 1236–1240.

Krstenansky, J., Wang, J., Chenail, G., Tiffany, M., Kuesters, G., Natke, B., Nestor, J., 2004. Probing Proteinase Active Sites Using Oriented Peptide Mixture Libraries – ADAM-10. Pharm. Sci. Res.

Kuba, K., Imai, Y., Rao, S., Gao, H., Guo, F., Guan, B., Huan, Y., Yang, P., Zhang, Y., Deng, W., Bao, L., Zhang, B., Liu, G., Wang, Z., Chappell, M., Liu, Y., Zheng, D., Leibbrandt, A., Wada, T., Slutsky, A.S., Liu, D., Qin, C., Jiang, C., Penninger, J.M., 2005. A crucial role of angiotensin converting enzyme 2 (ACE2) in SARS coronavirus-induced lung injury. Nat. Med. 11, 875–879.

Kuhn, P.-H., Wang, H., Dislich, B., Colombo, A., Zeitschel, U., Ellwart, J.W., Kremmer, E., Rossner, S., Lichtenthaler, S.F., 2010. ADAM10 is the physiologically relevant, constitutive alpha-secretase of the amyloid precursor protein in primary neurons. EMBO J. 29, 3020–3032.

Kveiborg, M., Jacobsen, J., Lee, M.-H., Nagase, H., Wewer, U.M., Murphy, G., 2010. Selective inhibition of ADAM12 catalytic activity through engineering of tissue inhibitor of metalloproteinase 2 (TIMP-2). Biochem. J. 430, 79–86.

Lai, Z.W., Hanchapola, I., Steer, D.L., Smith, A.I., 2011. Angiotensin-converting enzyme 2 ectodomain shedding cleavage-site identification: determinants and constraints. Biochemistry (Mosc.) 50, 5182–5194.

Lai, Z.W., Lew, R.A., Yarski, M.A., Mu, F.-T., Andrews, R.K., Smith, A.I., 2009. The identification of a calmodulin-binding domain within the cytoplasmic tail of angiotensin-converting enzyme-2. Endocrinology 150, 2376–2381.

Lambert, D.W., Clarke, N.E., Hooper, N.M., Turner, A.J., 2008. Calmodulin interacts with angiotensin-converting enzyme-2 (ACE2) and inhibits shedding of its ectodomain. FEBS Lett. 582, 385–390.

Lattion, A.-L., Soubrier, F., Allegrini, J., Hubert, C., Corvol, P., Alhenc-Gelas, F., 1989. The testicular transcript of the angiotensin I-converting enzyme encodes for the ancestral, non-duplicated form of the enzyme. FEBS Lett. 252, 99–104.

Le Gall, S.M., Bobé, P., Reiss, K., Horiuchi, K., Niu, X.-D., Lundell, D., Gibb, D.R., Conrad, D., Saftig, P., Blobel, C.P., 2009. ADAMs 10 and 17 represent differentially regulated components of a general shedding machinery for membrane proteins such as transforming growth factor alpha, L-selectin, and tumor necrosis factor alpha. Mol. Biol. Cell 20, 1785–1794.

Le Gall, S.M., Maretzky, T., Issuree, P.D.A., Niu, X.-D., Reiss, K., Saftig, P., Khokha, R., Lundell, D., Blobel, C.P., 2010. ADAM17 is regulated by a rapid and reversible mechanism that controls access to its catalytic site. J. Cell Sci. 123, 3913–3922.

Lieberman, J., 1975. Elevation of serum angiotensin-converting-enzyme (ACE) level in sarcoidosis. Am. J. Med. 59, 365–372.

Manon-Jensen, T., Multhaupt, H.A.B., Couchman, J.R., 2013. Mapping of matrix metalloproteinase cleavage sites on syndecan-1 and syndecan-4 ectodomains. FEBS J. 280, 2320–2331.

Maretzky, T., Yang, G., Ouerfelli, O., Overall, C.M., Worpenberg, S., Hassiepen, U., Eder, J., Blobel, C.P., 2009. Characterization of the catalytic activity of the membrane-anchored metalloproteinase ADAM15 in cell-based assays. Biochem. J. 420, 105–113.

Marshall, R.D., 1974. The nature and metabolism of the carbohydrate-peptide linkages of glycoproteins. Biochem. Soc. Symp. 17–26.

McIlwain, D.R., Lang, P.A., Maretzky, T., Hamada, K., Ohishi, K., Maney, S.K., Berger, T., Murthy, A., Duncan, G., Xu, H.C., Lang, K.S., Häussinger, D., Wakeham, A., Itie-Youten, A., Khokha, R., Ohashi, P.S., Blobel, C.P., Mak, T.W., 2012. iRhom2 regulation of TACE controls TNF-mediated protection against Listeria and responses to LPS. Science 335, 229–232.

Merlos-Suárez, A., Arribas, J., 1999. Mechanisms controlling the shedding of transmembrane molecules. Biochem. Soc. Trans. 27, 243–246.

Migaki, G.I., Kahn, J., Kishimoto, T.K., 1995. Mutational analysis of the membrane-proximal cleavage site of L-selectin: relaxed sequence specificity surrounding the cleavage site. J. Exp. Med. 182, 549–557.

Naim, H.Y., 1996. Secretion of human intestinal angiotensin-converting enzyme and its association with the differentiation state of intestinal cells. Biochem. J. 316 (Pt 1), 259–264.

Nakayama, H., Fukuda, S., Inoue, H., Nishida-Fukuda, H., Shirakata, Y., Hashimoto, K., Higashiyama, S., 2012. Cell surface annexins regulate ADAM-mediated ectodomain shedding of proamphiregulin. Mol. Biol. Cell 23, 1964–1975.

Naperova, I.A., Baliasnikova, I.V., Petrov, M.N., Vakhitova, A.V., Evdokimov, V.V., Danilov, S.M., Kost, O.A., 2008. [Characteristics of monoclonal antibody binding with the C domain of human angiotensin converting enzyme]. Bioorg. Khim. 34, 358–364.

Natesh, R., Schwager, S.L.U., Sturrock, E.D., Acharya, K.R., 2003. Crystal structure of the human angiotensin-converting enzyme-lisinopril complex. Nature 421, 551–554.

Naus, S., Reipschläger, S., Wildeboer, D., Lichtenthaler, S.F., Mitterreiter, S., Guan, Z., Moss, M.L., Bartsch, J.W., 2006. Identification of candidate substrates for ectodomain shedding by the metalloprotease-disintegrin ADAM8. Biol. Chem. 387, 337–346.

Nchinda, A.T., Chibale, K., Redelinghuys, P., Sturrock, E.D., 2006. Synthesis of novel keto-ACE analogues as domain-selective angiotensin I-converting enzyme inhibitors. Bioorg. Med. Chem. Lett. 16, 4612–4615.

Nesterovitch, A.B., Hogarth, K.D., Adarichev, V.A., Vinokour, E.I., Schwartz, D.E., Solway, J., Danilov, S.M., 2009. Angiotensin I-converting enzyme mutation (Trp1197Stop) causes a dramatic increase in blood ACE. PloS One 4, e8282.

Nievergall, E., Lackmann, M., Janes, P.W., 2012. Eph-dependent cell-cell adhesion and segregation in development and cancer. Cell. Mol. Life Sci. CMLS 69, 1813–1842.

Nikolaeva, M.A., Balyasnikova, I.V., Alexinskaya, M.A., Metzger, R., Franke, F.E., Albrecht, R.F., 2nd, Kulakov, V.I., Sukhikh, G.T., Danilov, S.M., 2006. Testicular isoform of angiotensin I-converting enzyme (ACE, CD143) on the surface of human spermatozoa: revelation and quantification using monoclonal antibodies. Am. J. Reprod. Immunol. New York N 1989 55, 54–68.

Nishie, W., Jackow, J., Hofmann, S.C., Franzke, C.-W., Bruckner-Tuderman, L., 2012. Coiled coils ensure the physiological ectodomain shedding of collagen XVII. J. Biol. Chem. 287, 29940–29948.

O'Neill, H.G., Redelinghuys, P., Schwager, S.L.U., Sturrock, E.D., 2008. The role of glycosylation and domain interactions in the thermal stability of human angiotensin-converting enzyme. Biol. Chem. 389, 1153–1161.

Oba, R., Igarashi, A., Kamata, M., Nagata, K., Takano, S., Nakagawa, H., 2005. The N-terminal active centre of human angiotensin-converting enzyme degrades Alzheimer amyloid beta-peptide. Eur. J. Neurosci. 21, 733–740.

Oppong, S.Y., Hooper, N.M., 1993. Characterization of a secretase activity which releases angiotensin-converting enzyme from the membrane. Biochem. J. 292 (Pt 2), 597–603.

Overall, C.M., Blobel, C.P., 2007. In search of partners: linking extracellular proteases to substrates. Nat. Rev. Mol. Cell Biol. 8, 245–257.

Pang, S., Chubb, A.J., Schwager, S.L., Ehlers, M.R., Sturrock, E.D., Hooper, N.M., 2001. Roles of the juxtamembrane and extracellular domains of angiotensin-converting enzyme in ectodomain shedding. Biochem. J. 358, 185–192.

Pantoliano, M.W., Holmquist, B., Riordan, J.F., 1984. Affinity chromatographic purification of angiotensin converting enzyme. Biochemistry (Mosc.) 23, 1037–1042.

Parkin, E., Harris, B., 2009. A disintegrin and metalloproteinase (ADAM)-mediated ectodomain shedding of ADAM10. J. Neurochem. 108, 1464–1479.

Parkin, E.T., Trew, A., Christie, G., Faller, A., Mayer, R., Turner, A.J., Hooper, N.M., 2002. Structure-activity relationship of hydroxamate-based inhibitors on the secretases that cleave the amyloid precursor protein, angiotensin converting enzyme, CD23, and pro-tumor necrosis factor-alpha. Biochemistry (Mosc.) 41, 4972–4981.

Parvathy, S., Karran, E.H., Turner, A.J., Hooper, N.M., 1998. The secretases that cleave angiotensin converting enzyme and the amyloid precursor protein are distinct from tumour necrosis factor-alpha convertase. FEBS Lett. 431, 63–65.

Parvathy, S., Oppong, S.Y., Karran, E.H., Buckle, D.R., Turner, A.J., Hooper, N.M., 1997. Angiotensin-converting enzyme secretase is inhibited by zinc metalloprotease inhibitors and requires its substrate to be inserted in a lipid bilayer. Biochem. J. 327 (Pt 1), 37–43.

Peiretti, F., Canault, M., Deprez-Beauclair, P., Berthet, V., Bonardo, B., Juhan-Vague, I., Nalbone, G., 2003. Intracellular maturation and transport of tumor necrosis factor alpha converting enzyme. Exp. Cell Res. 285, 278–285.

Qi, B., Newcomer, R.G., Sang, Q.-X.A., 2009. ADAM19/adamalysin 19 structure, function, and role as a putative target in tumors and inflammatory diseases. Curr. Pharm. Des. 15, 2336–2348.

Ramchandran, R., Sen, I., 1995. Cleavage processing of angiotensin-converting enzyme by a membrane-associated metalloprotease. Biochemistry (Mosc.) 34, 12645–12652.

Ramchandran, R., Sen, G.C., Misono, K., Sen, I., 1994. Regulated cleavage-secretion of the membrane-bound angiotensin-converting enzyme. J. Biol. Chem. 269, 2125–2130.

Sabatini, R.A., Bersanetti, P.A., Farias, S.L., Juliano, L., Juliano, M.A., Casarini, D.E., Carmona, A.K., Paiva, A.C.M., Pesquero, J.B., 2007. Determination of angiotensin I-converting enzyme activity in cell culture using fluorescence resonance energy transfer peptides. Anal. Biochem. 363, 255–262.

Sadhukhan, R., Santhamma, K.R., Reddy, P., Peschon, J.J., Black, R.A., Sen, I., 1999. Unaltered cleavage and secretion of angiotensin-converting enzyme in tumor necrosis factor-alpha-converting enzyme-deficient mice. J. Biol. Chem. 274, 10511–10516.

Sadhukhan, R., Sen, G.C., Ramchandran, R., Sen, I., 1998. The distal ectodomain of angiotensin-converting enzyme regulates its cleavage-secretion from the cell surface. Proc. Natl. Acad. Sci. U. S. A. 95, 138–143.

Sadhukhan, R., Sen, G.C., Sen, I., 1996. Synthesis and cleavage- secretion of enzymatically active rabbit angiotensin-converting enzyme in Pichia pastoris. J. Biol. Chem. 271, 18310–18313.

Sadhukhan, R., Sen, I., 1996. Different glycosylation requirements for the synthesis of enzymatically active angiotensin-converting enzyme in mammalian cells and yeast. J. Biol. Chem. 271, 6429–6434.

Saftig, P., Reiss, K., 2011. The “A Disintegrin And Metalloproteases” ADAM10 and ADAM17: novel drug targets with therapeutic potential? Eur. J. Cell Biol. 90, 527–535.

Schechter, I., Berger, A., 1967. On the size of the active site in proteases. I. Papain. Biochem. Biophys. Res. Commun. 27, 157–162.

Schlomann, U., Wildeboer, D., Webster, A., Antropova, O., Zeuschner, D., Knight, C.G., Docherty, A.J.P., Lambert, M., Skelton, L., Jockusch, H., Bartsch, J.W., 2002. The metalloprotease disintegrin ADAM8. Processing by autocatalysis is required for proteolytic activity and cell adhesion. J. Biol. Chem. 277, 48210–48219.

Schwager, S.L., Chubb, A.J., Scholle, R.R., Brandt, W.F., Eckerskorn, C., Sturrock, E.D., Ehlers, M.R., 1998. Phorbol ester-induced juxtamembrane cleavage of angiotensin-converting enzyme is not inhibited by a stalk containing intrachain disulfides. Biochemistry (Mosc.) 37, 15449–15456.

Schwager, S.L., Chubb, A.J., Scholle, R.R., Brandt, W.F., Mentele, R., Riordan, J.F., Sturrock, E.D., Ehlers, M.R., 1999. Modulation of juxtamembrane cleavage (“shedding”) of angiotensin-converting enzyme by stalk glycosylation: evidence for an alternative shedding protease. Biochemistry (Mosc.) 38, 10388–10397.

Schwager, S.L., Chubb, A.J., Woodman, Z.L., Yan, L., Mentele, R., Ehlers, M.R., Sturrock, E.D., 2001. Cleavage of disulfide-bridged stalk domains during shedding of angiotensin-converting enzyme occurs at multiple juxtamembrane sites. Biochemistry (Mosc.) 40, 15624–15630.

Schwager, S.L., Chubb, A.J., Woodman, Z.L., Yan, L., Mentele, R., Ehlers, M.R., Sturrock, E.D., 2001. Cleavage of disulfide-bridged stalk domains during shedding of angiotensin-converting enzyme occurs at multiple juxtamembrane sites. Biochemistry (Mosc.) 40, 15624–15630.

Schwager, S.L., Carmona, A.K., Sturrock, E.D., 2006. A high-throughput fluorimetric assay for angiotensin I-converting enzyme. Nat. Protoc. 1, 1961–1964.

Skeggs, L.T., Jr, Kahn, J.R., Shumway, N.P., 1956. The preparation and function of the hypertension converting enzyme. J. Exp. Med. 103, 295–299.

Smalley, D.M., Ley, K., 2005. L-selectin: mechanisms and physiological significance of ectodomain cleavage. J. Cell. Mol. Med. 9, 255–266.

Soubrier, F., Alhenc-Gelas, F., Hubert, C., Allegrini, J., John, M., Tregear, G., Corvol, P., 1988. Two putative active centers in human angiotensin I-converting enzyme revealed by molecular cloning. Proc. Natl. Acad. Sci. U. S. A. 85, 9386–9390.

Stawikowska, R., Cudic, M., Giulianotti, M., Houghten, R.A., Fields, G.B., Minond, D., 2013. Activity of ADAM17 (a disintegrin and metalloprotease 17) is regulated by its noncatalytic domains and secondary structure of its substrates. J. Biol. Chem. 288, 22871–22879.

Surawska, H., Ma, P.C., Salgia, R., 2004. The role of ephrins and Eph receptors in cancer. Cytokine Growth Factor Rev. 15, 419–433.

Takeda, S., Igarashi, T., Mori, H., Araki, S., 2006. Crystal structures of VAP1 reveal ADAMs' MDC domain architecture and its unique C-shaped scaffold. EMBO J. 25, 2388–2396.

Takeda, S., Takeya, H., Iwanaga, S., 2012. Snake venom metalloproteinases: structure, function and relevance to the mammalian ADAM/ADAMTS family proteins. Biochim. Biophys. Acta 1824, 164–176.

Tanabe, C., Hotoda, N., Sasagawa, N., Futai, E., Komano, H., Ishiura, S., 2010. ADAM19 autolysis is activated by LPS and promotes non-classical secretion of cysteine-rich protein 2. Biochem. Biophys. Res. Commun. 396, 927–932.

Taylor, D.R., Parkin, E.T., Cocklin, S.L., Ault, J.R., Ashcroft, A.E., Turner, A.J., Hooper, N.M., 2009. Role of ADAMs in the ectodomain shedding and conformational conversion of the prion protein. J. Biol. Chem. 284, 22590–22600.

Tzakos, A.G., Galanis, A.S., Spyroulias, G.A., Cordopatis, P., Manessi-Zoupa, E., Gerothanassis, I.P., 2003. Structure-function discrimination of the N- and C- catalytic domains of human angiotensin-converting enzyme: implications for Cl- activation and peptide hydrolysis mechanisms. Protein Eng. 16, 993–1003.

Urban, A., Neukirchen, S., Jaeger, K.E., 1997. A rapid and efficient method for site-directed mutagenesis using one-step overlap extension PCR. Nucleic Acids Res. 25, 2227–2228.

Walcheck, B., Alexander, S.R., St Hill, C.A., Matala, E., 2003. ADAM-17-independent shedding of L-selectin. J. Leukoc. Biol. 74, 389–394.

Wang, Y., Herrera, A.H., Li, Y., Belani, K.K., Walcheck, B., 2009. Regulation of mature ADAM17 by redox agents for L-selectin shedding. J. Immunol. Baltim. Md 1950 182, 2449–2457.

Watanabe, H., Kondoh, G., 2011. Mouse sperm undergo GPI-anchored protein release associated with lipid raft reorganization and acrosome reaction to acquire fertility. J. Cell Sci. 124, 2573–2581.

Watermeyer, J.M., Kröger, W.L., O'Neill, H.G., Sewell, B.T., Sturrock, E.D., 2010. Characterization of domain-selective inhibitor binding in angiotensin-converting enzyme using a novel derivative of lisinopril. Biochem. J. 428, 67–74.

Wei, L., Alhenc-Gelas, F., Corvol, P., Clauser, E., 1991a. The two homologous domains of human angiotensin I-converting enzyme are both catalytically active. J. Biol. Chem. 266, 9002–9008.

Wei, L., Alhenc-Gelas, F., Soubrier, F., Michaud, A., Corvol, P., Clauser, E., 1991b. Expression and characterization of recombinant human angiotensin I-converting enzyme. Evidence for a C-terminal transmembrane anchor and for a proteolytic processing of the secreted recombinant and plasma enzymes. J. Biol. Chem. 266, 5540–5546.

Wei, L., Clauser, E., Alhenc-Gelas, F., Corvol, P., 1992. The two homologous domains of human angiotensin I-converting enzyme interact differently with competitive inhibitors. J. Biol. Chem. 267, 13398–13405.

Willems, S.H., Tape, C.J., Stanley, P.L., Taylor, N.A., Mills, I.G., Neal, D.E., McCafferty, J., Murphy, G., 2010. Thiol isomerases negatively regulate the cellular shedding activity of ADAM17. Biochem. J. 428, 439–450.

Wong, S.K., Li, W., Moore, M.J., Choe, H., Farzan, M., 2004. A 193-amino acid fragment of the SARS coronavirus S protein efficiently binds angiotensin-converting enzyme 2. J. Biol. Chem. 279, 3197–3201.

Woodman, Z.L., Oppong, S.Y., Cook, S., Hooper, N.M., Schwager, S.L., Brandt, W.F., Ehlers, M.R., Sturrock, E.D., 2000. Shedding of somatic angiotensin-converting enzyme (ACE) is inefficient compared with testis ACE despite cleavage at identical stalk sites. Biochem. J. 347 Pt 3, 711–718.

Woodman, Z.L., Schwager, S.L.U., Redelinghuys, P., Carmona, A.K., Ehlers, M.R.W., Sturrock, E.D., 2005. The N domain of somatic angiotensin-converting enzyme negatively regulates ectodomain shedding and catalytic activity. Biochem. J. 389, 739–744.

Woodman, Z.L., Schwager, S.L.U., Redelinghuys, P., Chubb, A.J., van der Merwe, E.L., Ehlers, M.R.W., Sturrock, E.D., 2006. Homologous substitution of ACE C-domain regions with N-domain sequences: effect on processing, shedding, and catalytic properties. Biol. Chem. 387, 1043–1051.

Wu, W., Jia, Z., Liu, P., Xie, Z., Wei, Q., 2005. A novel PCR strategy for high-efficiency, automated site directed mutagenesis. Nucleic Acids Res. 33, e110. doi:10.1093/nar/gni115

Yang, H.Y., Erdös, E.G., Levin, Y., 1970. A dipeptidyl carboxypeptidase that converts angiotensin I and inactivates bradykinin. Biochim. Biophys. Acta 214, 374–376.

Yu, X.C., Sturrock, E.D., Wu, Z., Biemann, K., Ehlers, M.R., Riordan, J.F., 1997. Identification of N-linked glycosylation sites in human testis angiotensin-converting enzyme and expression of an active deglycosylated form. J. Biol. Chem. 272, 3511–3519.

Zettl, M., Adrain, C., Strisovsky, K., Lastun, V., Freeman, M., 2011. Rhomboid family pseudoproteases use the ER quality control machinery to regulate intercellular signaling. Cell 145, 79–91.

Zhao, L.C., Edgar, J.B., Dailey, M.O., 2001. Characterization of the rapid proteolytic shedding of murine L-selectin. Dev. Immunol. 8, 267–277.

Zheng, Y., Saftig, P., Hartmann, D., Blobel, C., 2004. Evaluation of the contribution of different ADAMs to tumor necrosis factor alpha (TNFalpha) shedding and of the function of the TNFalpha ectodomain in ensuring selective stimulated shedding by the TNFalpha convertase (TACE/ADAM17). J. Biol. Chem. 279, 42898–42906.

Zou, J., Zhang, R., Zhu, F., Liu, J., Madison, V., Umland, S.P., 2005. ADAM33 enzyme properties and substrate specificity. Biochemistry (Mosc.) 44, 4247–4256.

Zou, J., Zhu, F., Liu, J., Wang, W., Zhang, R., Garlisi, C.G., Liu, Y.-H., Wang, S., Shah, H., Wan, Y., Umland, S.P., 2004. Catalytic activity of human ADAM33. J. Biol. Chem. 279, 9818–9830.

Zou, K., Maeda, T., Watanabe, A., Liu, J., Liu, S., Oba, R., Satoh, Y., Komano, H., Michikawa, M., 2009. Abeta42-to-Abeta40- and angiotensin-converting activities in different domains of angiotensin-converting enzyme. J. Biol. Chem. 284, 31914–31920.

Zou, K., Yamaguchi, H., Akatsu, H., Sakamoto, T., Ko, M., Mizoguchi, K., Gong, J.-S., Yu, W., Yamamoto, T., Kosaka, K., Yanagisawa, K., Michikawa, M., 2007. Angiotensin-converting enzyme converts amyloid beta-protein 1-42 (Abeta(1-42)) to Abeta(1-40), and its inhibition enhances brain Abeta deposition. J. Neurosci. Off. J. Soc. Neurosci. 27, 8628–8635.